Downregulation of Natriuretic Peptide Receptor-A:

Evidence for Clathrin- and Dynamin-Independent Internalization

A DISSERTATION SUBMITTED TO THE FACULTY OF

THE GRADUATE SCHOOL OF THE UNIVERSITY OF MINNESOTA

BY

Darcy Rae Flora

IN PARTIAL FULFILLMENT OF THE REQUIREMENTS FOR THE DEGREE OF

DOCTOR OF PHILOSOPHY

Adviser: Lincoln R. Potter

December 2009

ACKNOWLEDGEMENT

Portions of the research presented here were supported by a predoctoral fellowship to Darcy R. Flora from the American Heart Association.

DEDICATION

This dissertation is dedicated to my parents,

Michael and Marsha Flora,

for their continuous support.

ABSTRACT

Atrial natriuretic peptide (ANP) and B-type natriuretic peptide (BNP) are endogenous cardiac hormones that are essential for cardiovascular homeostasis. To decrease blood pressure and cardiac hypertrophy, ANP and BNP bind to the transmembrane guanylyl cyclase natriuretic peptide receptor-A (NPR-A). Activation of NPR-A leads to the synthesis of the intracellular second messenger cGMP, which mediates the physiological effects of the natriuretic peptides. Under cardiovascular stress serum ANP and BNP concentrations are elevated. Initially, these cardiac peptides stimulate compensatory hemodynamic functions, but over time their cardiac unloading effects wane despite continued elevation of serum ANP and BNP levels. Unfortunately, the underlying molecular mechanisms responsible for the diminished effect are poorly understood.

Transaortic banding was performed to induce congestive heart failure in mice; failed hearts had both reduced ANP-dependent guanylyl cyclase activity and NPR-A protein levels compared to control hearts, indicating that NPR-A is downregulated in the failed heart. Consistent with the *in vivo* studies, cell culture experiments demonstrated that prolonged ANP exposure resulted in degradation of NPR-A in multiple cell lines. To investigate potential mechanisms involved in NPR-A downregulation, a novel antibody-based intracellular accumulation assay was developed. The assay revealed that NPR-A is basally internalized by a relatively slow clathrin- and dynamin-independent process that is stimulated by ANP. Dynamin inactivation increased intracellular accumulation of NPR-A at long, but not short, time periods after initiation of internalization, which is consistent with the notion of NPR-A recycling in a dynamin-dependent process. Surprisingly, the rate of NPR-A internalization was accelerated in clathrin-depleted cells. Understanding the molecular mechanisms underlying NPR-A downregulation will aid in

the development of potential therapeutic strategies that disrupt this process and prolong the beneficial compensatory effects of natriuretic peptides in patients with cardiovascular disease.

TABLE OF CONTENTS

LIST OF TABLES

LIST OF FIGURES

CHAPTER 1:

Introduction to Natriuretic Peptides and Natriuretic Peptide Receptors

History of Natriuretic Peptides

Decades before their contents or significance were appreciated, specific atrial granules were described in electron microscope studies of mammalian atrial cardiac muscle (Stenger and Spiro, 1961; Jamieson and Palade, 1964). Adolfo de Bold became interested in these secretory-like differentiations found exclusively in the atria, and made it a personal challenge over the course of 12 years to unravel the functional nature of the atrial granules. In 1981, de Bold and colleagues reported that atrial, but not ventricular, extracts contained a blood pressure-lowering component that functions through its rapid and potent natriuretic (sodium excretion) and diuretic (water excretion) effects (de Bold *et al.*, 1981). This paper marked the discovery of the first natriuretic peptide. de Bold would later provide evidence suggesting that the specific atrial granules are a storage site for the newly identified natriuretic peptide (de Bold, 1982). Shortly after de Bold's landmark paper numerous groups purified and sequenced atrial peptides of various sizes with natriuretic, diuretic, and/or smooth muscle relaxing effects (Flynn *et al.*, 1983; Currie *et al.*, 1984; Forssmann *et al.*, 1984; Kangawa *et al.*, 1984). These peptides were given names such as atrial natriuretic factor, cardionatrin, cardiodilatin, and atriopeptin; however, current literature commonly refers to the peptide as atrial natriuretic peptide (ANP).

B-type natriuretic peptide (BNP) was the second member of the mammalian natriuretic peptide family to be identified. Because BNP was purified and sequenced from porcine brain, it was originally named brain natriuretic peptide (Sudoh *et al.*, 1988). However, subsequent studies have shown that BNP is more highly concentrated in cardiac tissue (Nakao *et al.*, 1990; Hosoda *et al.*, 1991). The third mammalian natriuretic peptide, C-type natriuretic peptide (CNP), was also purified and sequenced from porcine

brain (Sudoh *et al.*, 1990). Phylogenetic studies of the natriuretic peptide family revealed that ANP and BNP evolved from CNP gene duplication events; thus, CNP is the oldest member of the family (Inoue *et al.*, 2003).

Natriuretic Peptides

The mammalian natriuretic peptide family consists of three members: atrial natriuretic peptide (ANP), B-type natriuretic peptide (BNP), and C-type natriuretic peptide (CNP). ANP and BNP are referred to as the cardiac peptides in reference to their well-established role in maintaining cardiovascular homeostasis. All of the peptide hormones are structurally homologous, but genetically distinct; they are the product of separate genes, synthesized as preprohormones, and contain a 17 amino acid disulfide-linked ring that is required for biological activity (Figure 1). Degradation of the three natriuretic peptides occurs through either enzymatic degradation by neutral endopeptidase (NEP), a zinc-dependent enzyme expressed on the plasma membrane (Stephenson and Kenny, 1987; Kenny *et al.*, 1993), or binding to the natriuretic peptide clearance receptor (NPR-C). NPR-C controls local natriuretic peptide concentrations via constitutive receptor-mediated internalization and degradation (Nussenzveig *et al.*, 1990).

Atrial Natriuretic Peptide

The gene encoding human atrial natriuretic peptide (ANP), *NPPA*, is located on chromosome 1p36.21 and consists of 3 exons and 2 introns. Translation of mRNA produces a 151 amino acid polypeptide known as preproANP, and cleavage of the amino terminal signal sequence yields a 126 amino acid peptide called proANP. ProANP is the primary form of ANP stored in atrial granules (Thibault *et al.*, 1987), and upon release from the atrial granules proANP is cleaved by the transmembrane cardiac serine

protease corin into the biologically active 28 amino acid form of ANP (Yan *et al.*, 2000). The mature 28 amino acid form of ANP is identical in humans, chimpanzees, dogs, pigs, horses, and sheep. Replacement of the methionine with isoleucine at position 12 in mature human ANP yields mature rat ANP. The sequence of mature ANP is identical in rats, mice, and rabbits.

Atrial wall stretch resulting from increased intravascular volume is the primary stimulus for proANP release from atrial granules (Lang *et al.*, 1985; Edwards *et al.*, 1988); however, pressor hormones such as endothelin and angiotensin II have also been linked to proANP release (Thibault *et al.*, 1999). Upon secretion and cleavage, mature ANP enters the coronary sinus and is distributed via the circulation to target organs. Plasma ANP levels are approximately 10 fmol/ml in normal individuals, and are elevated under cardiovascular stress (Cody *et al.*, 1986). The plasma half-life of ANP is approximately 2 min in humans (Nakao *et al.*, 1986; Yandle *et al.*, 1986).

ANP is primarily expressed in the cardiac atria; however, it is also present at much lower concentrations in a variety of other tissues such as the cardiac ventricle, kidney, and lung (Sakamoto *et al.*, 1985; Gardner *et al.*, 1986). Deletion of the ANP gene in mice resulted in hypertension that was not correlated with dietary salt intake (John *et al.*, 1996). Mice deficient in corin, the cardiac protease that cleaves proANP into its biologically active form, had elevated proANP levels but no detectable ANP levels, and exhibited hypertension and cardiac hypertrophy (Chan *et al.*, 2005).

B-Type Natriuretic Peptide

NPPB, the gene encoding human B-type natriuretic peptide (BNP), is located on chromosome 1p36.2 and, similar to *NPPA*, it consists of 3 exons and 2 introns. PreproBNP is cleaved from 134 amino acids into 108 amino acids to yield proBNP.

Further cleavage by an unidentified protease produces the biologically active 32 amino acid form of human BNP. BNP has the lowest species homology of the natriuretic peptide family, thus the length of mature BNP between mammalian species varies. Mature BNP is 32 amino acids in length in humans and pigs, and is composed of 45 amino acids in rats and mice.

Although low levels of BNP are stored with ANP in atrial granules, the cardiac ventricle secretes the greatest amount of BNP. Ventricular BNP is not stored in granules. Instead, BNP synthesis is transcribed in response to cardiac wall stretch; the transcription factor GATA4 plays a role in regulating this process (Grepin *et al.*, 1994; Thuerauf *et al.*, 1994). Plasma concentrations of BNP are approximately 1 fmol/ml in normal individuals, or roughly $1/10^{th}$ of plasma ANP levels (Mukoyama *et al.*, 1991). Under cardiovascular stress, such as congestive heart failure, BNP serum levels are dramatically elevated, and these increasing levels are correlated with disease progression (Richards *et al.*, 1993b). Hence, BNP has become a powerful tool for the diagnosis and prognosis of cardiovascular disease (Richards *et al.*, 2004). Additionally, of the natriuretic peptides, BNP has the longest half-life in humans (approximately 20 min) and is most resistant to neutral endopeptidase degradation (Richards *et al.*, 1993a; Smith *et al.*, 2000).

Mice with targeted disruption of the BNP gene are normotensive and display ventricular fibrotic lesions that increase in size and number in response to ventricular pressure overload, suggesting a role for BNP in ventricular remodeling (Tamura *et al.*, 2000). BNP plasma levels were elevated up to 100-fold in transgenic mice overexpressing the BNP gene, and these mice had significantly lower blood pressure compared to their nontransgenic littermates (Ogawa *et al.*, 1994).

C-Type Natriuretic Peptide

The human gene encoding C-type natriuretic peptide (CNP), *NPPC*, consists of 2 exons and 1 intron located on chromosome 2. PreproCNP is made up of 126 amino acids and cleavage of the 23 amino acid signal sequence results in a 103 amino acid peptide known as proCNP. Mature CNP is processed into both a 53- and a 22-amino acid form. The mature 53 amino acid form of CNP is cleaved from proCNP by the endoprotease furin (Wu *et al.*, 2003); however, the protease responsible for further cleavage into the 22 amino acid form of CNP is unknown. Both forms of mature CNP similarly bind and activate their receptor, natriuretic peptide receptor-B (NPR-B) (Yeung *et al.*, 1996). Not only is CNP the most ancient member of the natriuretic peptide family, but it is also the most conserved between species. PreproCNP in chimpanzees, dogs, and rats has a homology of 99, 96, and 94%, respectively, compared to the human form. The 22 amino acid form of CNP is identical in humans, chimpanzees, dogs, pigs, horses, sheep, rats, and mice.

CNP is not stored in granules and, in endothelial cells, its secretion is upregulated by sheer stress and growth factors such as transforming growth factor (TGF)-β, tumor necrosis factor (TNF)-α, and interleukin (IL)-1 (Suga *et al.*, 1992b; Suga *et al.*, 1993; Chun *et al.*, 1997). Plasma concentrations of CNP are approximately 1 fmol/ml in normal individuals (Igaki *et al.*, 1996). In heart failure plasma CNP levels are elevated, although to a much lesser extent than ANP and BNP levels (Kalra *et al.*, 2003; Del Ry *et al.*, 2005; Charles *et al.*, 2006). The reported half-life of CNP in humans is 2.6 min (Hunt *et al.*, 1994).

CNP is the most highly expressed natriuretic peptide in the brain and is also highly expressed in chondrocytes and endothelial cells (Ogawa *et al.*, 1992; Suga *et al.*, 1992b;

Hagiwara *et al.*, 1994). Targeted disruption of the CNP gene in mice causes dwarfism and premature death; however, these effects are rescued with targeted expression of CNP in the growth plate chondrocytes (Chusho *et al.*, 2001). A spontaneous single nucleotide mutation in the CNP gene in the long bone abnormality (lbab) mouse results in dwarfism due to a reduced ability of CNP to bind and activate its receptor (Jiao *et al.*, 2007; Yoder *et al.*, 2008). In humans, separation of putative negative transcriptional regulators in the NPPC gene caused by a balanced translocation results in elevated CNP plasma levels and Marfornoid-like skeletal overgrowth (Bocciardi *et al.*, 2007; Moncla *et al.*, 2007).

Natriuretic Peptide Receptors

There are three known mammalian receptors that bind natriuretic peptides: natriuretic peptide receptor-A (NPR-A), natriuretic peptide receptor-B (NPR-B), and natriuretic peptide receptor-C (NPR-C). NPR-A and NPR-B are particulate (transmembrane) guanylyl cyclases, enzymes that catalyze the synthesis of the intracellular second messenger cGMP from GTP. Hence, they are also referred to as guanylyl cyclase-A (GC-A) and guanylyl cyclase-B (GC-B), respectively. NPR-C, commonly called the natriuretic peptide clearance receptor, lacks guanylyl cyclase activity.

Natriuretic Peptide Receptor-A

Natriuretic peptide receptor-A (NPR-A) is the principal receptor of ANP and BNP and exhibits natriuretic peptide selectivity in the order ANP ≥ BNP >> CNP (Bennett *et al.*, 1991; Suga *et al.*, 1992a). The human gene encoding NPR-A is located on chromosome 1q21-22 and consists of 22 exons and 21 introns (Lowe *et al.*, 1990; Takahashi *et al.*,

1998). The general structural topology of NPR-A consists of an extracellular ligand binding domain (~450 amino acids), a single hydrophobic membrane-spanning region (21 amino acids), and an intracellular domain (~570 amino acids) (Figure 2) (Lowe *et al.*, 1989; Pandey and Singh, 1990). The intracellular domain is further divided into a kinase homology domain (~280 amino acids), an amphipathic coiled-coil dimerization region (~40 amino acids), and a carboxyl-terminal guanylyl cyclase catalytic domain (~250 amino acids). NPR-A exists as a homodimer or homotetramer in its native state, and oligomerization is ligand-independent (Iwata *et al.*, 1991; Chinkers and Wilson, 1992). The receptor-to-ligand stoichiometry is 2:1 (Ogawa *et al.*, 2004).

There are three intramolecular disulfide bonds between Cys60 and Cys86, Cys164 and Cys213, and Cys423 and Cys432 in the extracellular domain of rat NPR-A, but no intermolecular disulfide bonds (Miyagi and Misono, 2000). The basic human NPR-A polypeptide is ~115 kDa; however, due to N-linked glycosylation of extracellular asparagine residues, NPR-A exhibits size heterogeneity when fractionated by SDS-PAGE (Lowe *et al.*, 1989; Lowe and Fendly, 1992). The effect of glycosylation on ligand binding is controversial (Lowe and Fendly, 1992; Koller *et al.*, 1993; Heim *et al.*, 1996; Miyagi *et al.*, 2000). Under basal conditions, rat NPR-A is phosphorylated on at least four serine (Ser497, Ser502, Ser506, and Ser510) and two threonine (Thr500 and Thr513) residues located within the kinase homology domain (Potter and Hunter, 1998b). Additional phosphorylation sites are likely in NPR-A since its sea urchin homolog contains approximately 18 moles of phosphate per mole of receptor (Vacquier and Moy, 1986). Phosphorylation is essential for activation of NPR-A and ligand-induced dephosphorylation causes desensitization of the receptor (Potter and Garbers, 1992;

Potter and Hunter, 1998b). The kinase or kinases that phosphorylate NPR-A have not been identified.

NPR-A and/or its mRNA is expressed in adipose, adrenal, brain, heart, kidney, lung, testis, and vascular smooth muscle tissue (Lowe *et al.*, 1989; Wilcox *et al.*, 1991; Nagase *et al.*, 1997; Goy *et al.*, 2001). NPR-A null mice exhibit chronic salt-resistant hypertension and cardiac hypertrophy and fibrosis (Lopez *et al.*, 1995; Oliver *et al.*, 1997; Kuhn *et al.*, 2002). A deletion in the human NPR-A gene was identified in nine Japanese individuals; eight individuals had essential hypertension and the normotensive individual with the deleted allele had left ventricular hypertrophy (Nakayama *et al.*, 2000).

Natriuretic Peptide Receptor-B

Natriuretic peptide receptor-B (NPR-B) is the principal receptor of CNP and exhibits natriuretic peptide selectivity in the order CNP >> ANP ≥ BNP (Bennett *et al.*, 1991; Koller *et al.*, 1991; Suga *et al.*, 1992a). The human NPR-B gene consists of 22 exons and 21 introns and is located on chromosome 9p12-21 (Lowe *et al.*, 1990; Rehemudula *et al.*, 1999). Several splice variants of NPR-B have been identified; the relative expression levels of these isoforms vary across tissues and may help to regulate full-length NPR-B (Hirsch *et al.*, 2003; Tamura and Garbers, 2003). The structural topology of NPR-B is similar to NPR-A (Figure 2). Rat NPR-B has a 43% and 78% amino acid sequence identity to the extracellular and intracellular domains, respectively, of rat NPR-A (Schulz *et al.*, 1989).

NPR-B exhibits similar glycosylation and intramolecular disulfide bonding patterns as NPR-A. Mutagenesis-based studies using rat NPR-B are consistent with the presence of intramolecular disulfide bonds between Cys53 and Cys79, Cys205 and Cys314, and Cys417 and Cys426 (Langenickel *et al.*, 2004). Like NPR-A, NPR-B is also regulated by

phosphorylation and five phosphorylation sites (Thr513, Thr516, Ser518, Ser523, and Ser526) have been reported within the amino-terminal portion of the kinase homology domain (Potter and Hunter, 1998a).

NPR-B and/or its mRNA is expressed in bone, brain, fibroblast, heart, kidney, lung, ovarian, uterine, and vascular smooth muscle tissue (Chrisman *et al.*, 1993; Langub *et al.*, 1995; Herman *et al.*, 1996; Nagase *et al.*, 1997; Yamashita *et al.*, 2000; Hirsch *et al.*, 2003; Dickey *et al.*, 2007). Targeted disruption of the NPR-B gene in mice resulted in dwarfism due to impaired endochondral ossification, female sterility, and neuronal disorders (Tamura *et al.*, 2004). The achondroplastic (cn/cn) mouse has a spontaneous mutation in NPR-B resulting from a T to G transversion that leads to the substitution of a highly conserved leucine with arginine in the guanylyl cyclase domain; this mutation inactivates the enzyme (Tsuji and Kunieda, 2005). Mice with two defective alleles display dwarfism due to disrupted endochondral ossification. NPR-B dominant negative mutant transgenic rats displayed long bone growth retardation as well as progressive, blood pressure-independent cardiac hypertrophy and an elevated heart rate (Langenickel *et al.*, 2006). A homologous loss-of-function mutation in human NPR-B results in a rare autosomal recessive skeletal dysplasia known as acromesomelic dysplasia, type Maroteaux (AMDM) (Bartels *et al.*, 2004). Individuals with one defective NPR-B allele are statistically shorter than the average person (Olney *et al.*, 2006).

Natriuretic Peptide Receptor-C

Natriuretic peptide receptor-C (NPR-C) binds all three mammalian natriuretic peptides and exhibits natriuretic peptide selectivity in the order ANP > CNP ≥ BNP (Bennett *et al.*, 1991; Suga *et al.*, 1992a). Compared to NPR-A and NPR-B, NPR-C has much less stringent specificity for structural variants of ANP and will bind with high

affinity to the ring-deleted ANP analog C-ANP(4-23) (Maack *et al.*, 1987). Osteocrin, an endogenous protein with well-conserved homology to members of the natriuretic peptide family, binds specifically and saturably to NPR-C, but not NPR-A or NPR-B (Moffatt *et al.*, 2007). Osteocrin may act to modulate the actions of the natriuretic peptide system in bone by blocking the clearance action of NPR-C, thus increasing local CNP levels (Moffatt *et al.*, 2007). The human NPR-C gene is located on chromosome 5p13-14 and contains 8 exons and 7 introns (Lowe *et al.*, 1990; Rahmutula *et al.*, 2002). A splice variant of NPR-C containing an additional cysteine residue has been identified and characterized (Mizuno *et al.*, 1993). The structural topology of NPR-C consists of an extracellular ligand binding domain (~440 amino acids) with ~30% sequence identity to NPR-A and NPR-B, a single membrane-spanning region, and a 37 amino acid intracellular domain (Figure 2) (Fuller *et al.*, 1988). In contrast to NPR-A and NPR-B, NPR-C lacks enzymatic guanylyl cyclase activity.

Human NPR-C has a molecular weight of ~68 kDa and exists as a homodimer (Stults *et al.*, 1994). Unlike NPR-A and NPR-B, human NPR-C has intermolecular disulfide bonds involved in homodimer formation at Cys428 and Cys431; only one intermolecular disulfide bond was identified at Cys469 in bovine NPR-C (Itakura *et al.*, 1994; Stults *et al.*, 1994). The extracellular domain of human NPR-C is glycosylated at three sites (Asn41, Asn248, and Asn349) and contains two intramolecular disulfide bonds between Cys63 and Cys91 and Cys168 and Cys216 (Stults *et al.*, 1994). NPR-C was reported to be phosphorylated exclusively on serine residues in the intracellular domain (Pedro *et al.*, 1998).

The main function of NPR-C, also known as the clearance receptor, is to clear circulating natriuretic peptides through receptor-ligand internalization, extensive receptor

recycling, and lysosomal hydrolysis of ligand (Nussenzveig *et al.*, 1990). Internalization of NPR-C occurs in the absence of ligand (Nussenzveig *et al.*, 1990). In other words, it internalizes in a constitutive manner. Hypertonic sucrose, which disrupts clathrin-mediated endocytosis through clathrin disassembly, reduced NPR-C internalization, consistent with endocytosis occurring via clathrin-coated pits (Cohen *et al.*, 1996). Although NPR-C has no known enzymatic activity, it has been reported to couple to inhibitory G proteins to cause inhibition of adenylyl cyclase and activation of phospholipase-C (Anand-Srivastava, 2005; Rose and Giles, 2008).

NPR-C is the most widely and abundantly expressed natriuretic peptide receptor; in endothelial cells NPR-C constitutes ~94% of the total ANP binding sites (Leitman *et al.*, 1986). NPR-C and/or its mRNA is expressed in adrenal, brain, heart, kidney, lung, mesentery, placenta, and vascular smooth muscle tissue (Porter *et al.*, 1990; Wilcox *et al.*, 1991; Suga *et al.*, 1992c; Nagase *et al.*, 1997). Mice with targeted inactivation of both NPR-C alleles by homologous recombination exhibit long bone overgrowth, hypotension, mild diuresis, reduced ability to concentrate urine, and blood volume depletion (Matsukawa *et al.*, 1999). Three different mice strains that contain loss-of-function mutations in the extracellular domain of NPR-C have been identified; all three strains display skeletal overgrowth from endochondral ossification defects (Jaubert *et al.*, 1999).

Physiological Effects of Natriuretic Peptides

Natriuretic peptides and their receptors mediate a diverse array of physiological effects ranging from blood pressure regulation to lipolysis to endochondral ossification. Activation of the transmembrane guanylyl cyclases NPR-A and NPR-B by their respective ligands generates the intracellular second messenger cGMP. cGMP locally

amplifies the natriuretic peptide signal and interacts with downstream cGMP binding effectors to elicit a physiological response. There are three known cGMP binding proteins: cGMP-dependent protein kinases (PKG), cGMP binding phosphodiesterases, and cyclic nucleotide-gated ion channels.

Physiological Effects of Natriuretic Peptide Receptor-A

Since the original report from de Bold and colleagues describing the discovery of ANP, the ANP/NPR-A pathway has been shown to regulate normal homeostatic blood pressure. In mice lacking ANP or NPR-A blood pressure is elevated 20-40 mm mercury (John *et al.*, 1995; Lopez *et al.*, 1995; Oliver *et al.*, 1997). Conversely, transgenic mice overexpressing ANP or BNP have significantly lower than normal blood pressures (Steinhelper *et al.*, 1990; Ogawa *et al.*, 1994). Another group reported that NPR-A gene dosage over a range of 0 to 4 alleles influenced ANP-dependent guanylyl cyclase activity and blood pressure in a dose-dependent manner; thus, mice with additional alleles had higher guanylyl cyclase activities and lower blood pressures (Oliver *et al.*, 1998).

NPR-A regulates blood pressure through natriuresis and diuresis, vasorelaxation, increased endothelium permeability, and antagonism of the renin-angiotensin-aldosterone system. To cause natriuresis and diuresis, ANP increases the glomerular filtration rate, inhibits sodium and water reabsorption, and reduces renin secretion in the kidney (Potter *et al.*, 2006). The natriuresis, diuresis, and vasorelaxation responses to ANP and/or BNP require NPR-A because the effects of ANP are completely lost in NPR-A deficient mice (Kishimoto *et al.*, 1996; Lopez *et al.*, 1997). The natriuretic and diuretic effects of ANP are not required for ANP-dependent vascular volume constriction because it precedes urination and occurs in nephrectomized rats; instead, ANP-dependent vascular volume constriction results from the ability of ANP to increase

endothelium permeability (Almeida *et al.*, 1986; Richards *et al.*, 1988). Mice with endothelium-restricted deletion of the NPR-A gene exhibit significant arterial hypertension, cardiac hypertrophy, and increased plasma volume (Sabrane *et al.*, 2005). It is estimated that approximately a third of the total hypotensive effects of ANP are due to the presence of NPR-A in the vascular endothelium (Sabrane *et al.*, 2005).

NPR-A is also a regulator of cardiac hypertrophy and remodeling. Mice lacking ANP or NPR-A have enlarged hearts (John *et al.*, 1995; Oliver *et al.*, 1997; Franco *et al.*, 1998), whereas the heart size is reduced by 27% in mice overexpressing ANP (Barbee *et al.*, 1994). Chronic hypertension can cause cardiac hypertrophy; however, NPR-A null mice chronically treated with antihypertensive drugs still have enlarged hearts (Knowles *et al.*, 2001). Cardiac hypertrophy was inhibited in NPR-A null mice with transgenic over-expression of NPR-A in their cardiomyocytes, yet blood pressure was not reduced in these mice despite the reduced cardiomyocyte size (Kishimoto *et al.*, 2001). Conversely, mice with cardiomyocyte-restricted NPR-A deletion exhibited mild cardiac hypertrophy and reduced blood pressure (Holtwick *et al.*, 2003). Meanwhile, mice with targeted disruption of BNP have increased ventricular fibrosis, but no signs of hypertension or cardiac hypertrophy (Tamura *et al.*, 2000). Based on these genetic studies in mice, activation of NPR-A by ANP inhibits cardiac hypertrophy, whereas BNP-dependent activation of NPR-A inhibits cardiac fibrosis.

More recently a role for NPR-A activation in lipolysis has emerged. ANP-dependent cGMP elevations had been reported in rat adipose tissue since the 1980s; however, more than a decade elapsed before ANP was shown to stimulated lipolysis in both isolated human fat cells and in situ in the abdominal subcutaneous adipose tissue of healthy individuals (Okamura *et al.*, 1988; Jeandel *et al.*, 1989; Sengenes *et al.*, 2000).

Later ANP-induced lipolysis was determined to be specific to primates (Sengenes *et al.*, 2002). NPR-A activation has been reported to stimulate lipolysis via a cGMP-dependent protein kinase (PKG) pathway independent of cAMP production and cAMP-dependent protein kinase (PKA) activity (Sengenes *et al.*, 2003). Activation of the PKG isoform PKGI by ANP induces phosphorylation of hormone-sensitive lipase, an enzyme that hydrolyzes triglycerides into free fatty acids (Sengenes *et al.*, 2003).

Physiological Effects of Natriuretic Peptide Receptor-B

Stimulation of long bone growth is the most obvious physiological effect of NPR-B activation. In vitro evidence demonstrated that chondrocytes exposed to CNP have elevated cGMP levels, and that in fetal mouse tibia cultures endochondral ossification is stimulated by CNP (Hagiwara *et al.*, 1994; Yasoda *et al.*, 1998). Mice with targeted disruption of CNP or NPR-B developed post-partum dwarfism due to impaired endochondral ossification; growth plate histology of these mice revealed reduced endochondral proliferative and hypertrophic zones (Chusho *et al.*, 2001; Tamura *et al.*, 2004; Tsuji and Kunieda, 2005). Conversely, enlarged growth plates and skeletal overgrowth were observed in mice with transgenic overexpression of CNP or reduced CNP degradation from disruption of NPR-C (Jaubert *et al.*, 1999; Matsukawa *et al.*, 1999; Yasoda *et al.*, 2004). The CNP/NPR-B pathway partially mediates long bone growth through its downstream effector cGMP-dependent protein kinase II (PKGII), a PKG isoform. Mice or rats lacking functional PKGII are dwarfs and, in contrast to CNP or NPR-B deficient mice, have an expanded growth plate (Pfeifer *et al.*, 1996; Chikuda *et al.*, 2004).

Skeletal effects resulting from alteration of the CNP/NPR-B pathway have been reported in humans as well. Individuals with a rare form of dwarfism known as

acromesomelic dysplasia, type Maroteaux (AMDM) have two loss-of-function alleles for NPR-B (Bartels *et al.*, 2004). Birth lengths and weights are normal in AMDM individuals; however, a year or more after birth the disproportionate limb-to-torso ratio characteristic of AMDM becomes obvious (Bartels *et al.*, 2004). Heterozygous mutations in NPR-B are associated with short stature and do not alter body proportions (Olney *et al.*, 2006). A balanced t(2;7)(q37.1;q21.3) translocation, which separates putative negative regulatory elements in the NPPC gene, was identified in individuals with Marfornoid-like skeletal overgrowth and abnormally elevated CNP plasma concentrations (Bocciardi *et al.*, 2007; Moncla *et al.*, 2007).

Growing evidence supports a role for the CNP/NPR-B pathway in the cardiovascular system. CNP is secreted from vascular endothelial cells, and secretion is enhanced in the presence of important regulators of vascular remodeling (Suga *et al.*, 1992b; Suga *et al.*, 1993). In the vasculature, CNP causes vasorelaxation, inhibits vascular smooth muscle proliferation, and inhibits vascular smooth muscle migration (Furuya *et al.*, 1991; Drewett *et al.*, 1995; Kohno *et al.*, 1997). CNP also suppresses intimal growth caused by vascular injury (Shinomiya *et al.*, 1994; Takeuchi *et al.*, 2003; Schachner *et al.*, 2004). Infusion of supraphysiological concentrations of CNP into dogs caused a decrease in blood pressure with no natriuresis effect (Clavell *et al.*, 1993b); however, mice lacking NPR-B are normotensive suggesting that the CNP/NPR-B pathway is not a fundamental regulator of basal blood pressure in these animals (Tamura *et al.*, 2004). Transgenic rats expressing a dominant negative mutant of NPR-B have a normal lifespan and renal function, but exhibited reduced overall length, elevated heart rate, and progressive, blood pressure-independent cardiac hypertrophy (Langenickel *et al.*, 2006). The hypertrophic phenotype was further enhanced upon the induction of congestive heart

failure (Langenickel *et al.*, 2006). Cardiomyocyte-restricted overexpression of CNP in mice prevented cardiac hypertrophy following myocardial infarction (Wang *et al.*, 2007).

Cardiac Natriuretic Peptides and Cardiovascular Disease

Cardiovascular disease is defined as a disease affecting the heart or blood vessels, and includes diseases such as coronary heart disease, heart failure, hypertension, and stroke. According to the American Heart Association, it is estimated that one out of every three American adults has at least one form of cardiovascular disease. Natriuretic peptides are beneficial endogenous regulators of cardiovascular homeostasis, and imbalances in the natriuretic peptide system are associated with cardiovascular disease. The plasma concentrations of natriuretic peptides are low in healthy individuals; however, under hemodynamic stress, natriuretic peptide levels rise dramatically and increases are correlated with disease progression (Burnett *et al.*, 1986; Richards *et al.*, 1986; Richards *et al.*, 1993b). Amino-terminal fragments of proANP and proBNP are also elevated in the plasma in cardiovascular disease (Hunt *et al.*, 1997; Ruskoaho, 2003).

Increased ANP and BNP plasma levels result from increased atrial and ventricular wall stretch, increased synthesis, renal impairment, and activation of autocrine and paracrine regulatory factors. ANP and BNP synthesis are increased within both the atrial and ventricular myocardium under chronic hemodynamic stress (de Bold *et al.*, 1996). In healthy individuals low levels of ANP are released from the cardiac ventricles; however, in individuals with dilated cardiomyopathy, ANP secretion from the left ventricle was significantly increased (Yasue *et al.*, 1989). Conversely, BNP is primarily concentrated in the ventricle in healthy individuals; however, individuals with left ventricular hypertrophy released significant amounts of BNP from the atrial myocardium, and atrium-derived

BNP was found to contribute significantly to the total elevated BNP levels (Murakami *et al.*, 2002). In addition to mechanical wall stretch, ANP and BNP gene expression and release are influenced by endothelin-1 and angiotensin II (McDonough *et al.*, 1993; Bruneau *et al.*, 1997; Leskinen *et al.*, 1997; Liang and Gardner, 1998).

Of the natriuretic peptides, BNP exhibits the greatest proportional increase in disease states (Ruskoaho, 2003). Studies indicate that BNP is also the superior diagnostic marker of left ventricular systolic dysfunction, left ventricular diastolic dysfunction, and left ventricular hypertrophy (Yamamoto *et al.*, 1996; Maeda *et al.*, 1998). Thus, BNP has become an important tool for the screening, diagnosis, prognosis, and management of cardiovascular disease. Immunoassays measuring the levels of BNP or proBNP have been approved in the United States by the Food and Drug Administration and are commonly used clinically.

Not only are natriuretic peptides used as diagnostic and prognostic tools, but their synthetic versions are approved for the treatment of heart failure. A synthetic 25 amino acid peptide lacking the first three amino-terminal residues of mature ANP is known as anaritide. Synthetic full length ANP is called carperitide, and in 1995 it was approved for the treatment of acute decompensated heart failure in Japan. Infusion of anaritide in healthy male individuals resulted in natriuresis, diuresis, and reduced systolic blood pressure; however, the change in natriuresis and diuresis was minimal in individuals with congestive heart failure (Cody *et al.*, 1986). Similar renal hyporesponsiveness was observed in congestive heart failed patients infused with the 28 amino acid form of ANP (Saito *et al.*, 1987). Studies investigating the effectiveness of anaritide in the treatment of renal disease indicated no significant benefit of anaritide in dialysis-free survival or

reduction of dialysis, and commented on the severe hypotension resulting from anaritide infusion (Allgren *et al.*, 1997; Lewis *et al.*, 2000).

Synthetic BNP is known as nesiritide, and in 2001 it was approved in the United States under the trade name Natrecor for the treatment of acute decompensated heart failure. Nesiritide, marketed as Noratak, became commercially available in Switzerland and Israel in 2003. Initial studies, which likely lead to approval of nesiritide, reported that BNP increased natriuresis, vasodilation, stroke volume, and cardiac output in both healthy and heart-failed individuals (McGregor *et al.*, 1990; Yoshimura *et al.*, 1991; Mills *et al.*, 1999). The drug quickly came under scrutiny after two meta-analysis studies indicated that patients receiving nesiritide therapy had increased mortality and worsened renal function (Sackner-Bernstein *et al.*, 2005a; Sackner-Bernstein *et al.*, 2005b). However, other studies suggest that nesiritide has no detrimental effect on renal function and does not increase patient mortality (Arora *et al.*, 2006; Witteles *et al.*, 2007; Yancy *et al.*, 2007). Current natriuretic peptide drug development is focused on novel designer natriuretic peptides. Designer natriuretic peptides are hybrid peptides engineered from the native natriuretic peptides through amino acid addition, deletion, or substitution. These hybrid peptides aim to preserve the favorable cardiorenal effects of the native natriuretic peptides while minimizing the undesirable systemic hypotension, and hold promise as a new generation of therapeutics for cardiorenal disease (Lee *et al.*, 2009).

Despite the significant elevation of plasma ANP and BNP levels under cardiovascular stress, their cardioprotective physiological responses are blunted. In patients with congestive heart failure and a dog model of congestive heart failure the renal responses to ANP and BNP are attenuated (Cody *et al.*, 1986; Clavell *et al.*, 1993a). Explanations for the blunted response include: reduced bioactivity of ANP and

BNP (Hawkridge *et al.*, 2005), increased local degradation of ANP and BNP (Iervasi *et al.*, 1995; Andreassi *et al.*, 2001; Knecht *et al.*, 2002), decreased NPR-A guanylyl cyclase activity (Tsutamoto *et al.*, 1993; Bryan *et al.*, 2007), and increased cGMP degradation (Valentin *et al.*, 1992; Margulies and Burnett, 1994; Supaporn *et al.*, 1996). Decreased NPR-A guanylyl cyclase activity may be a result of receptor dephosphorylation and/or increased NPR-A degradation (Tsutamoto *et al.*, 1993; Singh *et al.*, 2006; Bryan *et al.*, 2007). Despite the growing evidence for NPR-A downregulation *in vivo*, there is not a consistent consensus that NPR-A is downregulated in cell culture systems in response to prolonged exposure to cardiac natriuretic peptides.

Internalization and Degradation of Natriuretic Peptide Receptor-A

Ligand-mediated internalization and degradation is a mechanism for terminating receptor-mediated signaling from the cell surface and has important physiological and pathophysiological consequences. It is widely accepted that NPR-C is constitutively internalized and recycled back to the cell surface (Nussenzveig *et al.*, 1990); however, the internalization and degradation of NPR-A, as well as NPR-B, is controversial. Previous reports on NPR-A internalization and degradation stem from ^{125}I-ANP binding studies where the ^{125}I-ANP-NPR-A complex is followed. Unfortunately, ^{125}I-ANP binding studies are subject to interpretation issues due to changing ligand-receptor binding affinities, difficulties in removing prior bound ANP from the receptor, and cells expressing two ANP receptors (NPR-A and NPR-C) (Schiffrin *et al.*, 1991; Jewett *et al.*, 1993).

Maack and colleagues reported that NPR-A is a membrane resident protein that neither internalizes itself at a detectable rate nor mediates internalization and lysosomal hydrolysis of ANP (Koh *et al.*, 1992). In rat glomerular mesangial and renomedullary

interstitial cells a rapid dissociation of ligand-receptor complexes was observed upon ^{125}I-ANP binding to endogenous NPR-A at physiological temperatures, but not at subphysiological temperatures (Koh *et al.*, 1992). The Maack group reported similar findings in Chinese hamster ovary cells transfected with wildtype NPR-A, and further found that deletion of the cytoplasmic domain of NPR-A dramatically slowed dissociation of the ligand-receptor complex and abolished the temperature-dependent dissociation of ANP (Vieira *et al.*, 2001). A separate group found that ANP binding to NPR-A stably expressed in 293 cells at 4°C was time-dependent, and concluded that the reduced binding over time was due to a diminished affinity of NPR-A for ANP and was not associated with receptor loss from the cell surface (Jewett *et al.*, 1993). Consistent with the previous reports, Fan and colleagues reported that the majority of ^{125}I-ANP bound to NPR-A overexpressed in 293T cells was rapidly released intact into culture medium when warmed from 4°C to 37°C (Fan *et al.*, 2005). Furthermore, this group found no evidence for NPR-A or NPR-B internalization or degradation in response to ligand binding despite the observed natriuretic peptide-dependent receptor desensitization (Fan *et al.*, 2005).

Meanwhile, other studies suggested an alternative fate for NPR-A. Exposure of rat vascular smooth muscle, PC-12, and HEK-293 cells to unlabelled ANP caused a time- and concentration-dependent loss of ^{125}I-ANP binding sites without any changes in the binding affinity, suggesting that NPR-A is downregulated (Cahill *et al.*, 1990; Rathinavelu and Isom, 1991; Pandey, 1992; Pandey *et al.*, 2002). 293 cells stably overexpressing NPR-A incubated with ANP for increasing time periods resulted in a biphasic decrease in hormone-dependent guanylyl cyclase activity; it was concluded that acute and chronic regulation of NPR-A occurs through receptor dephosphorylation and degradation

(downregulation), respectively (Potter and Hunter, 1999). Pandey and colleagues repeatedly demonstrated in a variety of cell lines expressing either endogenous or transfected NPR-A that ANP-NPR-A complexes are internalized at physiological temperatures, and that both intact and degraded ligand are released into culture medium (Pandey, 1992, 1993; Pandey *et al.*, 2002). In intact COS-7 cells expressing NPR-A with various deleted intracellular regions, receptor internalization and sequestration was reduced; the greatest impact on internalization occurred with deletion of both the intracellular kinase homology and guanylyl cyclase domains (Pandey *et al.*, 2000). A GDAY motif identified in the carboxyl-terminal domain of NPR-A was reported to regulate NPR-A internalization and trafficking; endocytosis of ANP-NPR-A complexes was reduced by almost 50% in transfected HEK-293 cells where the glycine and/or tyrosine residues in the GDAY motif of NPR-A were mutated to alanine (Pandey *et al.*, 2005).

Following receptor internalization and sequestration into subcellular compartments, NPR-A is thought to diverge into either a recycling or degradation pathway (Rathinavelu and Isom, 1991; Pandey, 1992, 1993; Pandey *et al.*, 2002). Pandey and colleagues reported that in HEK-293 cells overexpressing NPR-A ~70-80% of internalized ^{125}I-ANP is processed through a lysosomal degradative pathway, whereas 20-25% of internalized ^{125}I-ANP is released intact into the cell medium via a retroendocytotic pathway (Pandey *et al.*, 2002). NPR-A recycling was disrupted by the lysosomotrophic agent chloroquine and the metabolic inhibitor dinitrophenol, which depletes cellular ATP, suggesting that NPR-A recycling is energy-dependent (Pandey, 1993; Pandey *et al.*, 2002). Although some groups have reported internalization, degradation, and recycling of NPR-A, the molecular mechanisms and trafficking pathways involved are virtually unexplored.

The research presented in the following chapters began as a continuation of our group's studies characterizing natriuretic peptide receptor guanylyl cyclase activity and phosphorylation and protein levels *in vi*vo during cardiovascular disease. The initial report from our group found that the renal hyporesponsiveness to ANP in congestive heart-failed mice resulted from reduced NPR-A protein levels; thus, NPR-A is downregulated in the kidney of heart-failed mice (Bryan *et al.*, 2007). In Chapter 2, the initial report is followed up with studies of both NPR-A and NPR-B in the heart of congestive heart-failed mice, as well as patients with heart failure. In failed mouse hearts, NPR-A was downregulated and, interestingly, NPR-B accounted for the majority of natriuretic peptide-dependent guanylyl cyclase activity. Chapter 3 demonstrates that *in vivo* NPR-A downregulation can be replicated in various cell culture systems, and indicates that NPR-A downregulation is a universal property, but that it varies with receptor levels and cell type. The controversial topic of NPR-A internalization is addressed in the following chapter with a newly developed assay that utilizes antibody binding to an extracellular receptor epitope to measure intracellular accumulation of receptor. Furthermore, Chapter 4 explores two well-studied components of endocytic pathways to suggest that the majority of NPR-A internalization occurs through a novel clathrin- and dynamin-independent pathway.

Figure 1

Expression, structure, and processing of the human natriuretic peptides. Atrial natriuretic peptide (ANP), B-type natriuretic peptide (BNP), and C-type natriuretic peptide (CNP) are expressed in the indicated tissues listed on the left of each panel. The structure and processing of the natriuretic peptide preprohormones are outlined in the middle of each panel. The final amino acid sequence and structure of the mature peptides, along with the major degradation product, are on the right of each panel. The sites of cleavage are indicated with scissors, the disulfide bond is shown in black, and invariant amino acids within the ring structure are shaded. Figure modified from: Potter, L.R., Yoder, A.R., Flora, D.R., Antos, L.K., and Dickey, D.M. (2009). Natriuretic peptides: their structures, receptors, physiologic functions and therapeutic applications. Handb Exp Pharmacol, 341-366.

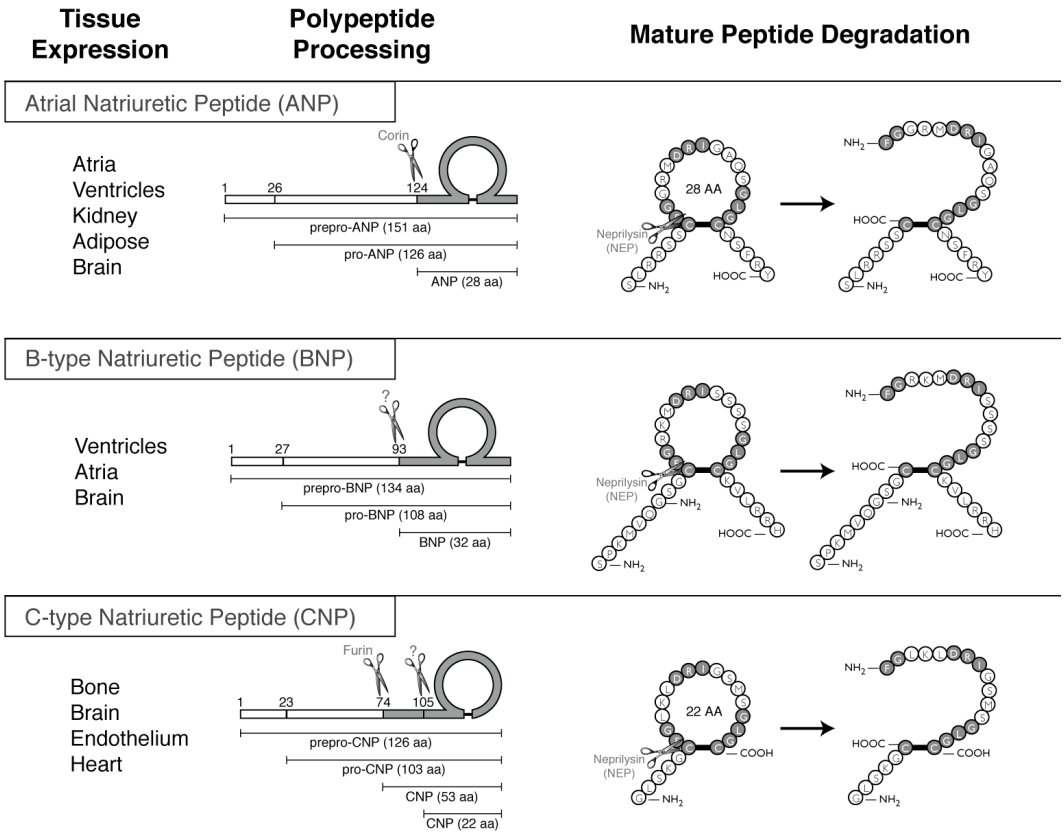
Tissue Expression
Polypeptide Processing
Mature Peptide Degradation
Atrial Natriuretic Peptide (ANP)
Atria
Ventricles
Kidney
Adipose
Brain
Corin
1
26
124
prepro-ANP (151 aa)
pro-ANP (126 aa)
ANP (28 aa)
28 AA
Neprilysin (NEP)
B-type Natriuretic Peptide (BNP)
Ventricles
Atria
Brain
?
1
27
93
prepro-BNP (134 aa)
pro-BNP (108 aa)
BNP (32 aa)
C-type Natriuretic Peptide (CNP)
Bone
Brain
Endothelium
Heart
Furin
?
1
23
74
105
prepro-CNP (126 aa)
pro-CNP (103 aa)
CNP (53 aa)
CNP (22 aa)
22 AA

Figure 2

Natriuretic peptide receptor ligand preferences and structural topology. Natriuretic peptide receptor-A (NPR-A), or guanylyl cyclase-A (GC-A), is activated by ANP and BNP, whereas natriuretic peptide receptor-B (NPR-B), or guanylyl cyclase-B (GC-B), is activated by CNP. Natriuretic peptide receptor-C (NPR-C) binds all three mammalian natriuretic peptides as well as osteocrin. NPR-A and NPR-B are transmembrane guanylyl cyclases consisting of an extracellular ligand binding domain, a single membrane-spanning region, and an intracellular kinase homology, dimerization, and catalytic guanylyl cyclase domain. NPR-C is ~30% identical to NPR-A and NPR-B in the extracellular ligand binding domain, but contains only 37 intracellular amino acids and lacks enzymatic guanylyl cyclase activity. Figure modified from: Potter, L.R., Abbey-Hosch, S., and Dickey, D.M. (2006). Natriuretic peptides, their receptors, and cyclic guanosine monophosphate-dependent signaling functions. Endocr Rev *27*, 47-72.

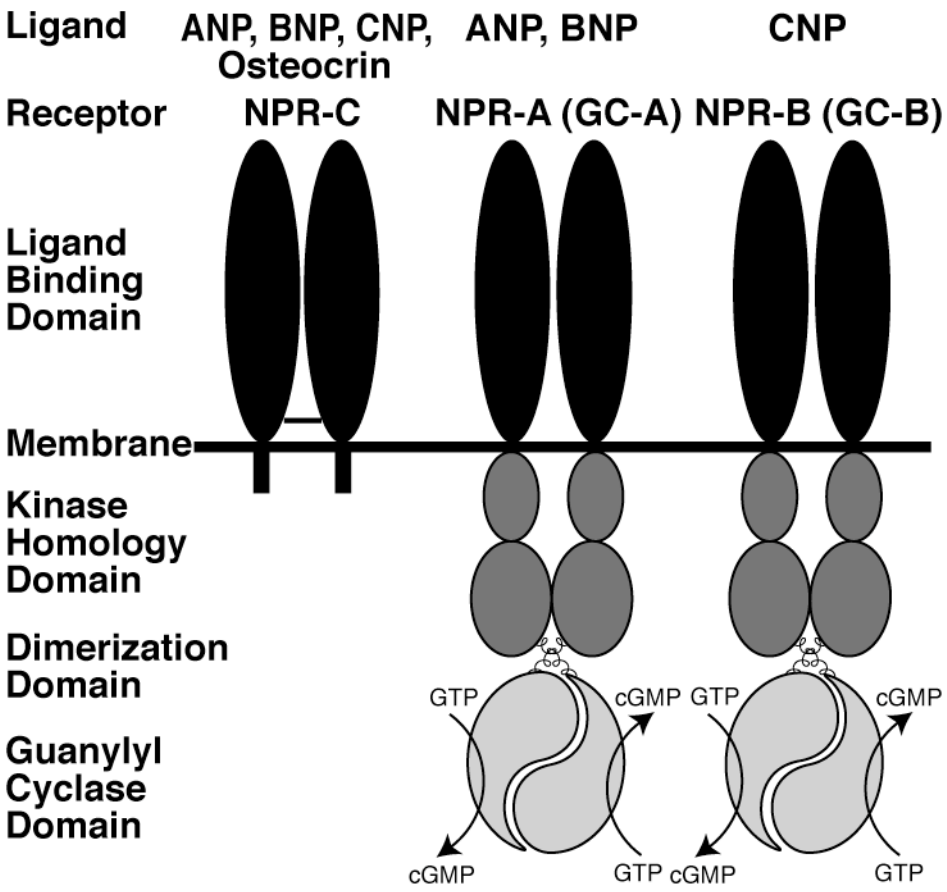
Ligand
ANP, BNP, CNP, Osteocrin
ANP, BNP
CNP
Receptor
NPR-C
NPR-A (GC-A)
NPR-B (GC-B)
Ligand Binding Domain
Membrane
Kinase Homology Domain
Dimerization Domain
Guanylyl Cyclase Domain
GTP
cGMP
GTP
cGMP
cGMP
GTP
cGMP
GTP

CHAPTER 2:

Differential Regulation of Membrane Guanylyl Cyclases in Congestive Heart Failure: Natriuretic Peptide Receptor (NPR)-A is Downregulated and Natriuretic Peptide Receptor-B, Not NPR-A, is the Predominant Natriuretic Peptide Receptor in the Failing Mouse Heart

This chapter is modified from:

Dickey, D.M., Flora, D.R., Bryan, P.M., Xu, X., Chen, Y., and Potter, L.R. (2007) Differential regulation of membrane guanylyl cyclases in congestive heart failure: natriuretic peptide receptor (NPR)-B, not NPR-A, is the predominant natriuretic peptide receptor in the failing heart. Endocrinology *148*, 3518-3522.

Disclosure

The research presented in Chapter 2 represents a collaborative effort. Deborah M. Dickey wrote the majority of the published article "Differential regulation of membrane guanylyl cyclases in congestive heart failure: natriuretic peptide receptor (NPR)-B, not NPR-A, is the predominant natriuretic peptide in the failing heart" on which Chapter 2 is based. The original text from the published article has been modified and additional information has been added by Darcy R. Flora to create Chapter 2. The following lists each contributor to the actual research as well as the contributions made:

Paula M. Bryan: Collection of Mouse Tissues, Preparation of Mouse Heart Membranes, NPR-A Protein Levels in Mouse Heart

Yingjie Chen: Aortic Banding of Mice, Echocardiographic Measurements in Mice

Deborah M. Dickey: Collection of Mouse Tissues, Preparation of Mouse Heart Membranes, Guanylyl Cyclase Activity in Mouse Heart, Preparation of Human Heart Membranes, Guanylyl Cyclase Activity in Human Heart

Dan Dries: Provided Human Heart Samples and Patient Information

Darcy R. Flora: Collection of Mouse Tissues, Preparation of Mouse Heart Membranes, NPR-B Protein Levels in Mouse Heart, Preparation of Human Heart Membranes, NPR Protein Levels in Human Heart

Ken Margulies: Provided Human Heart Samples and Patient Information

Xin Xu: Aortic Banding of Mice, Echocardiographic Measurements in Mice

Introduction

Three genetically distinct but highly similar natriuretic peptides exist in mammals: atrial natriuretic peptide (ANP), B-type natriuretic peptide (BNP), and C-type natriuretic peptide (CNP) (Potter *et al.*, 2006). ANP and BNP elicit their cardioprotective effects by binding and activating the cell surface guanylyl cyclase natriuretic peptide receptor-A (NPR-A), whereas CNP activates the homologous natriuretic peptide receptor-B (NPR-B) (Kuhn, 2003). All three natriuretic peptides also bind the natriuretic peptide clearance receptor, which chiefly controls the local concentrations of these peptides through receptor-mediated internalization and degradation (Maack, 1992; Matsukawa *et al.*, 1999). ANP and BNP are primarily released from the atria and ventricles of the heart, respectively, in response to cardiomyocyte stretch. The accepted production sites for CNP are endothelium, brain, and bone, but a role for CNP in the heart has been bolstered by studies showing increased CNP levels in patients with chronic heart failure in a manner that positively correlates with mean pulmonary capillary wedge pressure and degree of failure (Kalra *et al.*, 2003; Del Ry *et al.*, 2005).

Natriuretic peptides are endogenous diuretic and vasorelaxation factors. In healthy individuals, circulating ANP and BNP levels are low, but they rise dramatically in response to cardiovascular stress. In fact, recent studies indicate that increased BNP concentrations are a hallmark indicator of several cardiovascular diseases, including congestive heart failure (Gardner, 2003; Ruskoaho, 2003). In normal patients, elevated ANP and BNP levels activate NPR-A to decrease blood pressure by stimulating natriuresis, diuresis, vasorelaxation, and generally antagonizing the renin-angiotensin-aldosterone system. In contrast, the renal and renin effects of ANP are attenuated in animal models and patients with congestive heart failure despite marked serum ANP and

BNP concentrations (Cody *et al.*, 1986; Garcia *et al.*, 1992; Tsutamoto *et al.*, 1993; Supaporn *et al.*, 1996). Several possible explanations exist for the blunted natriuretic peptide response, including increased local natriuretic peptide degradation (Iervasi *et al.*, 1995; Knecht *et al.*, 2002), reduced bioactivity of ANP and BNP (Hawkridge *et al.*, 2005), increased degradation of cGMP (Valentin *et al.*, 1992; Margulies and Burnett, 1994), and decreased NPR-A guanylyl cyclase activity (Tsutamoto *et al.*, 1993).

Mice lacking ANP (John *et al.*, 1995) or NPR-A (Lopez *et al.*, 1995; Oliver *et al.*, 1997) are hypertensive and exhibit cardiac hypertrophy (Kishimoto *et al.*, 2001; Knowles *et al.*, 2001; Holtwick *et al.*, 2003). Mice lacking functional NPR-A display greater cardiac hypertrophy in response to pressure overload than wildtype animals (Knowles *et al.*, 2001), whereas the opposite is true for animals overexpressing a constitutively active form of NPR-A in the heart (Zahabi *et al.*, 2003). In contrast, mice lacking CNP (Chusho *et al.*, 2001) or NPR-B (Tamura *et al.*, 2004) are normotensive but have a decreased life span due to defective bone growth. To overcome the complications of reduced lifespan, Langenickel *et al.* used a transgenic dominant-negative approach to inhibit NPR-B but not NPR-A (Langenickel *et al.*, 2006). They found that the transgenic rats displayed reduced NPR-B guanylyl cyclase activity, progressive blood pressure-independent cardiac hypertrophy, and increased heart rate. The transgenic animals also displayed marked hypertrophy in response to pressure overload, which is consistent with previous data showing that CNP inhibits cardiomyocyte hypertrophy in culture (Tokudome *et al.*, 2004). Thus, recent data suggests that NPR-B may play a more important role in the regulation of cardiac hypertrophy than previously appreciated.

For the first time, we measured ANP/NPR-A-dependent and CNP/NPR-B-dependent guanylyl cyclase activities as well as determined NPR-A and NPR-B protein levels in

failed mouse and human ventricles. We found that CNP-dependent activity is only slightly less than the ANP-dependent activity in the normal mouse heart. However, in the failed mouse heart, ANP-dependent activity is markedly reduced, whereas CNP-dependent activity is statistically unchanged. Consistent with the trends in hormone-dependent activity, NPR-A and NPR-B protein levels are decreased and increased, respectively, in failed mouse hearts. Surprisingly, in the failed mouse heart, CNP-dependent activity is twice as high as ANP-dependent activity. The data from human hearts did not yield conclusive results; however, compared to the mouse data, similar trends in guanylyl cyclase activities are observed in the final, most complete, human heart trial. These data suggest that drugs designed to activate NPR-B alone or in combination with NPR-A may provide more effective cardiac therapy for congestive heart failure than the FDA-approved drug nesiritide, which activates only NPR-A.

Materials and Methods

Materials

Rat ANP, CNP, and microcystin LR were purchased from Sigma-Aldrich (St. Louis, MO). The cGMP RIA kit was purchased from PerkinElmer (Waltham, MA). All animal protocols were approved by the University of Minnesota Institutional Animal Care and Use Committee.

Human Heart Samples

Frozen human left ventricle samples from non-failed and failed hearts were obtained from Dan Dries and Ken Margulies (University of Pennsylvania; Philadelphia, PA). Each sample weighed approximately 2 g.

Aortic Banding of Mice

Male C57 black mice were anesthetized with a mixture of 80 mg/kg ketamine and 30 mg/kg xylazine intraperitoneally. The neck and upper chest were shaved, and a horizontal incision was made at the level of the suprasternal notch to allow direct visualization of the transverse aorta without entering the pleural space. Aortic constriction was performed by ligating the aorta between the right innominate artery and the left carotid arteries over a 26-gauge needle using 5-0 silk sutures and a dissecting microscope. The needle was then removed leaving the constriction in place, and the skin was closed. For control mice, sham surgeries were performed without constricting the aorta.

Echocardiographic Measurement

Echocardiography was performed in mice anesthetized with 1.5% isoflurane by inhalation. Left ventricular (LV) wall thickness, LV end-diastolic dimension (LVEDD), LV end-systolic dimension (LVESD), LV end-systolic wall thickness, and end-diastolic wall thickness were measured using two-dimensional echocardiography. LV ejection fraction (LVEF) was calculated by the cubic method: $LVEF = [(LVEDD)^3 – (LVESD)^3]/(LVEDD)^3 \times 100\%$. LV fractional shortening (FS) was calculated as: $FS = (LVEDD – LVESD)/LVEDD \times 100\%$.

Collection of Mouse Tissues

The mice were euthanized with a mixture of 80 mg/kg ketamine and 30 mg/kg xylazine intraperitoneally. Hearts were removed, trimmed of most of the atria, cleaned in sterile saline, weighed, and placed in ice-cold phosphatase inhibitor buffer (PIB) containing 25 mM HEPES (pH 7.4), 50 mM NaCl, 20% glycerol, 50 mM NaF, 2 mM EDTA, 0.5 μM microcystin LR, and 1.3X Complete protease inhibitors (Roche Diagnostics; Indianapolis, IN).

Membrane Preparation

Mouse and human heart samples were homogenized in phosphatase inhibitor buffer (PIB) and then centrifuged at 10,000 x g for 10 min at 4°C. The supernatant was removed, and the pellet was washed three times in PIB by resuspension and centrifugation. After the final wash, the samples were resuspended in PIB, and total protein concentrations were determined by the Bradford method. The protein concentrations of the membranes were normalized to 3.5 mg/ml and then used for cyclase determinations without freezing.

Guanylyl Cyclase Assay

Membrane fractions containing approximately 80 μg protein were assayed for guanylyl cyclase activity by addition of ATP/Mg^{2+} alone (for basal determination) or with ATP/Mg^{2+} plus 50 nM ANP (mouse only), 1 μM ANP, 50 nM or 100 nM CNP (mouse only), or 1 μM CNP. The receptor was stimulated by addition of 60 μl of cocktail containing 25 mM HEPES (pH 7.4), 50 mM NaCl, 0.1% BSA, 500 μM isobutylmethylxanthine (IBMX), 1 mM GTP, 5 mM $MgCl_2$, 5 mM creatine phosphate, and 0.1 mg/ml creatine kinase. Mouse and human membranes were assayed for 3 or 5 min, respectively. The reactions were stopped with 400 μl ice-cold 50 mM sodium acetate solution containing 5 mM EDTA. One fifth of the reaction was then removed and assayed for cGMP concentrations by RIA according to the manufacturer's instructions.

Immunoprecipitation and Immunoblotting

Mouse heart tissue homogenate was pooled into sham and banded groups, and each group was split in half (one half for peptide block). Human heart tissue homogenate was kept separate, and at least one sample was designated for the peptide block. Total protein concentrations were determined by the Bradford method. After normalizing for

total protein levels, tissue homogenate was pelleted by centrifugation at 10,000 x g for 10 min at 4°C. Each pellet was solubilized for 2 h at 4°C in 10 ml modified RIPA buffer containing 50 mM Tris-HCl (pH 7.5), 100 mM NaCl, 1% NP-40, 0.5% sodium deoxycholate, 0.1% SDS, 10 mM NaH_2PO_4, 50 mM NaF, 2 mM EDTA, 0.5 μM microcystin LR, and 2.5X Complete protease inhibitors. Solubilized mouse tissue was incubated twice for 30 min at 4°C with 500 μl protein A (RepliGen, Waltham, MA) and 30 μl rabbit serum, and human tissue was incubated twice for 30 min at 4°C with only 50 μl protein A. NPR-A was immunoprecipitated overnight at 4°C using 50 μl protein A and 2.3 or 7 μl (human and mouse, respectively) of polyclonal rabbit 6325 antiserum, which recognizes the last 17 carboxyl-terminal amino acids of rat NPR-A (Bryan *et al.*, 2007). The next day the protein A beads were pelleted by centrifugation and the supernatant was reserved for sequential immunoprecipitation of NPR-B using polyclonal rabbit 6328 antiserum, which recognizes the last 10 carboxyl-terminal amino acids of rat NPR-B. Protein A beads were washed three times with 1 ml of ice-cold RIPA buffer (the third wash without NaCl), boiled in 2X reducing sample buffer, fractionated by SDS-PAGE, and transferred to polyvinylidene fluoride (PVDF) membrane.

Primary antibodies for immunoblot analysis were polyclonal rabbit 6325 (1:2500) or 6328 (1:2500) to NPR-A or NPR-B, respectively (Abbey and Potter, 2002). Secondary antibody was peroxidase-conjugated donkey anti-rabbit IgG (1:20,000; GE Healthcare; Buckinghamshire, UK).

Quantification and Statistical Analysis

Immunoblots were quantified with ImageJ software. GraphPad Prism software was used for the statistical analysis of the data. Unpaired t tests were conducted to determine the

p values of the mean differences between sham or non-failed and banded or failed samples. Data are represented as mean ± SEM.

Results

Induction of Congestive Heart Failure in Mice

Transverse aortic constriction surgery was performed to induce heart failure in mice in two independent trials. The first trial was small and included 5 sham (control) and 5 banded mice. The second trial was much larger and included 18 sham and 20 banded animals. The banded and sham animals were evaluated 8 weeks after surgery in both trials. Echocardiography of anesthetized animals was performed to determine the degree of heart failure. All 10 of the animals in the first trial were analyzed. However, only eight sham and 10 banded animals were analyzed in the second trial. The parameters from both trials are summarized in Table 1. The banded animals displayed increased left ventricular (LV) anterior and posterior wall thicknesses, 50% reductions in mean ejection fractions, and a 62% reduction in LV shortening compared with sham-operated animals. Similarly, the systolic aortic pressure, mean aortic pressure, and LV systolic pressure were measured in four sham and six banded mice. The banding resulted in significantly increased systolic aortic pressure (94.8 ± 3.9 vs. 160 ± 17 mm Hg, $p < 0.05$), mean aortic pressure (82.4 ± 5.0 vs. 110 ± 10.5 mm Hg, $p < 0.05$), and LV systolic pressure (98.3 ± 3.7 vs. 163 ± 16 mm Hg, $p < 0.05$). Hence, the banded animals in both trials clearly progressed to overt heart failure as a result of the increased pressure induced by transverse aortic constriction.

After euthanizing the animals and removing their organs, cardiac hypertrophy was indicated by increased heart weights and increased heart weight-to-body weight ratios.

An increase in lung weight and the lung-to-body weight ratio, which is indicative of pulmonary edema due to congestive heart failure, was also evident in both trials, although the increased lung weight was not statistically significant in the second trial. In summary, animals that underwent the minimally invasive transaortic constriction procedure reached a stage of advanced heart failure after 8 weeks.

Cardiac NPR-A Activity is Reduced in Heart-Failed Mice

To determine the responsiveness of NPR-A to hormonal stimulation, we measured the guanylyl cyclase activities of heart membranes derived from sham or banded mice in the presence of 0 (basal), 50 nM, or 1 μM ANP. Fifty nanomolar ANP was chosen as the representative low dose of ANP; previous preliminary experiments had determined that using doses lower than 50 nM did not yield reproducible changes in cGMP production compared with basal levels. One micromolar ANP was used to represent saturating concentrations as our previous experience indicates that this dose elicits maximal hormone-stimulated activity. In the first trial, conversion of GTP into cGMP under basal conditions (no ANP) was not different in cardiac membranes obtained from the two groups (2.58 pmol/mg/min for sham vs. 2.59 pmol/mg/min for banded) (Figure 1A). However, cyclase activity in response to ANP was significantly reduced in the banded compared with the sham animals. ANP concentrations of 50 nM and 1 μM increased cyclase activity by 3.6- and 6.3-fold, respectively, in membranes from the sham animals. In contrast, the lower concentrations of ANP had no significant effect on cGMP production in membranes from banded animals, whereas the higher concentrations increased activity only 1.8-fold. The reduction in activity was statistically significant when analyzed using unpaired t tests with p values of 0.01 and 0.015 at 50 nM and 1 μl ANP concentrations, respectively.

When this experiment was repeated using a larger sample size, we observed very similar data (Figure 1B). In this study, activities were elevated 10- and 13.6-fold by 50 nM and 1 μM concentrations of ANP in sham membranes, whereas the same hormone conditions elevated cGMP levels by only 2.5- and 4-fold, respectively, in membranes from the heart-failed animals. The p values were < 0.0001 for both concentrations of ANP. The basal activities were not statistically different (2.21 pmol/mg/min for sham vs. 3.00 pmol/mg/min for banded). These data clearly demonstrate that ANP-dependent guanylyl cyclase activity is dramatically reduced in the hearts from mice with congestive heart failure.

NPR-B, Not NPR-A, is the Most Active NPR in the Failed Mouse Heart

Because NPR-B was recently shown to inhibit cardiac hypertrophy in rats (Langenickel *et al.*, 2006), we investigated the contribution of NPR-B to the natriuretic peptide-dependent guanylyl cyclase response in hearts from the sham and banded mice. We found that 100 nM and 1 μM concentrations of CNP increased guanylyl cyclase activities 2.6- and 4.7-fold in membranes from sham animals, and the maximal concentration of CNP elevated cGMP levels to 74% of the levels elicited by the maximal ANP concentration (Figure 1A). However, in contrast to the ANP scenario, the CNP-dependent responses were not decreased in preparations from heart-failed animals. In fact, the CNP-dependent responses were increased to 2.9- and 5.7-fold, respectively, in membranes from the banded hearts, although the differences were not statistically significant. Importantly, the fact that the CNP responses are increased or unchanged when the ANP responses are decreased clearly indicates that the CNP-dependent activity is not due to cross-activation of NPR-A.

When the experiment was repeated with more animals, we observed similar CNP-dependent increases in particulate guanylyl cyclase activities at the two different concentrations in cardiac membranes from sham animals (Figure 1B). Maximum CNP-dependent activity accounted for 67% of maximum ANP response. Again, guanylyl cyclase activities measured under identical conditions in membranes from the banded animals were slightly, but not significantly, increased ($p = 0.13$ for 50 nM and 0.34 for 1 μM CNP). Maximal CNP-dependent activity was about twice that of maximal ANP-dependent activity in the failed heart. Hence, although NPR-A and NPR-B account for similar amounts of natriuretic peptide-dependent particulate guanylyl cyclase activity in the normal mouse heart, NPR-B, not NPR-A, accounts for the majority of natriuretic peptide-dependent activity in the failed mouse heart.

Differential Regulation of NPR-A and NPR-B Protein Levels in the Failed Mouse Heart

To determine if the changes in ANP- and CNP-dependent guanylyl cyclase activity in failed mouse hearts could be explained by changes in receptor protein levels, we measured NPR-A and NPR-B protein levels in cardiac membranes by immunoprecipitation-immunoblot analysis (Figure 2). Previous experiments had determined that NPR protein levels were below the limit of detection in heart membranes from one mouse; thus, cardiac NPR protein levels were only determined in the larger second trial where membranes from multiple mouse hearts could be combined. A caveat to pooling the mouse hearts was that each condition had a N of 1, which made statistically significant distinctions between groups impossible to determine. Furthermore, high background staining in the NPR-A immunoblot made interpretation difficult. Nevertheless, initial data are consistent with reduced protein levels in hearts from banded mice compared to sham mouse hearts (Figure 2, A and C). Meanwhile,

NPR-B concentrations appeared to be elevated in the banded compared to the sham animals (Figure 2, B and C). These limited data are consistent with the decreased ANP-dependent and slightly increased CNP-dependent guanylyl cyclase activities observed in heart-failed mice.

Guanylyl Cyclase Activities and Protein Concentrations of NPR-A and NPR-B in Failed Human Hearts

Since we observed differential regulation of NPR-A and NPR-B in a mouse model of congestive heart failure and biomedical research is aimed at improving human health, we examined NPR-A and NPR-B in the left ventricle of patients with non-failed and failed hearts. Samples from 35 individuals were tested for guanylyl cyclase activity and/or protein levels over the course of three separate trials; several individuals were tested in more than one trial. Sample information from all three trials is summarized in Table 2. All of the failed samples in the third trial were from individuals with dilated heart failure. The mean left ventricular ejection fraction was 12% and 61% in failed and non-failed hearts, respectively, in this trial.

Although guanylyl cyclase activities were measured in all three trials (Figure 3), the first two trials lacked a sufficient number of non-failed samples for statistical analysis. In all three trials, basal guanylyl cyclase activities from failed hearts were slightly elevated compared to non-failed hearts, and in the third trial this elevation was determined statistically significant at a p value of 0.02. It is possible that the elevated basal levels result from residual ANP and BNP contained in the heart samples from heart-failed patients. ANP-dependent guanylyl cyclase activity was increased in failed membranes in the first trial; however, this activity was reduced in the subsequent studies. The ANP-dependent activities in the third trial were not statistically different (2.327 pmol/mg/min

for non-failed vs. 2.086 pmol/mg/min for failed). Similar to the mouse studies, CNP-dependent responses in all three human trials were increased in heart-failed samples by 1.4-, 1.1-, and 1.3-fold, respectively. Nevertheless, the CNP-dependent increase observed in the third trial from 3.953 pmol/mg/min in non-failed samples to 5.205 pmol/mg/min in failed samples was not significant ($p = 0.09$). Thus, no statistically significant differences in ANP- or CNP-stimulated guanylyl cyclase activities were observed from non-failed or failed human hearts.

NPR-A and NPR-B protein levels from individual human heart samples were measured; receptors were purified by immunoprecipitation and detected by immunoblot analysis in the first two trials (Figure 4). Due to reagent complications receptor protein levels were not obtained in the final trial. As mentioned previously, the limited number of non-failed samples in the first two trials hampered comparison between the two groups making it difficult to determine accurate trends in the protein levels. Regardless, this data is significant because, to our knowledge, it is the first to demonstrate purification and detection of natriuretic peptide receptors from human heart tissue.

Discussion

Increased serum ANP and BNP levels are hallmark indicators of heart failure (Gardner, 2003; Ruskoaho, 2003). Despite these elevations, the body's response to these peptides is diminished in heart failure (Cody *et al.*, 1986). Here, we show that NPR-A activity is significantly reduced, whereas NPR-B activity is increased or statistically unchanged in the failed mouse heart. Reduced NPR-A protein explains, at least in part, the reduced ANP-dependent activity and indicates that NPR-A is downregulated in mice with pressure overload-induced congestive heart failure.

Consistent with the slightly increased NPR-B activity in failing mouse hearts, NPR-B concentrations also increased. Unfortunately, statistics on the changes in NPR protein levels could not be determined since N = 1 for each condition, a consequence of pooling the mouse hearts. Significantly, NPR-B accounts for almost as much natriuretic peptide-dependent guanylyl cyclase activity as NPR-A in normal mouse hearts and about twice as much activity as NPR-A in failed hearts. Since different antibodies were used to purify and detect each receptor, the predominant natriuretic peptide receptor in the failed heart could not be determined directly from the immunoblot analysis.

To take the research a step further towards the clinic, heart samples from patients with non-failing or failed hearts were examined. Importantly, for the first time to our knowledge, these studies measured natriuretic peptide receptor guanylyl cyclase activity and concentrations in human tissue. The human studies were significantly more challenging. Unlike the mouse studies, where the age, genetic background, and environment of each mouse is controlled, the human samples were plagued with differences such as age, gender, race, medications, and disease etiology and severity. Control samples were from non-failed hearts, but they were not from disease or trauma-free individuals. Collection of the human tissues was controlled by a third-party; therefore, variation in collection methods could contribute to the reduced guanylyl cyclase activities observed in the human samples compared to the mouse samples. Unfortunately, due to miscommunication with collaborators, problems with reagents, and the inherent variability in human samples, no firm conclusions can be drawn from these three incomplete trials. Nevertheless, it is interesting that the changes in hormone-dependent guanylyl cyclase activity from the third, most complete, trial had similar trends

as those obtained in the mouse studies. These initial studies provide a foundation upon which to base future studies of natriuretic peptide receptor regulation in the human heart.

NPR-A guanylyl cyclase activity is elicited by binding ANP or BNP, whereas NPR-B is activated by CNP (Kuhn, 2003); however, at high peptide concentrations, cross-reactivity does occur (Koller *et al.*, 1991; Suga *et al.*, 1992a). Whether ANP and BNP cross-activate NPR-B in the mouse heart is unknown but remains an intriguing possibility. In our results, only a small increase in activity is seen in membranes from banded animals when maximal vs. low dose of ANP are included in the cyclase assay. Unfortunately, because there are no specific antagonists to these receptors, whether some of the ANP-dependent activity is due to cross-activation of NPR-B cannot be determined.

There are a number of reasons why this work is particularly timely and why the role of the cardiac CNP/NPR-B system should be considered more seriously than it has in the past. First, CNP is increased in the human heart in a manner that correlates with increased pulmonary wedge pressures and degree of failure (Kalra *et al.*, 2003; Del Ry *et al.*, 2005). Second, inhibition of NPR-B in the rat results in cardiac hypertrophy that is exacerbated by congestive heart failure (Langenickel *et al.*, 2006). Third, CNP prevents cardiac remodeling after myocardial infarction in rats (Soeki *et al.*, 2005). Finally, our work indicates that NPR-B accounts for about 70% of the activity attributable to NPR-A in the non-failing mouse heart and, more importantly, that in the failing mouse heart NPR-B protein levels are not decreased and NPR-B is responsible for the majority of particulate guanylyl cyclase activity. Together, these independent observations suggest that NPR-B is playing a very important role in regulating cardiac hypertrophy and remodeling. The implications of these combined findings are that NPR-B may be an

equally important drug target for the treatment of heart failure as NPR-A, the receptor for the FDA-approved drug nesiritide. One important question that we were unable to answer since we measured guanylyl cyclase activities from whole ventricles is whether or not NPR-A and NPR-B are expressed in the same or different cell types. Clearly, this is a critical distinction to make in order to determine whether single or bifunctional activators of NPR-B can be used as potential therapeutics for congestive heart failure.

Changes in natriuretic peptide activity in the heart were previously reported in a monocrotaline model for right ventricular hypertrophy (Kim *et al.*, 1999). Using membranes prepared from endocardial cells of the right ventricle, Kim and colleagues found that the cyclase activities of both NPR-A and NPR-B were reduced in membranes from the monocrotaline-treated animals (Kim *et al.*, 1999). Interestingly, they found that NPR-B-dependent guanylyl cyclase activity was greater than NPR-A-dependent guanylyl cyclase activity in membranes from the sham animals. It will be interesting to determine whether the differences in NPR-B activity in heart failure reported by our group and Kim's are due to the experimental models (monocrotaline vs. banding), heart regions (right ventricle vs. total ventricle), or the membranes assayed (endocardial cells in the right ventricle vs. all cell types in both ventricles).

Singh et al. recently reported interesting data suggesting that NPR-A levels are decreased in heart failure (Singh *et al.*, 2006). This conclusion was based on the binding of a radiolabeled snake venom ligand, *Dendroaspis* natriuretic peptide (^{125}I-DNP), which binds to NPR-A but not NPR-B. However, the initial characterization of DNP indicated that DNP also binds to the natriuretic peptide clearance receptor (Schweitz *et al.*, 1992). That DNP binding is not specific for NPR-A is also supported by the data of Singh and colleagues because CNP was able to displace the majority of the ^{125}I-DNP binding to left

ventricle sections (Singh *et al.*, 2006). If binding was specific for NPR-A, then CNP should have been a much less potent competitor than ANP and BNP, but it was not. Furthermore, it has been reported many times that the clearance receptor is the most abundant natriuretic peptide receptor in most tissues (Maack, 1992). Therefore, although the data supports our findings, no protein level or guanylyl cyclase measurements were performed to verify that NPR-A and ANP-dependent activity were reduced in the failed hearts.

In conclusion, our study indicates that NPR-A is downregulated in the failed mouse heart and that, for the first time to our knowledge, NPR-B is responsible for a significant and previously unappreciated amount of natriuretic peptide-dependent guanylyl cyclase activity in the non-failed heart and the majority of activity in the failed heart. Thus, NPR-B represents an exciting new potential drug target for the treatment of congestive heart failure.

Table 1

Mouse heart failure parameters. Values are represented as the mean ± SEM. HW, Heart weight; BW, body weight; LW, lung weight; LVEDD, left ventricular end-diastolic dimension; LVESD, left ventricular end-systolic dimension; LVAWT, left ventricular anterior wall thickness; LVPWT, left ventricular posterior wall thickness; LV-EF, left ventricular ejection fraction; LV-FS, left ventricular fractional shortening.

Echocardiograph data contained in this table was generated by Xin Xu and Yingjie Chen.

	First Trial			Second Trial		
	Sham (n = 5)	Banded (n = 5)	P	Sham (n = 8)	Banded (n = 10)	P
Body Weight (g)	25.46 + 0.61	27.42 + 1.17	0.1769	29.45 + 0.57	28.48 + 1.02	0.4498
Heart Weight (g)	0.1011 ± 0.0020	0.2061 ± 0.0090	< 0.0001	0.1187 ± 0.0047	0.1980 ± 0.0114	< 0.0001
Lung Weight (g)	0.1306 ± 0.0037	0.2013 ± 0.0302	0.0489	0.1680 ± 0.0046	0.2374 ± 0.0345	0.0944
HW/BW (mg/g)	3.976 ± 0.072	7.600 ± 0.5785	0.0003	4.038 ± 0.174	7.082 ± 0.574	0.0003
LW/BW (mg/g)	5.138 ± 0.172	7.590 ± 1.520	0.1477	5.708 ± 0.121	8.756 ± 1.620	0.1144
LVEDD (mm)	0.3911 ± 0.0133	0.5098 ± 0.0314	0.0083	0.4060 ± 0.0094	0.4889 ± 0.0210	0.044
LVESD (mm)	0.2434 ± 0.0149	0.4366 ± 0.0283	0.0003	0.2305 ± 0.0161	0.4127 ± 0.0291	0.0001
LVAWT (mm)	0.0680 ± 0.0013	0.0830 ± 0.0062	0.0468	0.0695 ± 0.0015	0.0949 ± 0.0034	< 0.0001
LVPWT (mm)	0.0680 ± 0.0013	0.0840 ± 0.0061	0.0334	0.0689 ± 0.0011	0.0948 ± 0.0034	< 0.0001
LV-EF (%)	75.60 ± 2.75	36.55 ± 4.32	< 0.0001	80.78 ± 2.89	40.19 ± 5.25	< 0.0001
LV-FS (%)	37.90 ± 2.47	14.27 ± 2.07	< 0.0001	43.43 ± 3.09	16.46 ± 2.61	< 0.0001

Figure 1

Changes in ANP- and CNP-dependent guanylyl cyclase activities in failed mouse hearts. Crude heart membranes were prepared from sham or banded animals. The membranes were assayed for guanylyl cyclase activity under basal conditions (no natriuretic peptide) or with the indicated concentrations of ANP or CNP. The 1 μM dose represents the maximal hormone-stimulated response. Results are shown for an initial trial (A), and a second larger trial (B). ** indicates statistical significance from non-failed samples where $p \leq 0.01$, and *** indicates statistical significance from non-failed samples where $p \leq 0.0001$. Data generated by Deborah M. Dickey.

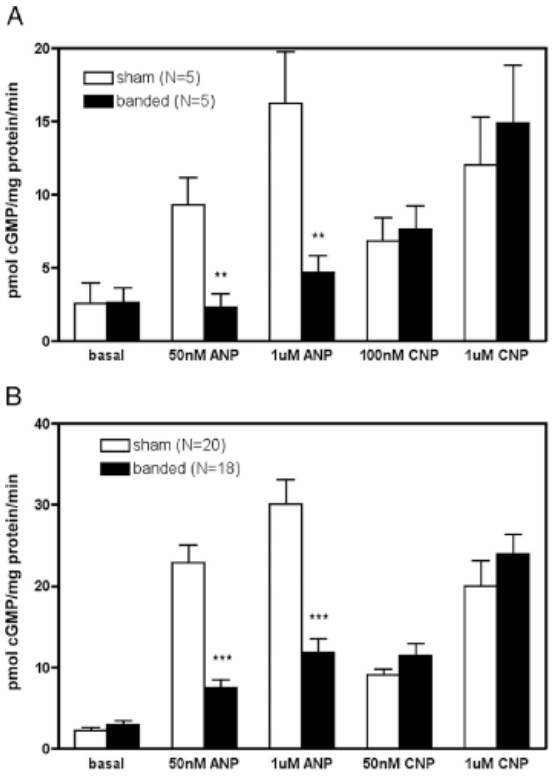
A
sham (N=5)
banded (N=5)
pmol cGMP/mg protein/min
20
15
10
5
0
**
**
basal
50nM ANP
1uM ANP
100nM CNP
1uM CNP
B
sham (N=20)
banded (N=18)
pmol cGMP/mg protein/min
40
30
20
10
0
***
***
basal
50nM ANP
1uM ANP
50nM CNP
1uM CNP

Figure 2

Changes in NPR-A and NPR-B protein levels in failed mouse hearts. Crude heart membranes were prepared and pooled from sham or banded animals in the second larger trial. NPR-A (A) and NPR-B (B) were sequentially purified by immunoprecipitation and detected by immunoblot. Each lane represents the equivalent of five mouse hearts. 293T NPR-A and 293T NPR-B are positive controls. (C) Data from (A) and (B) were quantified, normalized to sham NPR protein levels, and presented in graphical form. Data generated by Paula M. Bryan (NPR-A) and Darcy R. Flora (NPR-B).

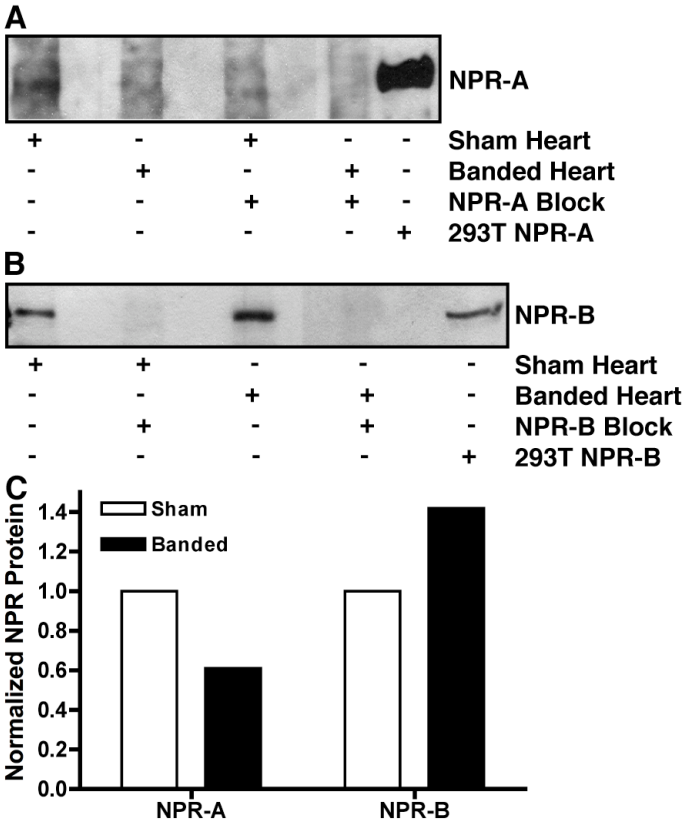
A
NPR-A
+ - + - - Sham Heart
- + - + - Banded Heart
- - + + - NPR-A Block
- - - - + 293T NPR-A
B
NPR-B
+ + - - - Sham Heart
- - + + - Banded Heart
- + - + - NPR-B Block
- - - - + 293T NPR-B
C
Normalized NPR Protein
Sham
Banded
1.4
1.2
1.0
0.8
0.6
0.4
0.2
0.0
NPR-A
NPR-B

Table 2

Human heart sample identification and patient characteristics. HF, Heart failure; LV-EF, left ventricular ejection fraction. Patient information provided by Dan Dries and Ken Margulies.

Sample ID #	First Trial Sample #	Second Trial Sample #	Third Trial Sample #	Age	Gender	Race	HF Etiology	Millrone Dose	Other Notes
601			12	61	Male		Non-Failed		LV-EF = 60%
606			13	44	Male	African America	Non-Failed		LV-EF = 60%
1003			1	64	Male	African America	Dilated HF	0.25	LV-EF = 28%
1004	10			58	Male	Caucasian	Ischemic HF	0.25	
1005		2		55	Male	Caucasian	Ischemic HF	0.5	
1007	12		9	60	Female	African America	Dilated HF	0.375	LV-EF = 5%
1008	7			49	Male	Caucasian	Ischemic HF	0.25	
1009		6	8	58	Female	Caucasian	Dilated HF	0.5	LV-EF = 10%
1010	11	1	2	44	Female	African America	Dilated HF	0.25	LV-EF = 28%
1011	2			58	Male	Caucasian	Ischemic HF		
1012		11	3	67	Male	Caucasian	Dilated HF		LV-EF = 18%
1013	6		7	53	Male	African America	Dilated HF	0.25	LV-EF = 12%
1017		13		58	Male	Caucasian	Ischemic HF		
1018	14		10	35	Male	African	Dilated HF	0.5	LV-EF = 8%
1020		12	4	35	Male	African America	Dilated HF	0.5	LV-EF = 18%
1021	13		5	47	Male	Caucasian	Dilated HF		LV-EF = 12%
1023		4		30	Male	African America	Dilated HF		
1027		15	18	46	Female	African America	Non-Failed		end stage renal disease, left ventricular hypertrophy
1029		5							
1031	8			63	Male	Caucasian	Ischemic HF	0.5	
1032		3	14	49	Male	Non-Hispanic	Non-Failed		LV-EF = 60%
1033		10	6	48	Male	Caucasian	Dilated HF		LV-EF = 15%
1034		14		62	Male	Caucasian	Non-Failed		
1035		7		64	Male	Caucasian	Ischemic HF	0.375	
1037		9							
1038			11	55	Female	Caucasian	Non-Failed		LV-EF = 65%
1040	3			67	Male	Caucasian	Ischemic HF	0.5	
1051		8							
1052			15	44	Male	African America	Non-Failed		LVEF = 48%
1067			16	66	Male	Hispanic	Non-Failed		LVEF = 65%
1068			17	18	Male	Caucasian	Non-Failed		LVEF = 70%
apex #4	9			47	Male	Caucasian	Non-Failed		gunshot victim
LV 060315	4								
LV 5-9-06	5								
LV 5-19-06	1								

Figure 3

ANP- and CNP-dependent guanylyl cyclase activities in failed human hearts.

Crude heart membranes were prepared from non-failed and failed hearts and assayed for guanylyl cyclase activity under basal conditions (no natriuretic peptide) or with 1 μM ANP or CNP. Results are shown for three separate trials: (A) first trial, (B) second trial, and (C) third trial. * indicates statistical significance from non-failed samples where $p < 0.05$. Data generated by Deborah M. Dickey.

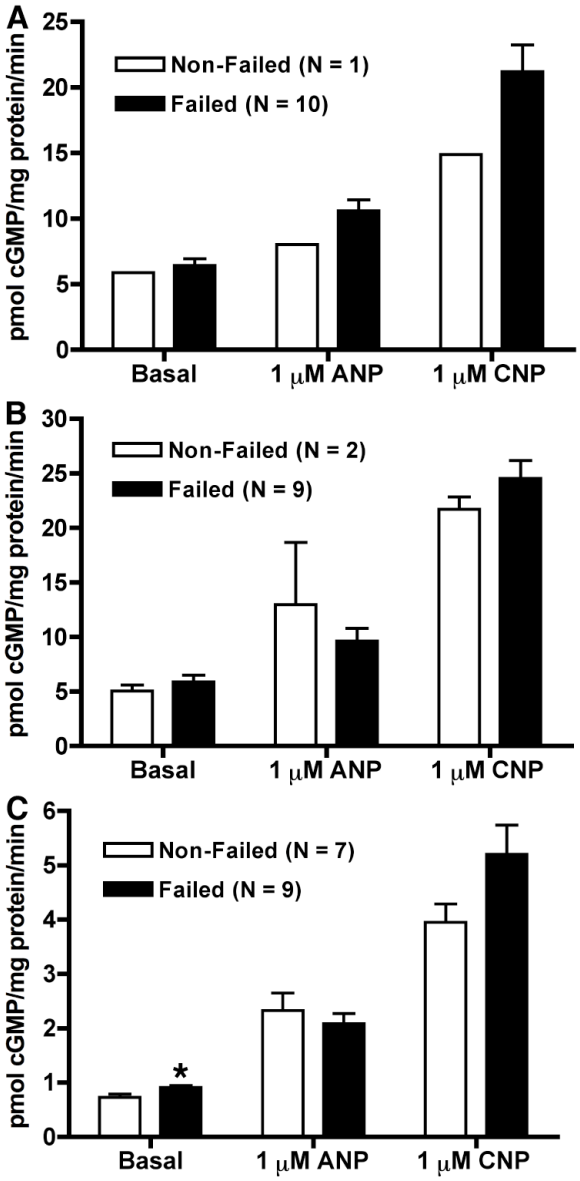
A
pmol cGMP/mg protein/min
25
20
15
10
5
0
Non-Failed (N = 1)
Failed (N = 10)
Basal
1 μM ANP
1 μM CNP
B
pmol cGMP/mg protein/min
30
25
20
15
10
5
0
Non-Failed (N = 2)
Failed (N = 9)
Basal
1 μM ANP
1 μM CNP
C
pmol cGMP/mg protein/min
6
5
4
3
2
1
0
Non-Failed (N = 7)
Failed (N = 9)
*
Basal
1 μM ANP
1 μM CNP

Figure 4

NPR-A and NPR-B protein levels in failed human hearts. Crude membranes were prepared from non-failed or failed human hearts. NPR-A (top) and NPR-B (bottom) were sequentially purified by immunoprecipitation and detected by immunoblot. Immunoblots from two of the three separate trials are shown: (A) first trial and (B) second trial. 293T NPR-A and 293T NPR-B are positive controls. Data generated by Darcy R. Flora.

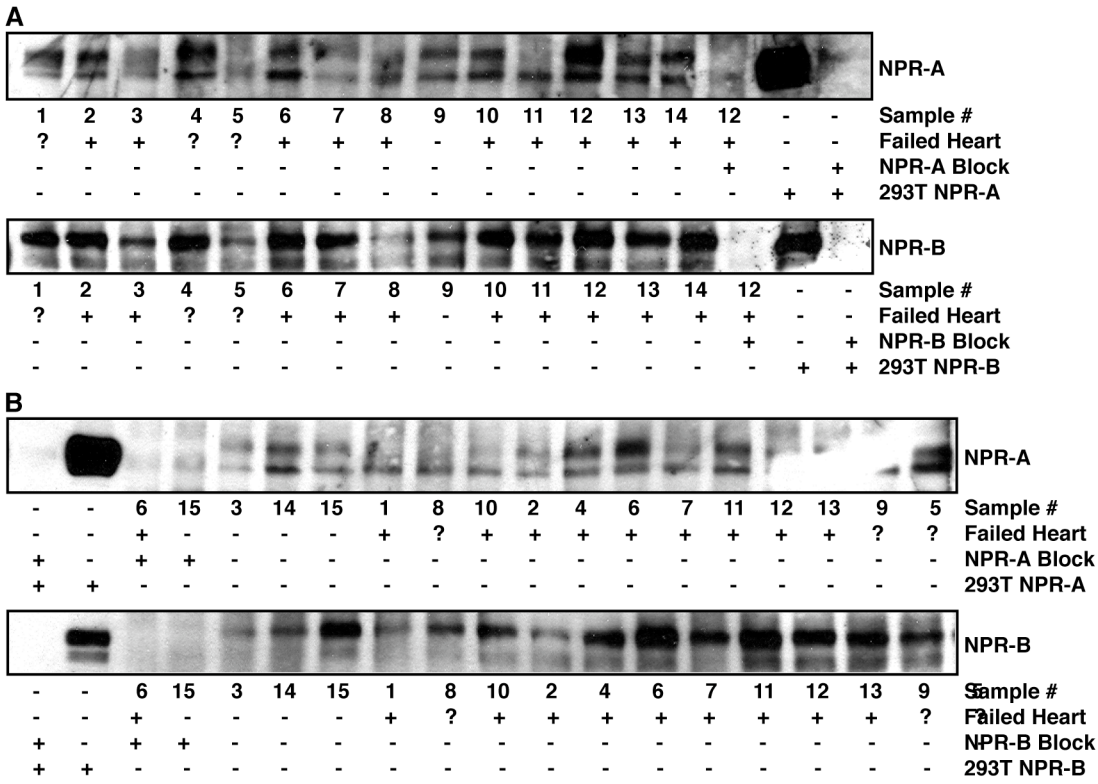
A
NPR-A
1 2 3 4 5 6 7 8 9 10 11 12 13 14 12 - - Sample #
? + + ? ? + + + - + + + + + + + - - Failed Heart
- - - - - - - - - - - - - - + - + NPR-A Block
- - - - - - - - - - - - - - - + + 293T NPR-A
NPR-B
1 2 3 4 5 6 7 8 9 10 11 12 13 14 12 - - Sample #
? + + ? ? + + + - + + + + + + + - - Failed Heart
- - - - - - - - - - - - - - + - + NPR-B Block
- - - - - - - - - - - - - - - + + 293T NPR-B
B
NPR-A
- - 6 15 3 14 15 1 8 10 2 4 6 7 11 12 13 9 5 Sample #
- - + - - - - + ? + + + + + + + + ? ? Failed Heart
+ - + + - - - - - - - - - - - - - - - NPR-A Block
+ + - - - - - - - - - - - - - - - - - 293T NPR-A
NPR-B
- - 6 15 3 14 15 1 8 10 2 4 6 7 11 12 13 9 5 Sample #
- - + - - - - + ? + + + + + + + + ? ? Failed Heart
+ - + + - - - - - - - - - - - - - - - NPR-B Block
+ + - - - - - - - - - - - - - - - - - 293T NPR-B

CHAPTER 3:

Prolonged Atrial Natriuretic Peptide Exposure Stimulates Degradation of Natriuretic Peptide Receptor-A

This chapter is modified from the manuscript:
Flora, D.R., and Potter, L.R. Prolonged atrial natriuretic peptide exposure stimulates guanylyl cyclase-A degradation.

Introduction

Atrial natriuretic peptide (ANP) and B-type natriuretic peptide (BNP) are released into the circulation from the atria and ventricles of the heart, respectively, in response to elevated blood pressure (Kuhn, 2003). Known collectively as the cardiac natriuretic peptides, ANP and BNP inhibit cardiac hypertrophy and decrease blood pressure through natriuresis, diuresis, vasorelaxation, and antagonism of the renin-angiotensin-aldosterone system (Potter *et al.*, 2009). ANP and BNP bind to and activate natriuretic peptide receptor-A (NPR-A), a cell surface guanylyl cyclase. NPR-A consists of an extracellular ligand binding domain, a single membrane-spanning region, and intracellular regulatory kinase homology, coiled-coil dimerization, and catalytic guanylyl cyclase domains (Potter, 2005). The latter synthesizes the intracellular second messenger cGMP, which mediates the physiological effects of the natriuretic peptides. ANP and BNP also bind to natriuretic peptide receptor-C (NPR-C). NPR-C, often referred to as the natriuretic peptide clearance receptor, lacks enzymatic guanylyl cyclase activity and functions to clear circulating natriuretic peptides through receptor-mediated, but ligand-independent, internalization and degradation (Nussenzveig *et al.*, 1990; Matsukawa *et al.*, 1999).

Healthy individuals have low plasma ANP and BNP levels; however, under cardiovascular stress, circulating cardiac natriuretic peptide levels are dramatically elevated. The rise in plasma ANP and BNP levels are correlated with disease progression; hence, the measurement of plasma natriuretic peptide levels, particularly BNP, has become a powerful tool in the diagnosis and prognosis of heart failure (Ruskoaho, 2003). Despite increased natriuretic peptide levels, the renal responsiveness to these peptides is diminished in patients with heart failure (Charloux *et al.*, 2003). One

explanation for the blunted response is accelerated NPR-A degradation resulting from ligand-dependent receptor degradation. Recent studies using ^{125}I-natriuretic peptide binding or antibody-mediated receptor detection indicate that NPR-A levels are reduced in tissues from heart-failed animals or patients compared to non-failed subjects (Tsutamoto *et al.*, 1993; Singh *et al.*, 2006; Bryan *et al.*, 2007; Dickey *et al.*, 2007).

Ligand-mediated internalization and degradation, a process referred to as downregulation, is a mechanism used by cell-surface signaling receptors to terminate receptor-mediated signaling from the plasma membrane. Although downregulation of NPR-A has been reported *in vivo*, it has been controversial when studied in cell culture. The majority of the studies on the downregulation of NPR-A use ^{125}I-ANP to follow NPR-A via the ^{125}I-ANP-NPR-A complex. Interpretation of the results from these studies can be challenging due to changing ligand-receptor binding affinities, difficulties in removing prior bound ligand from the receptor, and cells expressing two ANP receptors (NPR-A and NPR-C) (Schiffrin *et al.*, 1991; Jewett *et al.*, 1993).

^{125}I-ANP binding studies from the Maack group indicated that NPR-A is a membrane resident protein that does not internalize in the absence or presence of ANP, and that the interaction between ANP and NPR-A is terminated by a rapid, temperature-dependent dissociation that occurs at the cell surface (Koh *et al.*, 1992; Vieira *et al.*, 2001). Consistent with these findings, Jewett and coworkers reported that ANP binding to NPR-A in 293 cells causes a transition from high to low affinity binding within 15 min at 4°C that is not associated with receptor loss from the cell surface (Jewett *et al.*, 1993). Similarly, our group found that 80% of ^{125}I-ANP bound to NPR-A overexpressed in 293T cells was released intact into cell culture medium after 10 min at 37°C (Fan *et al.*, 2005). Meanwhile other groups reported that NPR-A is downregulated because a time- and

concentration-dependent loss of ^{125}I-ANP binding was observed in cells exposed to unlabelled ANP (Cahill *et al.*, 1990; Pandey, 1992; Pandey *et al.*, 2002). Pandey and colleagues further reported that the ^{125}I-ANP-NPR-A complex internalizes and is processed through a lysosomal degradation pathway (Pandey, 2005). Our group reported that in 293 cells stably expressing NPR-A, the reduced hormone-dependent guanylyl cyclase activity following a 4 h ANP exposure was due to receptor downregulation (Potter and Hunter, 1999). However, a more recent study from our group found that NPR-A overexpressed in 293T cells was not detectably downregulated by a 14 h ANP exposure (Fan *et al.*, 2005). Thus, the effect of ANP on NPR-A downregulation in cell culture is decidedly unclear.

Recent studies from our laboratory suggested that NPR-A is downregulated in mice with congestive heart failure (Bryan *et al.*, 2007; Dickey *et al.*, 2007). Here, we sought to reproduce our *in vivo* findings in cell culture, as a cell culture model of NPR-A downregulation may be further used to gain insight into the mechanisms involved in NPR-A downregulation. Primary, immortalized, and overexpressing cell lines were studied to develop a consistent understanding of the problem. Furthermore, we specifically avoided ^{125}I-ANP binding studies due to the previously described interpretation issues. Instead, receptor protein levels were estimated from guanylyl cyclase activities and immunoprecipitation-immunoblot analysis with antibodies against natural intracellular and artificial extracellular receptor epitopes. NPR-A protein loss from the plasma membrane was qualitatively examined using a new immunolocalization procedure that, for the first time to our knowledge, permitted NPR-A to be visualized exclusively at the cell surface. We found that ANP unequivocally stimulates NPR-A degradation in all cell types examined by a process that occurs over hours, not minutes.

Materials and Methods

Materials

Rat ANP, cycloheximide, microcystin LR, and FLAG peptide were purchased from Sigma-Aldrich (St. Louis, MO). Complete protease inhibitors and bovine serum albumin (BSA) were from Roche Diagnostics (Indianapolis, IN). Cyclic GMP RIA kit was purchased from PerkinElmer (Waltham, MA).

Cell Culture

Primary bovine aortic endothelial cells (bAEC) were purchased from Lonza (Walkersville, MD) and maintained in endothelial cell growth medium (Lonza). Stably transfected 293T-NPR-A cells were grown as previously described (Fan *et al.*, 2005). CHO-pCEP6 cells were a generous gift from Dr. Kathy Griendling (Emory University; Atlanta, GA) and were maintained in DMEM containing 10% FBS, 100 units/ml penicillin, 100 μg/ml streptomycin, 500 μg/ml hygromycin B, and 20 μg/ml L-proline.

FLAG-NPR-A Construct

Rat NPR-A was excised from pCMV3-GC-A (Potter and Garbers, 1992) by digestion with NotI and BglII and subcloned into the same sites in the multiple cloning region of pFLAG-CMV1 (Sigma-Aldrich), which contains a FLAG epitope inserted carboxyl-terminal to the Met-preprotrypsin coding sequence. The resulting plasmid generates an amino-terminal FLAG-tagged receptor after cleavage of the signal sequence.

Small Interfering RNA (siRNA) Knock Down

Silencer GAPDH siRNA and siRNAs targeting human NPR-A (NPR1) [#143349: sense: 5'-CCCAGAUAAUCCCGAGUACtt-3', anti-sense: 5'-GUACUCGGGAUUAUCUGGGtc-3'; #143350: sense: 5'-GCAUAUUAUAAGGGCAACCtt-3', anti-sense: 5'-

GGUUGCCCUUAUAAUAUGCtg-3'; #143351: sense: 5'-CCGUAAACGCAUUGAGCUGtt-3', anti-sense: 5'-CAGCUCAAUGCGUUUACGGtt-3'] were from Ambion (Austin, TX). Thirty nmol siRNA were transfected into HeLa cells using Lipofectamine 2000 (Invitrogen; Carlsbad, CA). Cells were incubated for 48-72 h post-transfection before analysis.

Membrane Preparation

Cells were washed with 4°C with phosphate-buffered saline (PBS) and scraped off the plate in the presence of phosphatase inhibitor buffer containing 25 mM HEPES (pH 7.4), 50 mM NaCl, 20% glycerol, 50 mM NaF, 2 mM EDTA, 0.5 μM microcystin LR, and 1X Roche Complete protease inhibitors. Suspended cells were sonicated for 1-2 s and centrifuged at 20,000 x g for 10 min at 4°C. The supernatant was aspirated, and the pellet was resuspended in the same buffer. Total protein concentrations were determined by the Bradford method.

Guanylyl Cyclase Assay

Twenty microliters of membranes were assayed for guanylyl cyclase activity in the presence of 1 mM ATP and 5 mM $MgCl_2$ (basal stimulation), 1 mM ATP, 5 mM $MgCl_2$, and 1 μM rat ANP (hormone stimulation), or 1% Triton X-100 and 5 mM $MnCl_2$ (detergent stimulation). The reaction was initiated by adding 55 μl prewarmed cocktail containing 25 mM HEPES (pH 7.4), 50 mM NaCl, 0.1% BSA, 0.5 mM 1-methyl-3-isobutylxanthine (IBMX), 1 mM GTP, 5 mM creatine phosphate, 0.1 μg/μl creatine kinase, 1 μM EDTA, and 1 μM microcystin LR. Reactions were performed at 37°C for 3 min and stopped with 400 μl of ice-cold 50 mM sodium acetate solution containing 5 mM EDTA. One hundred microliters of the reaction was assayed for cGMP concentrations by radioimmunoassay.

Immunoprecipitation and Immunoblotting

Cells were solubilized in 1 ml of ice-cold modified RIPA buffer containing 50 mM Tris (pH 7.5), 100 mM NaCl, 1% NP-40, 0.5% sodium deoxycholate, 0.1% SDS, 10 mM NaH_2PO_4, 50 mM NaF, 2 mM EDTA, 0.5 μM microcystin LR, and 1X Complete protease inhibitors. To reduce nonspecific binding, solubilized cells were incubated at 4°C with 50 μl protein A (RepliGen; Waltham, MA) for at least 30 min. NPR-A was immunoprecipitated overnight at 4°C using 2 μl of polyclonal rabbit 6325 antiserum, which recognizes the last 17 carboxyl-terminal amino acids of rat NPR-A, and 50 μl protein A. The FLAG epitope was immunoprecipitated with 40 μl anti-FLAG M2 affinity gel (Sigma-Aldrich) overnight at 4°C. Immunocomplexes were washed three times with 1 ml of ice-cold RIPA buffer, fractionated by SDS-PAGE, and transferred to polyvinylidene fluoride (PVDF) membrane.

Primary antibodies for immunoblot analysis were polyclonal rabbit 6325 (1:2500) to NPR-A (Abbey and Potter, 2002) or monoclonal anti-FLAG M2 (1:5000; Sigma-Aldrich) to the FLAG epitope. Secondary antibodies were peroxidase-conjugated donkey anti-rabbit IgG (1:20,000; GE Healthcare; Buckinghamshire, UK), peroxidase-conjugated sheep anti-mouse IgG (1:20,000; GE Healthcare), or goat anti-rabbit IRDye 680 (1:10,000; LI-COR Biosciences; Lincoln, NE).

Whole Cell cGMP Elevation Assay

293neo cells, grown on poly-D-lysine-coated 24-well plates, were transfected using a calcium phosphate protocol. The day of the assay, the cells were incubated in serum-free medium for at least 4 h. Medium was aspirated, and the cells were incubated for 20 min at 37°C in Dulbecco's modified Eagle's medium (DMEM) containing 20 mM HEPES (pH 7.4) and 0.5 mM IBMX. This medium was then replaced with the same medium

containing 1 μM rat ANP, a 1:2000 dilution of anti-FLAG M2 antibody, or both 1 μM rat ANP and a 1:2000 dilution of anti-FLAG M2 antibody, and stimulated for 5 min. The reaction was terminated by aspirating the medium and adding 1 ml of ice-cold 80% ethanol. One hundred and fifty microliters of the resulting supernatant was dried in a centrifugal vacuum concentrator and analyzed for cGMP content by radioimmunoassay.

Immunolocalization of FLAG-NPR-A

Cells were grown on glass coverslips and transfected with a FLAG-NPR-A construct using Lipofectamine 2000. The next day cells were incubated with DMEM containing 10 μg/ml cycloheximide in the absence or presence of 200 nM rat ANP for various periods of time. Cells were fixed in PBS solution containing 4% formalin and 0.2% Triton X-100 for 20 min. The cells were then washed in PBS containing 0.2% Triton X-100 and incubated overnight at 4°C in a humidity chamber. After washing two additional times, the cells were blocked with PBS containing 10 mg/ml BSA, 0.5% donkey serum, and 0.2% Triton X-100 at 37°C for 60 min. The coverslips were then incubated with anti-FLAG M2 antibody (1:2000) or antibody to NPR-A (6325; 1:1000) for 60 min at 37°C. To observe FLAG-NPR-A on the cell surface, live cells were blocked and incubated with anti-FLAG M2 antibody before fixation. Cells were washed five times, and incubated for 45 min at 37°C with FITC-conjugated goat anti-mouse IgG (1:500; Jackson ImmunoResearch Laboratories; West Grove, PA) or FITC-conjugated goat anti-rabbit IgG (1:500; Jackson ImmunoResearch Laboratories). Nuclei were stained by including Hoechst 33342 (1:5000; Molecular Probes; Eugene, OR) in the final wash. To identify the plasma membrane, Alexa Fluor 594-conjugated wheat germ agglutinin (1 μg/ml; Molecular Probes) was added to two washes following incubation with the primary antibody. Fixed cells were mounted on slides with Vectashield (Vector Laboratories;

Bulingame, CA) and imaged using a multiphoton confocal microscope (Olympus FluoView 1000).

Quantification

Immunoblots were quantified on an Odyssey Infrared Imaging System (LI-COR Biosciences).

Results

ANP-Dependent Degradation of Endogenous NPR-A

Our laboratory recently reported two confounding observations. First, NPR-A is not downregulated by ligand exposure in 293T cells overexpressing NPR-A (Fan *et al.*, 2005), and second, NPR-A is downregulated in a mouse model of congestive heart failure (Bryan *et al.*, 2007; Dickey *et al.*, 2007). Because ANP and BNP are highly elevated in congestive heart failure and NPR-A mRNA levels are not decreased in failing hearts (Brown *et al.*, 1993; Christoffersen *et al.*, 2006), we reexamined whether NPR-A is downregulated in response to prolonged ligand exposure in cultured cells.

Initial experiments were conducted in primary bovine aortic endothelial cells (bAEC) because these cells are physiologically relevant, express detectable levels of endogenous NPR-A, and are more likely to exhibit physiological regulation than immortalized or transfected cells. Exposure of bAEC to saturating levels of ANP for 1 h reduced ANP-dependent guanylyl cyclase activity by 75% (Figure 1A). To determine whether decreased receptor protein levels explained the reduced guanylyl cyclase activity, cellular NPR-A levels from cells exposed to ANP for increasing periods of time were determined by immunoblot analysis (Figure 1B). A characteristic doublet detection pattern for NPR-A was observed, which consists of the more prominent upper

completely glycosylated and phosphorylated band and lower incompletely glycosylated and unphosphorylated band (Koller *et al.*, 1993). Importantly, immunoblot signals obtained from cells incubated with or without ANP for 1 h were not significantly different, indicating that decreases in receptor protein levels do not explain the reduced ANP-dependent guanylyl cyclase activity (Figure 1B). Previous studies indicate that NPR-A dephosphorylation is tightly correlated with early losses in ANP-dependent guanylyl cyclase activities in 293 cells and likely explains the initial activity declines in the bAEC as well (Potter and Garbers, 1992; Koller *et al.*, 1993; Potter and Hunter, 1999; Joubert *et al.*, 2001). Exposure of the bAEC to ANP for 4, 8, or 20 hours resulted in a more gradual loss of ANP-dependent cyclase activity and immunoblot analysis indicated that NPR-A levels declined in a time-dependent manner that was correlated with reductions in guanylyl cyclase activities (Figure 1, A and B). To our knowledge, this is the first report to directly demonstrate large time-dependent reductions in NPR-A protein and guanylyl cyclase levels in response to ANP exposure in primary cells.

ANP-dependent downregulation of endogenous NPR-A was also examined in immortalized human cervical HeLa cells. HeLa cells are robust, express higher levels of endogenous NPR-A than bAEC, and are commonly used to study the molecular machinery involved in downregulation. To focus on protein degradation in the absence of new protein synthesis these cells were treated with 10 μg/ml cycloheximide. Cycloheximide clearly blocked protein synthesis because the lower migrating precursor form of NPR-A was not present in immunoblots from cells incubated with the protein synthesis inhibitor (Figure 1D). As was observed in the bAEC, exposure to 200 nM ANP for 1 h markedly reduced hormone-dependent guanylyl cyclase activity without affecting NPR-A protein levels (Figure 1, C and D). However, exposure to hormone for 2, 4, 8, or

12 hours further reduced ANP-dependent guanylyl cyclase activity, and the reductions were nicely correlated with decreased NPR-A protein levels as revealed by immunoblot analysis (Figure 1, C and D).

In both bAEC and HeLa cells, about half of the protein was lost after exposure to ANP for 4 h. In HeLa cells, we also measured guanylyl cyclase activity in the presence of 1% Triton X-100 and manganese as the divalent metal cofactor. These non-physiologic conditions activate the enzyme in a hormone- and phosphorylation-independent manner. Hence, they are a reliable indicator of total NPR-A protein levels (Potter and Hunter, 1998b). Guanylyl cyclase activity determined in the presence of detergent declined gradually and paralleled the diminishing immunoblot signal (Figure 1, C and D).

To verify that NPR-A alone was responsible for the ANP- and Triton X-100-dependent guanylyl cyclase activities observed in HeLa cells, guanylyl cyclase activity was measured following a three-minute basal, hormone, or detergent stimulation in HeLa cells transfected with siRNA against NPR-A mRNA to reduce NPR-A protein. Three separate siRNAs targeting different regions of NPR-A produced similar results (Figure 2). In Figure 2A, note that the lower immature band of NPR-A is present, as no cycloheximide was added in this experiment. Both ANP-dependent and –independent guanylyl cyclase activities were reduced by approximately 80% in cells expressing NPR-A specific siRNA, which indicates that NPR-A is responsible for the vast majority of guanylyl cyclase activity in these cells (Figure 2B). Thus, two independent assays, detergent-dependent guanylyl cyclase activities and immunoblot detection, indicate that prolonged ANP exposure causes NPR-A degradation in HeLa cells.

ANP-Dependent Degradation of Overexpressed NPR-A

Previously our laboratory reported that NPR-A was not internalized or degraded in response to ANP in 293T cells overexpressing NPR-A (Fan *et al.*, 2005). Since we observed endogenous NPR-A downregulation in a mouse model of congestive heart failure (Bryan *et al.*, 2007; Dickey *et al.*, 2007) and in ANP-exposed "regular" 293 (Potter and Hunter, 1999), bAEC, and HeLa cells, we reexamined the effect of prolonged ANP exposure on NPR-A stably expressed in 293T cells. To optimize our ability to detect ANP-dependent degradation in the 293T NPR-A cells, several modifications were made to the original downregulation protocol (Fan *et al.*, 2005). Specifically, the time of incubation in the presence of ANP was extended, new protein synthesis was blocked with cycloheximide, and fresh ANP was added several times throughout the incubation period in order to replenish ANP levels resulting from possible peptide proteolysis. Under these conditions, ANP-dependent degradation of NPR-A in 293T cells was observed (Figure 3). However, the rate and extent of NPR-A degradation was significantly reduced compared to degradation observed in bAEC and HeLa cells. Visually, NPR-A protein levels were not obviously reduced until after 16 h of ANP exposure (Figure 3, top). Quantification of these data indicated that NPR-A protein levels were reduced by 17%, 38%, and 48% after being exposed to ANP for 8, 16, or 24 hours, respectively (Figure 3, bottom).

ANP Stimulates the Degradation of FLAG-NPR-A

Effective antibodies recognizing the extracellular amino-terminus of NPR-A are not available. Therefore, to follow receptors on the cell surface, an NPR-A construct with an amino-terminal FLAG epitope was created. 293neo cells transfected with FLAG-NPR-A generated cGMP upon ANP stimulation in a whole cell assay similarly to cells expressing the wildtype receptor (Figure 4A). Simultaneous additions of ANP and anti-FLAG M2

antibody caused a comparable increase in cGMP levels, and addition of the anti-FLAG M2 antibody alone did not stimulate cGMP production (Figure 4A). Thus, FLAG-NPR-A is expressed at the cell surface and neither the FLAG epitope nor its accompanying antibody stimulated or hindered receptor activation.

To determine if FLAG-NPR-A undergoes ANP-dependent degradation similar to wildtype receptor, Chinese hamster ovary (CHO) cells were transfected with FLAG-NPR-A and incubated with cycloheximide in the absence or presence of ANP for 10 h. Consistent with the wildtype NPR-A receptor in bAEC, HeLa, and 293T cells, prolonged exposure to ANP markedly reduced FLAG-NPR-A protein levels in CHO cells (Figure 4B). No endogenous NPR-A was detected in untransfected CHO cells (Figure 4B, top). Importantly, detection of FLAG-NPR-A was determined by reactivity to an epitope at the amino and carboxyl terminus of the receptor. Thus, loss of antibody reactivity to both the amino and carboxyl termini of NPR-A is consistent with ANP exposure stimulating the complete degradation of NPR-A. Furthermore, after reanalysis of NPR-A degradation in 293T cells, all data from the primary, immortalized, and transfected cells are consistent and in strong agreement with previous *in vivo* observations for ANP-dependent NPR-A downregulation.

Novel Immunolocalization Assay Visualizes FLAG-NPR-A at the Cell Surface

For further validation of NPR-A downregulation we turned to immunolocalization. Using a typical immunolocalization protocol, HeLa cells transfected with FLAG-NPR-A were fixed in formaldehyde, blocked in a solution containing BSA and donkey serum, and sequentially incubated with anti-FLAG M2 and FITC-conjugated anti-mouse IgG antibodies. All of the solutions contained Triton X-100, which permeabilizes the plasma membrane. Similar to previous unpublished observations within our group, and

immunolocalization observations of NPR-A (Airhart *et al.*, 2003; Abdelalim and Tooyama, 2009) and the related natriuretic peptide receptor-B (NPR-B) (Hume *et al.*, 2009) in cultured cells from other groups, FLAG-NPR-A had a diffuse intracellular localization under these conditions (Figure 5D). Methanol fixation yielded similar results (image not shown).

NPR-A is a transmembrane receptor and previous immunolocalization studies failed to convincingly demonstrate that the signal observed was from a natriuretic peptide receptor, thus, we performed several controls to verify that the diffuse intracellular staining was specific to NPR-A. HeLa cells that were not transfected with the FLAG-NPR-A construct failed to show specific staining (Figure 5A). FLAG-NPR-A transfected cells not exposed to primary anti-FLAG M2 antibody (Figure 5B), not exposed to secondary FITC-conjugated anti-mouse IgG antibody (Figure 5C), or exposed to primary anti-FLAG M2 antibody in the presence of FLAG peptide (Figure 5F) also failed to exhibit specific staining. Cells were permeabilized in this initial immunolocalization protocol, therefore, polyclonal antibodies recognizing the intracellular carboxyl-terminus of NPR-A (6325) could be used. The anti-FLAG M2 and carboxyl-terminal NPR-A antibodies both revealed a diffuse intracellular localization of NPR-A (Figure 5, D and E). Specific staining was not observed in non-transfected HeLa cells exposed to carboxyl-terminal NPR-A antibodies (image not shown), indicating that endogenous NPR-A is not detectable by immunofluorescence in HeLa cells.

Since we ultimately wanted to investigate the effect of ANP on NPR-A at the plasma membrane, the diffuse intracellular signal had to be eliminated. In the initial immunolocalization protocol, permeabilization of the cells allowed the primary antibody to recognize all receptors, regardless of the location; thus, to limit binding of anti-FLAG

M2 antibody to cell-surface FLAG-NPR-A, Triton X-100 was removed from solutions. No FLAG-NPR-A specific signal was observed under these detergent-free conditions (image not shown). In a subsequent attempt to eliminate the intracellular signal, FLAG-NPR-A transfected cells were, in the absence of Triton X-100, blocked and incubated with anti-FLAG M2 antibody as live cells. After incubation with the primary antibody, the cells were fixed with formalin solution and incubated with secondary antibody. Imaging revealed a FLAG-NPR-A signal that appeared to be only on the cell surface (Figure 5G). Overlay of the staining from FLAG-NPR-A (Figure 5G) and Alexa Fluor 594-conjugated wheat germ agglutinin (Figure 5H), a plasma membrane marker, indicated that, using this new immunolocalization protocol, FLAG-NPR-A was visible at the plasma membrane (Figure 5I).

Prolonged ANP Exposure Results in Loss of Cell-Surface FLAG-NPR-A

To examine the effect of ANP on FLAG-NPR-A at the plasma membrane, FLAG-NPR-A transfected HeLa cells were exposed to ANP and antibody to the FLAG epitope prior to fixation and incubation with secondary antibody. No significant differences in cell-surface FLAG-NPR-A were observed in cells exposed to ANP for short periods of time (≤ 1 h) (Figure 6, A-C). In a separate experiment, FLAG-NPR-A transfected HeLa cells were incubated either in the absence (Figure 6D, top) or presence (Figure 6D, bottom) of ANP for 8 h prior to fixation. Despite heterogeneity due to varying FLAG-NPR-A expression levels, FLAG-NPR-A staining at the plasma membrane was visibly reduced in the ANP-exposed cells (Figure 6D). This observation is consistent with reduced total receptor protein levels following prolonged ANP exposure.

Discussion

Here, we show that prolonged ANP exposure results in a time-dependent increase in NPR-A degradation in a variety of cell culture models including 293T cells. Unlike previous cell culture studies, which reported the downregulation of NPR-A indirectly through the measurement of either ^{125}I-ANP binding (Cahill *et al.*, 1990; Pandey, 1992; Pandey *et al.*, 2002) or guanylyl cyclase activity (Potter and Hunter, 1999), the current study uses immunoprecipitation-immunoblot techniques to examine the receptor itself. This approach eliminates the concern for changing ligand-receptor binding affinities, ligand prebound to the receptor (prior receptor occupation), and cell lines expressing more than one ANP receptor (Schiffrin *et al.*, 1991; Jewett *et al.*, 1993). ^{125}I-ANP binds NPR-C, which is not only the most widely and abundantly distributed natriuretic peptide receptor, but is also constitutively internalized (Nussenzveig *et al.*, 1990). Because ANP-dependent NPR-A degradation is observed in a variety of cell culture models, including a primary and immortalized cell line expressing endogenous NPR-A as well as transfected cell lines, it is unlikely that this phenomenon is specific to cell type as indicated in previous reports. The decreased receptor levels result from increased degradation, not reduced synthesis, because cycloheximide blocked new NPR-A synthesis without affecting the NPR-A degradation rate as measured by immunoblot or Triton X-100-dependent guanylyl cyclase activities.

The reason we did not observe significant ANP-dependent NPR-A degradation in our previous studies with 293T cells may result from the slow rate of degradation in these cells (Fan *et al.*, 2005). However, it is also noteworthy that ANP was frequently added to the cell culture medium to insure constant natriuretic peptide concentrations and cycloheximide was added to inhibit new protein synthesis in the present but not previous study. It is also relevant that the time span for epidermal growth factor (EGF)-induced

EGF receptor downregulation increases in cells expressing high receptor concentrations, which is consistent with reduced trafficking due to saturation of the basal endocytic machinery (Gilligan *et al.*, 1992; Sorkin and Goh, 2008). The 293T cell line used in the previous study expressed very high numbers of NPR-A (~10^6 receptors/cell); hence, it is not unreasonable for NPR-A to have a slower rate of degradation in the 293T cells. However, we cannot rule out the possibility that the majority of NPR-A is not on the cell surface and, therefore, is unable to be regulated by ligand binding in these cells. Regardless, the previous report examined ANP-dependent degradation of cell-surface NPR-A following 0, 10, 60, or 840 min of ANP exposure. Although endogenous NPR-A in bAEC and HeLa cells degraded more rapidly than NPR-A in the 293T NPR-A cells, even in the bAEC and HeLa cells there was virtually no difference in receptor protein levels after 1 h of ligand exposure. After 16 h of ANP exposure, we observed only a 38% reduction in NPR-A protein levels in the 293T NPR-A cells. Thus, a slight reduction in NPR-A protein levels at the 14 h time point in the previous study was not detected.

Consistent with published NPR immunolocalization studies in cell culture (Airhart *et al.*, 2003; Abdelalim and Tooyama, 2009; Hume *et al.*, 2009), NPR-A has a diffuse intracellular distribution in our initial immunolocalization experiments. In all of these studies the cells were fixed in formaldehyde and permeabilized prior to the addition of antibodies. Despite the similar observations for NPR-A localization, all of the previous studies failed to show that the staining was specific to a natriuretic peptide receptor. Airhart and colleagues examined co-localization of NPR-A and its downstream effector cGMP-dependent protein kinase (PKG) following ANP exposure in HEK-NPR-A cells (Airhart *et al.*, 2003). Recombinant PKG protein was added to effectively block the PKG signal and demonstrate specificity of the anti-PKG antibody, but this type of control was

not performed for NPR-A. No staining was reported in the absence of primary antibody; however, this data was not shown and it is unclear as to whether this control was performed in the absence of antibody to NPR-A, PKG, or both. Meanwhile, Abdelalim and Tooyama completely neglected to show or mention controls for their NPR-A and NPR-B immunolocalization studies in mouse embryonic stem cells (Abdelalim and Tooyama, 2009). Since all of the mammalian natriuretic peptide receptors are cell-surface receptors, Hume and colleagues used GFP-labeled H-Ras as a plasma membrane marker in their immunolocalization study of NPR-B mutants (Hume *et al.*, 2009). Not only did NPR-B staining appear to be intracellular in the HeLa cells, but, unimpressively, the plasma membrane marker also appeared to be cytoplasmic. No controls for the NPR-B signal were shown or reported in this study. Hence, it was essential for our study to demonstrate that the observed staining is specific to NPR-A prior to additional investigation.

Cells exposed to primary antibody prior to permeabilization show FLAG-NPR-A-specific staining at the plasma membrane. To our knowledge, this is the first NPR-A immunolocalization assay that visualizes NPR-A exclusively at the cell surface. Although prolonged exposure of FLAG-NPR-A transfected HeLa cells to ANP causes a visibly reduced NPR-A signal at the cell surface, it does not indicate where the receptors have gone. The immunoblot data indicates that a significant portion of the total receptors is degraded following prolonged hormone exposure; however, it is also possible that ANP-exposed NPR-A is accumulating in intracellular vesicles as well. Using our current experimental approach, it is difficult to quantitatively measure the decrease in FLAG-NPR-A signal because of the heterogeneous FLAG-NPR-A expression levels introduced by the transient transfection. Attempts to generate HeLa cells stably expressing high

levels of FLAG-NPR-A and alleviate this problem were unsuccessful. Live cell imaging may provide more insight on the trafficking path of FLAG-NPR-A in future studies, as the same cells expressing FLAG-NPR-A could be monitored over time with ANP.

In conclusion, data from primary, immortalized, and transfected cells are consistent and in agreement with the *in vivo* observations for ANP-dependent NPR-A downregulation. In other words, prolonged cellular exposure to ANP stimulates NPR-A degradation. The Pandey group used ligand binding assays to suggest that ANP binding stimulates NPR-A downregulation as early as 1986 (Pandey *et al.*, 1986), and now the majority of long-term exposure data confirm this hypothesis. However, similarly to the Maack group (Koh *et al.*, 1992; Vieira *et al.*, 2001), and unlike the results from Pandey and colleagues, we failed to observe significant NPR-A degradation within the first hour of ANP exposure. A caveat to this interpretation is that our studies measure reductions in the total cellular pool of NPR-A, and if the amount of NPR-A that is degraded at the cell surface is low compared to the total cellular receptor population then changes in extracellular NPR-A levels may not be detectable with our methods. Nevertheless, this study provides the foundation for studies on the mechanisms of NPR-A downregulation.

Figure 1

Endogenous NPR-A is downregulated by ANP. bAEC (A and B) or HeLa (C and D) cells were incubated in 200 nM ANP for the indicated periods of time; HeLa cells were also incubated in 10 μg/ml cycloheximide. Membranes were prepared and assayed for guanylyl cyclase activity and plotted as a function of time in the presence of ANP (A and C). In a parallel experiment, NPR-A was purified by immunoprecipitation and detected by immunoblot (B and D). 293T NPR-A is a positive control. Data points are represented as mean ± SEM, where N = 3. The data are representative of at least three separate experiments.

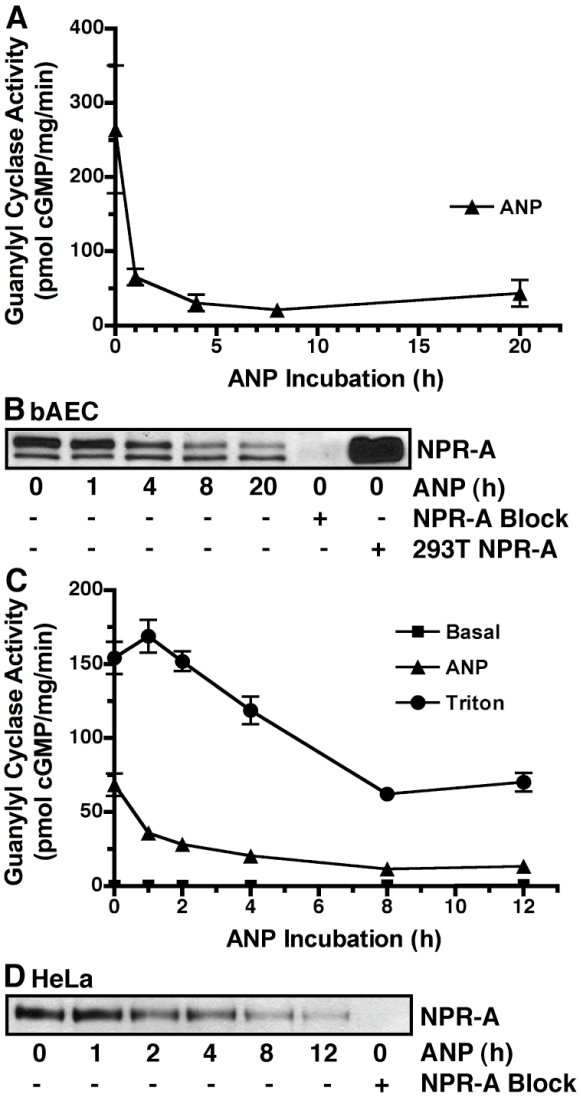
A
Guanylyl Cyclase Activity
(pmol cGMP/mg/min)
400
300
200
100
0
0
5
10
15
20
ANP Incubation (h)
ANP
B bAEC
NPR-A
0 1 4 8 20 0 0 ANP (h)
- - - - - + - NPR-A Block
- - - - - - + 293T NPR-A
C
Guanylyl Cyclase Activity
(pmol cGMP/mg/min)
200
150
100
50
0
0 2 4 6 8 10 12
ANP Incubation (h)
Basal
ANP
Triton
D HeLa
NPR-A
0 1 2 4 8 12 0 ANP (h)
- - - - - - + NPR-A Block

Figure 2

Endogenous NPR-A is responsible for the majority of ANP-dependent and – independent guanylyl cyclase activity in HeLa cells. HeLa cells were transfected with siRNA against glyceraldehyde-3-phosphate dehydrogenase (GAPDH) or NPR-A. (A) NPR-A was immunoprecipitated and detected by immunoblot to verify the NPR-A knock down. (B) Membranes were prepared and assayed for guanylyl cyclase activity following a 3 min basal, ANP, or Triton X-100 stimulation. Data points are represented as mean ± SEM, where N = 3.

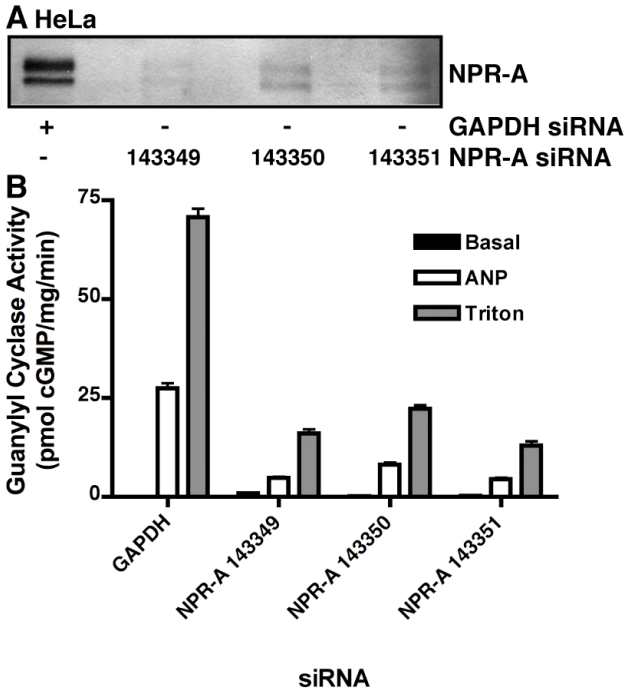
A HeLa
NPR-A
+ - - - GAPDH siRNA
- 143349 143350 143351 NPR-A siRNA
B
Guanylyl Cyclase Activity (pmol cGMP/mg/min)
75
50
25
0
Basal
ANP
Triton
GAPDH
NPR-A 143349
NPR-A 143350
NPR-A 143351
siRNA

Figure 3

ANP stimulates NPR-A downregulation in 293T NPR-A cells. (Top) 293T cells stably overexpressing NPR-A were incubated in 10 μg/ml cycloheximide and 1 μM ANP for indicated periods of time and then NPR-A protein levels were detected by sequential immunoprecipitation-immunoblotting. (Bottom) Data from the immunoblot was quantitated and presented in graphical form as a mean and range, where N = 2. Error bars are within the symbols. 293T NPR-A data is representative of three similar experiments.

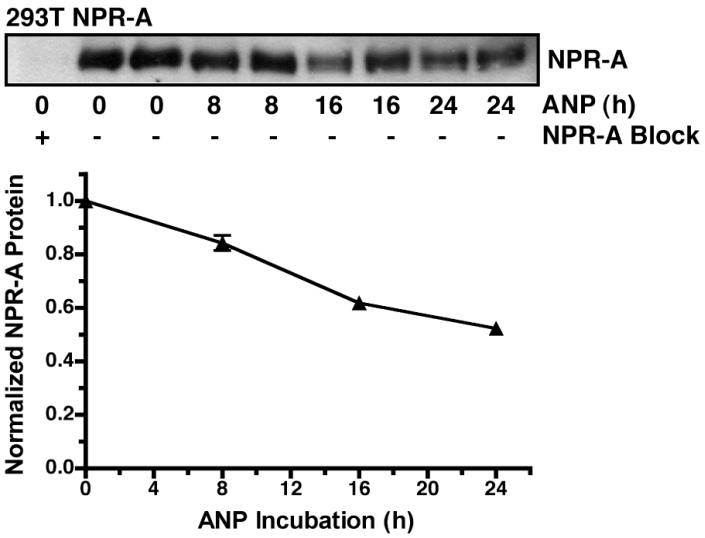
293T NPR-A
NPR-A
0 0 0 8 8 16 16 24 24 ANP (h)
+ - - - - - - - - NPR-A Block
Normalized NPR-A Protein
1.0
0.8
0.6
0.4
0.2
0.0
0 4 8 12 16 20 24
ANP Incubation (h)

Figure 4

FLAG-NPR-A is expressed and activated by ANP at the cell surface, and ANP exposure causes FLAG-NPR-A degradation. (A) 293neo cells transfected with GFP, NPR-A (wildtype), or FLAG-NPR-A were stimulated with 1 μM ANP for 3 min and cGMP levels were measured. FLAG-NPR-A transfected cells were stimulated with anti-FLAG M2 antibody or both ANP and anti-FLAG M2 antibody as well. Data points are represented as mean ± SEM, where N = 8. (B) CHO-pCEP6 cells were transiently transfected with or without FLAG-NPR-A and incubated with 10 μg/ml cycloheximide in the absence or presence of 200 nM ANP for 10 h. FLAG-NPR-A was immunoprecipitated and detected by immunoblot using antibody to both NPR-A (top) and the FLAG epitope (bottom). NPR-A isolated from 293T NPR-A cells was used as a positive control.

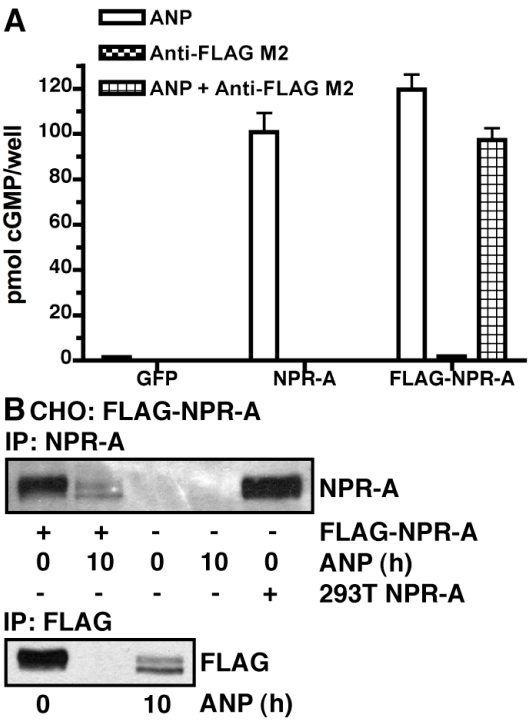
A
ANP
Anti-FLAG M2
ANP + Anti-FLAG M2
pmol cGMP/well
120
100
80
60
40
20
0
GFP
NPR-A
FLAG-NPR-A
B CHO: FLAG-NPR-A
IP: NPR-A
NPR-A
+ + - - - FLAG-NPR-A
0 10 0 10 0 ANP (h)
- - - - + 293T NPR-A
IP: FLAG
FLAG
0 10 ANP (h)

Figure 5

Controls for immunolocalization of NPR-A. HeLa cells transfected with FLAG-NPR-A (B-I) were grown on coverslips and fixed in 4% formalin/0.2% Triton X-100. Cells were washed, blocked for 1 h at 37°C, and then incubated with anti-FLAG M2 antibody (A-D, F-I) or antibody to the carboxyl-terminus of NPR-A (E) for 1 h at 37°C. To observe cell surface NPR-A, live cells were blocked and incubated with anti-FLAG M2 antibody prior to fixing (G-I). Cells were then washed, incubated with FITC-conjugated anti-mouse or –rabbit IgG for 45 min at 37°C, washed, and mounted on slides. (A) Mock transfected cells. (B) No primary antibody added. (C) No secondary antibody added. (D) NPR-A identified with antibody to the FLAG epitope. (E) NPR-A identified with antibody to NPR-A. (F) Anti-FLAG M2 antibody incubated with FLAG peptide. (G) NPR-A (green) at the cell surface. (H) Plasma membrane marker (red) (Alexa Fluor 594-conjugated wheat germ agglutinin). (I) Co-localization of NPR-A (G) and the plasma membrane marker (H).

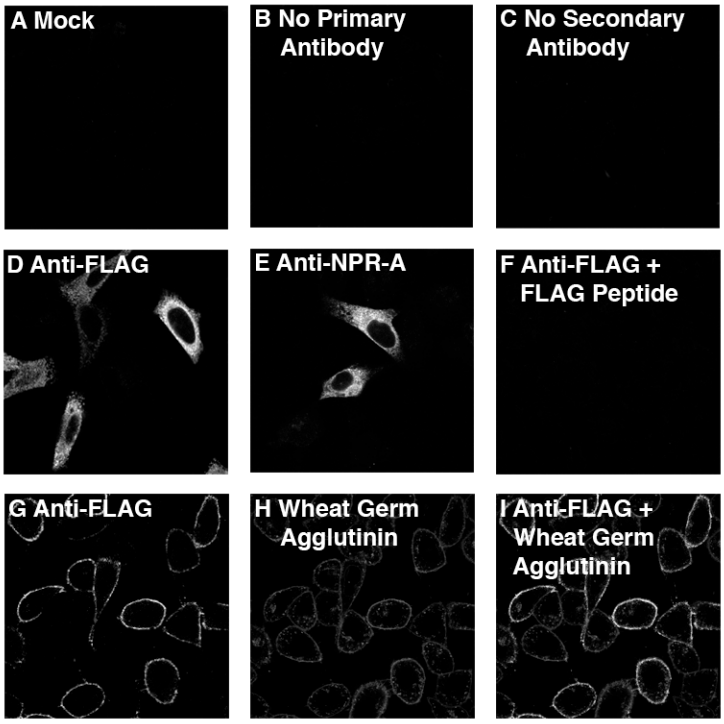
A Mock
B No Primary Antibody
C No Secondary Antibody
D Anti-FLAG
E Anti-NPR-A
F Anti-FLAG + FLAG Peptide
G Anti-FLAG
H Wheat Germ Agglutinin
I Anti-FLAG + Wheat Germ Agglutinin

Figure 6

Prolonged ANP exposure results in decreased cell-surface FLAG-NPR-A. HeLa cells transfected with FLAG-NPR-A were grown on coverslips. Cells were incubated in 10 μg/ml cycloheximide and were blocked and incubated with anti-FLAG M2 antibody prior to fixing and incubation with FITC-conjugated anti-mouse IgG. (A-C) Live cells were incubated with 200 nM ANP for 0 min (A), 10 min (B), or 60 min (C). (D) In a separate experiment, live cells were incubated in the absence (top) or presence (bottom) of 200 nM ANP for 8 h. Unless noted (B and C), images were captured at 60X. Images are representative of at least three separate experiments.

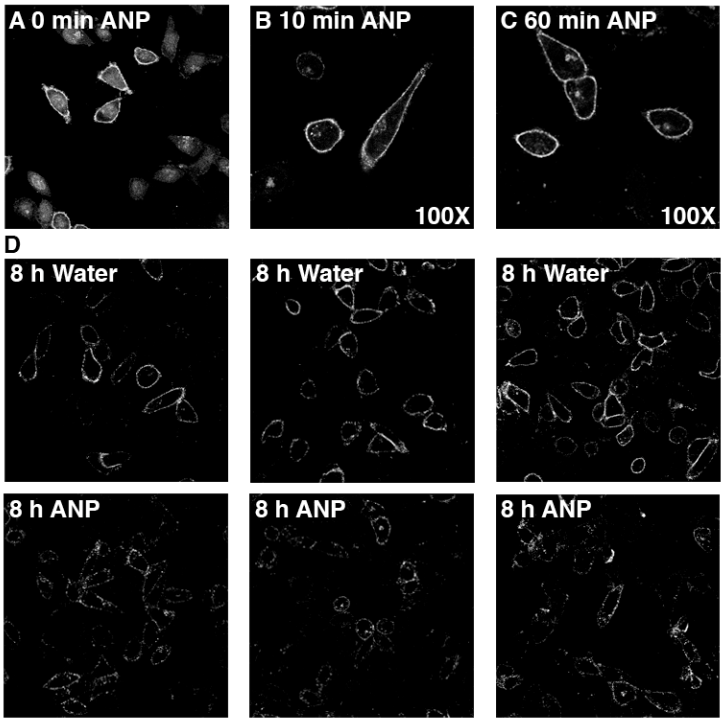
A 0 min ANP
B 10 min ANP
100X
C 60 min ANP
100X
D
8 h Water
8 h Water
8 h Water
8 h ANP
8 h ANP
8 h ANP

CHAPTER 4

Atrial Natriuretic Peptide and Clathrin Suppression Increase Natriuretic Peptide Receptor-A Internalization: Evidence for Clathrin- and Dynamin-Independent Internalization

This chapter is modified from the manuscript:

Flora, D.R., and Potter, L.R. Atrial natriuretic peptide and clathrin suppression increase guanylyl cyclase-A internalization: evidence for a novel trafficking pathway.

Introduction

Atrial natriuretic peptide (ANP) and B-type natriuretic peptide (BNP) are pleiotropic endogenous cardiac hormones that are essential for cardiovascular homeostasis. Both peptides elicit their beneficial effects by binding natriuretic peptide receptor-A (NPR-A), also known as guanylyl cyclase-A. NPR-A is a transmembrane receptor guanylyl cyclase consisting of an extracellular ligand-binding domain, a single membrane-spanning domain, and multiple intracellular regions including a guanylyl cyclase catalytic domain (Potter and Hunter, 2001). Activation of NPR-A leads to the synthesis of the intracellular second messenger cGMP, which mediates the vast majority of natriuretic peptide effects by regulating cGMP-dependent protein kinases, phosphodiesterases, and ion channels (Potter *et al.*, 2006). Natriuretic peptides also bind the natriuretic peptide clearance receptor (NPR-C), which lacks guanylyl cyclase activity and controls local natriuretic peptide concentrations via receptor-mediated ligand internalization and degradation (Nussenzveig *et al.*, 1990; Matsukawa *et al.*, 1999).

Elevated circulating ANP and BNP levels are markers for cardiovascular stress and are used clinically to gauge severity of disease (Gardner, 2003; Ruskoaho, 2003). Initially, these cardiac peptides stimulate compensatory hemodynamic functions, but over time natriuretic peptide-dependent cardiac unloading effects wane despite continued elevation of serum ANP and BNP concentrations (Cody *et al.*, 1986). Reduced NPR-A levels resulting from ligand-dependent receptor degradation contribute to the loss of natriuretic peptide response in heart-failed patients and animal models (Tsutamoto *et al.*, 1993; Bryan *et al.*, 2007; Dickey *et al.*, 2007). Unfortunately, the molecular mechanisms and trafficking pathways underlying NPR-A downregulation are not known, which impedes the development of potential therapeutic strategies that disrupt this

process and prolong the beneficial compensatory effects of natriuretic peptides in patients with cardiovascular disease.

Previous studies regarding the intracellular trafficking of NPR-A have exclusively focused on measuring ligand-dependent NPR-A internalization and degradation as detected by ^{125}I-ANP binding to whole cells. Although this is a useful and reasonable first approach to this problem, interpretation of data from these experiments is hindered due to changing binding affinities, difficulties in removing prior bound ANP from receptors (prior receptor occupation), and the common scenario of cells expressing two surface ANP binding proteins (NPR-A and NPR-C) (Schiffrin *et al.*, 1991; Jewett *et al.*, 1993). As a result of these studies, contradictory results have been reported for the internalization and degradation of NPR-A. Some groups reported relatively fast internalization and degradation of NPR-A after exposure of cells to ANP for 1 h, whereas others observed no internalization and degradation under similar conditions (Koh *et al.*, 1992; Pandey, 1992; Pandey *et al.*, 2002; Fan *et al.*, 2005). To complicate matters, we recently observed that endogenous NPR-A is not detectably degraded after exposure to ANP for 1 h, but is degraded after prolonged exposure to ligand, where the half-life ($t_{1/2}$) for degradation is approximately 4 h (Chapter 3).

What is clearly lacking in the analysis of the degradation of NPR-A are basic studies describing the mechanisms that control receptor downregulation. Here, we examined NPR-A trafficking in the well-characterized HeLa cell model using a newly developed assay employing monoclonal antibody binding to an extracellular receptor epitope that allows the measurement of NPR-A removal from the plasma membrane. To our knowledge, this is the first report to characterize basal and ligand-dependent NPR-A internalization and the first to use molecular loss-of-function approaches to link NPR-A to

common internalization pathways. We found that NPR-A is removed from the plasma membrane by a slow clathrin- and dynamin-independent process that is increased by ANP. Surprisingly, we found that clathrin depletion stimulates NPR-A uptake.

Materials and Methods

Materials

Rat ANP, cycloheximide, microcystin LR, and monoclonal anti-FLAG M2 antibody were purchased from Sigma-Aldrich (St. Louis, MO). Antibody against human CD8 was obtained from ATCC (51.1 mouse hybridoma cell line, HB-230; Manassas, VA) and was cultured using standard protocols. Cyclic GMP RIA kit, ^{125}I-anti-mouse IgG (goat), and ^{125}I-transferrin (human) were purchased from PerkinElmer (Waltham, MA).

FLAG-NPR-A Construct

Rat NPR-A was excised from pCMV3-GC-A (Potter and Garbers, 1992) by digestion with NotI and BglII and subcloned into the same sites in the multiple cloning region of pFLAG-CMV1 (Sigma-Aldrich), which contains a FLAG epitope inserted carboxyl-terminal to the Met-preprotrypsin coding sequence to generate pCMV1-FLAG-NPR-A. The resulting plasmid generates an amino-terminal FLAG-tagged receptor after cleavage of the signal sequence.

Cell Culture

Stably transformed tetracycline transactivator (tTA) HeLa cells were cultured as previously described (Sever *et al.*, 2000).

Transfections

HeLa or tTA HeLa cells were transfected with Lipofectamine 2000 (Invitrogen; Carlsbad, CA) according to manufacturer's instructions 24-48 h prior to analysis.

Adenoviruses and Infections

CD8 and rat NPR-A were excised by digestion with HindIII and NotI from pCR2.1-CD8-LDLR (Dr. Sandra Schmid; Scripps Institute; La Jolla, CA) and with NotI from pCMV3-GC-A (Potter and Garbers, 1992), respectively. The inserts were amplified by polymerase chain reaction (PCR) and subcloned into the HindIII/NotI sites of both pAdCMV(+) and pAdtet7 for adenovirus production (Damke *et al.*, 1995). The resulting plasmids generate an amino-terminal CD8-tagged form of NPR-A. The cDNA for an amino-terminal hemagglutinin (HA)-tagged dominant negative K44A mutant of dynamin-1 was a generous gift from Dr. Sandra Schmid (Scripps Institute) and was used for adenovirus production as previously described (Damke *et al.*, 1995).The pAdtet adenovirus was used as an infection control and does not express any form of dynamin. Adenovirus was added to the cell medium 10-12 h before analysis.

Small Interfering RNA (siRNA) Knock Down

Silencer GAPDH siRNA, Silencer negative control #2 siRNA, and siRNAs targeting human clathrin heavy chain [#146528: sense: 5'-CGUGUUAUGGAGUAUAUUAtt-3'; anti-sense: 5'-UAAUAUACUCCAUAACACGtg-3' and #107565: sense: 5'-GGCUCAUACCAUGACUGAUtt-3'; anti-sense: 5'-AUCAGUCAUGGUAUGAGCCtt-3'] were purchased from Ambion (Austin, TX). Thirty nmol siRNA were transfected into HeLa or tTA HeLa cells using Lipofectamine 2000 (Invitrogen). Cells were incubated for 48-72 h post-transfection before analysis.

Intracellular Accumulation of NPR-A

HeLa or tTA HeLa cells transfected with FLAG-NPR-A, or tTA HeLa cells infected with CD8-NPR-A adenovirus, were removed from 10 cm plates with PBS containing 5 mM EDTA. To slow internalization, suspended cells were cooled to 4°C and washed in 1 ml

DMEM containing 10% FBS. Fifty microliters of cell suspension were removed to determine expression of various proteins by immunoblot. Cells were incubated for 30 min with the anti-FLAG M2 (1:250) or anti-CD8 (1:50) antibody, washed in DMEM containing 0.5% bovine serum albumin (BSA), and then incubated with ^{125}I-anti-mouse IgG for 30 min. After washing in DMEM containing 0.5% BSA, the cells were resuspended in DMEM containing 10% FBS. Fifty microliters of cells were dispensed into tubes and incubated in a 37°C water bath for 0, 2, 5, 10, 15, 20, 40, or 60 min. All tubes except those designated "total counts" were washed with 0.2 M acetic acid and 0.5 M NaCl for 5 min at 4°C to remove ^{125}I-anti-mouse IgG bound to the cell surface. The cells were then pelleted, the supernatant removed, and the amount of radioactivity in the pellets was determined in a gamma counter. Total radioactivity was approximately 30-fold higher in FLAG-NPR-A transfected cells compared to cells expressing the wildtype receptor with no FLAG tag (mock) under control conditions. Nonspecific counts, obtained from mock-transfected cells, were subtracted from the counts generated from each time point and graphed as a percentage of the "total counts". Linear regression was used to determine the initial rate of intracellular accumulation, and a paired t-test was used to determine statistical significance.

Whole Cell cGMP Elevation Assay

tTA HeLa cells, grown on 24-well plates, were transfected with pEGFP or pCMV3-GC-A using Lipofectamine 2000 or infected with CD8-NPR-A adenovirus. The day of the assay, the cells were incubated in serum-free medium for at least 4 h. Medium was aspirated, and the cells were incubated for 20 min at 37°C in DMEM containing 20 mM HEPES (pH 7.4) and 0.5 mM IBMX. This medium was then replaced with the same medium containing 1 μM rat ANP, a 1:200 dilution of anti-CD8 antibody, or both 1 μM rat

ANP and a 1:200 dilution of anti-CD8 antibody, and stimulated for 5 min. The reaction was terminated by aspirating the medium and adding 1 ml of ice-cold 80% ethanol. One hundred and fifty microliters of the resulting supernatant was dried in a centrifugal vacuum concentrator and analyzed for cGMP content by radioimmunoassay.

Immunoprecipitation and Immunoblotting

Cells were solubilized in 1 ml of ice-cold modified RIPA buffer containing 50 mM Tris (pH 7.5), 100 mM NaCl, 1% NP-40, 0.5% sodium deoxycholate, 0.1% SDS, 10 mM NaH_2PO_4, 50 mM NaF, 2 mM EDTA, 0.5 μM microcystin LR, and 1X Complete protease inhibitors (Roche Diagnostics; Indianapolis, IN). To reduce nonspecific binding, solubilized cells were incubated at 4°C with 50 μl protein A (RepliGen; Waltham, MA) for at least 30 min. NPR-A was immunoprecipitated overnight at 4°C using 2 μl of polyclonal rabbit 6325 antiserum, which recognizes the last 17 carboxyl-terminal amino acids of rat NPR-A, and 50 μl protein A. Immunocomplexes were washed three times with 1 ml of ice-cold RIPA buffer, fractionated by SDS-PAGE, and transferred to polyvinylidene fluoride (PVDF) membrane.

Primary antibodies for immunoblot analysis were polyclonal rabbit CD8-α (H-160) (1:1000; Santa Cruz Biotechnology; Santa Cruz, CA) to CD8, monoclonal TD.1 (1:2500; Covance Research Products; Denver, PA) to clathrin heavy chain (Nathke *et al.*, 1992), polyclonal rabbit 6325 (1:2500) to NPR-A (Abbey and Potter, 2002), monoclonal 12CA5 (1:1000) to the HA epitope (Wilson *et al.*, 1984), or monoclonal E7 (1:5000) to β-tubulin. Secondary antibodies were peroxidase-conjugated donkey anti-rabbit IgG (1:20,000; GE Healthcare; Buckinghamshire, UK), peroxidase-conjugated sheep anti-mouse IgG (1:20,000; GE Healthcare), or goat anti-rabbit IRDye 680 (1:10,000; LI-COR Biosciences; Lincoln, NE).

Immunolocalization of Transferrin

DMEM containing 0.5% BSA and 5-10 μg/ml Alexa Fluor 488-conjugated transferrin (Invitrogen) was added to cells grown on glass coverslips and incubated at 37°C. After 5-20 min, the coverslips were transferred to ice and fixed with 4% formaldehyde. The coverslips were mounted with Vectashield (Vector Laboratories; Bulingame, CA) and imaged using a Zeiss Axioskop 2 microscope.

Intracellular Accumulation of Transferrin

A portion of cells harvested for the NPR-A accumulation assay were removed and pelleted by low speed centrifugation. To slow internalization, pelleted cells were moved to 4°C and resuspended in 500 μl of a PBS solution containing 1 mM $MgCl_2$, 1 mM $CaCl_2$, 5 mM glucose, and 0.2% BSA. Suspended cells were incubated with ^{125}I-transferrin for 30-40 min. Cells were then pelleted, resuspended in DMEM containing 10% FBS, aliquoted (50 μl) into tubes, and incubated in a 37°C water bath for 0, 1, 3, 5, 7, or 9 min. All tubes except those designated “total counts” were washed with 0.2 M acetic acid and 0.5 M NaCl for 5 min at 4°C. The cells were then pelleted, the supernatant removed, and the radioactivity level of the pellets was determined in a gamma counter. Counts from each time points were graphed as percentage of the “total counts”.

Quantification and Statistical Analysis

Immunoblots were quantified on a FLA-5000 imaging system with ImageGauge software (FUJIFILM Life Science) or an Odyssey Infrared Imaging System (LI-COR Biosciences). Microsoft Excel and GraphPad Prism software were used for statistical analysis of the data. The specific statistical tests performed are indicated in the figure legends.

Results

Development of a NPR-A Intracellular Accumulation Assay

To examine NPR-A internalization, a whole cell intracellular accumulation assay utilizing an amino-terminal FLAG-tagged version of NPR-A was developed (Figure 1). At 4°C anti-FLAG M2 antibody was added to whole cells to bind NPR-A at the cell surface. ^{125}I-conjugated anti-mouse IgG secondary antibody was subsequently added at 4°C to bind the primary antibody and radioactively label the extracellular receptor-primary antibody complex. Radioactivity measured at this step represents the total number of surface receptors at the time of labeling (total receptors). To initiate internalization, cells were transferred to a 37°C water bath in the presence or absence of ANP for increasing periods of time. The cells were acid washed at 4°C to remove surface radioactivity and subjected to gamma counting to determine the amount of receptors inside the cell (internalized receptors). The ratio of internalized to total receptors was plotted as a function of time at 37°C and represents the fraction of the initial surface receptors that are inside the cell after a given 37°C incubation period.

ANP Exposure Increases the FLAG-NPR-A Internalization Rate

In the absence of ANP (basal), NPR-A was internalized in a linear manner for up to 10 min (Figure 2A). Nearly 7% of the surface receptors were internalized during this period. A slight decrease in the internalization rate of FLAG-NPR-A was observed from 10 to 20 min, and maximum receptor accumulation was obtained at 40 min and maintained at 60 min. When the cells were warmed to 37°C in the presence of saturating amounts of ANP, the initial rate of intracellular NPR-A accumulation increased 1.4-fold, and after 60 min, total intracellular NPR-A was increased 1.8-fold compared to levels detected in cells not exposed to ANP.

The effect of prolonged ANP exposure on the internalization rate of NPR-A was also examined (Figure 2C). These studies were performed similarly to those described in Figure 2A except that the cells were incubated without or with ANP for 8 h at 37°C prior to conducting the accumulation assay. Total radioactivity detected in ANP-exposed cells was 47% of that detected in cells not exposed to ANP, indicating that prolonged ANP exposure reduces the number of receptors at the cell surface by approximately half (Figure 2B). In the absence of ANP, the initial internalization rate was linear between 2 and 10 min but declined at 15 min and maintained a steady, slow accumulation rate until the end of the assay. In contrast, the initial internalization rate remained linear between 2 and 20 min before slowing in cells exposed to ANP for 8 h. Comparison between the initial internalization rates revealed a 2-fold increase with ANP exposure, which was slightly greater than the increase observed in cells only exposed to ANP during the internalization assay. After 60 min, cells exposed to ANP had accumulated 3.6-fold more receptor than cells not exposed to ANP.

CD8-NPR-A is Internalized, But an 8 h ANP Exposure Does Not Degrade CD8-NPR-A

To overcome the low and varying FLAG-NPR-A expression levels associated with the transient transfections, two adenoviruses expressing amino-terminal CD8-tagged NPR-A were created. CD8-NPR-A expression is controlled by a tet-off system in one of the adenoviruses (pAdtet7-CD8-NPR-A). Similar to cells expressing wildtype receptor, cGMP levels were elevated in CD8-NPR-A-infected cells in the presence of ANP (Figure 3A). Simultaneous additions of ANP and anti-CD8 antibody caused a comparable increase in cGMP levels (Figure 3A). Addition of the anti-CD8 antibody alone did not stimulated cGMP production, which indicates that this receptor is not activated in the absence of ANP (Figure 3A). Similar responses were observed for both CD8-NPR-A

adenoviruses. Thus, CD8-NPR-A is expressed and activated at the cell surface, and neither the CD8 epitope nor its accompanying antibody stimulated or hindered receptor activation.

Since no problems with the CD8-NPR-A construct were identified in the whole cell stimulation, tetracycline transactivator (tTA) expressing HeLa cells were infected with CD8-NPR-A adenovirus to examine NPR-A internalization. CD8-NPR-A internalization was observed in the absence and presence of ligand; however, in contrast to the FLAG-NPR-A data, the difference in the initial internalization rates (0.49%/min for basal vs. 0.59%/min for ANP) was not statistically significant (Figure 3B). After 15 min, the rate of NPR-A accumulation between the two groups began to diverge, and by 60 min intracellular NPR-A accumulation had nearly doubled in the ANP-exposed cells.

Initial experiments aimed to examine the effect of prolonged ANP exposure on CD8-NPR-A internalization revealed that, contrary to the FLAG-NPR-A data (Figure 2B), total radioactivity in the ANP-exposed cells was not reduced. Thus, we investigated whether CD8-NPR-A was downregulated following an 8 h ANP exposure. Surprisingly, CD8-NPR-A protein levels were not noticeably degraded in ANP-exposed cells infected with CD8-NPR-A adenovirus compared to similarly infected cells not exposed to ANP (Figure 3C, top). Cells transfected with both of the CD8-NPR-A constructs had a similar resistance to CD8-NPR-A degradation in the presence of ANP (Figure 3C, bottom). Because we previously observed that both endogenous NPR-A and FLAG-NPR-A concentrations were markedly reduced in these same cells following an 8 h ANP exposure, no further experiments were performed with CD8-NPR-A.

Clathrin Reduction or Dynamin Inactivation Does Not Decrease ANP-Dependent NPR-A Degradation

Because clathrin-dependent internalization and degradation contributes to the regulation of most cell surface signaling receptors (Sorkin and von Zastrow, 2009) and lysosomal degradation of NPR-A has been previously reported (Pandey *et al.*, 2002), we investigated whether ANP-dependent NPR-A degradation was inhibited by reduced clathrin-mediated endocytosis. Transfection of HeLa cells, which endogenously express NPR-A, with siRNA against the heavy chain of human clathrin caused a reduction in clathrin heavy chain protein compared to cells transfected with control siRNA against glyceraldehyde 3-phosphate dehydrogenase (GAPDH) (Figure 4A). The reductions were functionally significant because transferrin internalization, a quintessential clathrin-dependent process, was markedly reduced in HeLa cells transfected with siRNA against clathrin (Figure 4B). Regardless, incubation with ANP for 10 h caused similar reductions in NPR-A protein levels in HeLa cells transfected with siRNA against GAPDH (84%) or clathrin heavy chain (87%) (Figure 4, C and D). Similar results were obtained using siRNA targeting two different exons of clathrin heavy chain. These data do not support a model where clathrin is required for ANP-stimulated NPR-A degradation in HeLa cells. However, we cannot rule out the possibility that residual functional clathrin is sufficient for normal NPR-A downregulation, particularly within this 10 h time frame.

The GTPase dynamin mediates vesicle scission required for many forms of endocytosis, including clathrin- and caveolin-mediated processes (Conner and Schmid, 2003; Doherty and McMahon, 2009). Thus, dynamin is required for more internalization pathways than clathrin. To study the possible involvement of dynamin in the ANP-dependent degradation of NPR-A, tTA HeLa cells were infected with an adenovirus encoding a dominant negative K44A mutant of dynamin-1 (K44A Dyn1), which inhibits dynamin-1 and dynamin-2 dependent internalization (Damke *et al.*, 1994). A large

reduction of transferrin uptake demonstrated that dynamin activity was markedly inhibited in cells infected with the K44A Dyn1 adenovirus (Figure 5A). However, prolonged ANP exposure reduced NPR-A protein levels by 37% and 49% in non-infected and K44A Dyn1-infected cells, respectively (Figure 5, B and C). These data are not consistent with dynamin being required for ANP-dependent degradation of NPR-A, but are also subject to the same caveats as the previously described clathrin knock down experiment.

Dynamin Inactivation Increases Long-Term Intracellular NPR-A Accumulation

Since dynamin is an established participant in the internalization of most cell surface receptors, we examined the effect of dynamin inhibition on FLAG-NPR-A internalization in tTA HeLa cells using the HA-tagged K44A Dyn1 adenovirus. Unlike the previous downregulation studies (Figures 4 and 5), this assay is not plagued by the problematic time lag between internalization and degradation. Furthermore, the expression of the K44A Dyn1 mutant was under the control of an inducible tet-off system; infected cells were grown in the absence or presence of tetracycline to allow or block expression of the K44A Dyn1 mutant, respectively. A separate group of cells were infected with a pAdtet adenovirus, which does not express dynamin, to control for viral load. Only cells infected with the adenovirus encoding K44A Dyn1 expressed this mutant protein and, furthermore, expression was severely reduced by the addition of tetracycline to the culture medium (Figure 6A).

In the absence of ANP, the initial rate of FLAG-NPR-A accumulation was similar in all three groups (pAdtet, K44A Dyn1, and K44A Dyn1 + Tetracycline) (Figure 6B). However, by 40 min cells expressing dominant negative K44A Dyn1 had higher intracellular FLAG-NPR-A levels than either control group (pAdtet or K44A Dyn1 + Tetracycline) and by 60

min intracellular receptor levels were twice that of the control groups. Intracellular accumulation in both control groups reached apparent steady state by 20 min with approximately 10% of the total labeled receptor pool internalized. Importantly, in cells where K44A Dyn1 expression was shut off by tetracycline exposure, intracellular NPR-A accumulation was not increased at 60 min.

Studies with the dominant negative K44A Dyn1 mutant were repeated in cells incubated with ANP (Figure 6C). Receptor accumulation was more variable under these conditions and no significant differences in initial rates were detected between cells expressing or not expressing K44A Dyn1. Intracellular accumulation throughout the assay was relatively similar between the two control groups and took slightly longer to reach apparent equilibrium compared to cells not incubated with ANP. Similarly to the basal internalization results, FLAG-NPR-A accumulation in cells expressing K44A Dyn1 did not reach equilibrium and uptake continued throughout the assay. After 60 min, the cells expressing K44A Dyn1 accumulated 1.7-fold more FLAG-NPR-A compared to cells not expressing K44A Dyn1.

Prior to the termination of the CD8-NPR-A studies, accumulation assays with CD8-NPR-A in the absence or presence of the K44A Dyn1 adenovirus were performed (Figure 7). The results were strikingly consistent to those of FLAG-NPR-A in Figure 6B. Basal intracellular accumulation between groups was nearly identical in the first 20 min of the assay. After 20 min, accumulation slowed in the non-infected cells, whereas the K44A Dyn1-infected cells continued to accumulate CD8-NPR-A in a linear manner. At 40 and 60 min, intracellular accumulation in cells expressing the K44A Dyn1 mutant were increased 1.4- and 2-fold, respectively.

Clathrin Reductions Increase Intracellular FLAG-NPR-A Accumulation

A siRNA approach was used to examine the requirement of clathrin in the NPR-A internalization process. siRNA against clathrin heavy chain dramatically reduced cellular clathrin levels compared to cells transfected with control siRNA (Figure 8A). More importantly, reduced clathrin heavy chain levels resulted in clear functional consequences. Intracellular ^{125}I-transferrin accumulation was reduced from 70% to 10% at 3 min in the cells transfected with control siRNA vs. siRNA against clathrin, respectively (Figure 8B).

Unexpectedly, initial basal FLAG-NPR-A uptake was increased in cells with reduced clathrin expression (Figure 8C). The initial internalization rate was elevated about 3.1-fold in cells transfected with siRNA against clathrin compared to cells transfected with control siRNA. The majority of receptor uptake in the clathrin-depleted cells occurred in the first 10 min and by 20 min the accumulation in both groups reached steady state. Receptor accumulation in the clathrin-depleted cells was almost double that of the control cells throughout the last 40 min of the assay.

Similar effects were observed in the presence of ANP (Figure 8D). The initial internalization rate was increased more than 2-fold in clathrin-depleted cells compared to control cells. Intracellular FLAG-NPR-A accumulation reached apparent steady state around 10 min in the clathrin knock down compared to more than 20 min in the control cells. However, by 60 min, accumulation in the control cells approached levels measured in cells lacking clathrin, which is consistent with the increased uptake effects of ANP and clathrin reductions converging on a common point in the NPR-A trafficking pathway.

Discussion

In this report, a novel antibody-based assay revealed that a relatively slow process that is stimulated by ligand internalizes NPR-A. Initially, ANP activates NPR-A and has little effect on downregulation; however, prolonged incubation with ANP decreases the number of receptors in the cell. We recently determined that the half-life of the total cellular NPR-A population (receptors at the cell surface and inside of the cell) in ANP-exposed primary bovine aortic endothelial and immortalized HeLa cells is about 4 h (Chapter 3; Figure 1). Here, we found that an 8 h ANP incubation decreases the number of receptors at the HeLa cell surface by 53% (Figure 2B). This is consistent with ligand-stimulated endocytosis reported for numerous of tyrosine kinase and G protein-coupled receptors (Sorkin and von Zastrow, 2009). Compared to the related cell surface receptor NPR-C, which reportedly internalizes at a rate of ~5%/min (Nussenzveig *et al.*, 1990), the basal NPR-A internalization rate of approximately 0.4-0.8%/min is sluggish. The disparity is not explained by a defect in the ability of the HeLa cells to undergo internalization because 70% of the labeled transferrin pool was internalized in 3 min, whereas less than 8% of the extracellular NPR-A pool had internalized after a 10 min exposure to ANP in the same cells (Figure 8, B and D). Rapid internalization is not just observed for nutrient receptors in HeLa cells because previous reports in these cells demonstrated that more than 70% of surface epidermal growth factor (EGF) receptors are internalized by 5 min (Vieira *et al.*, 1996). It is likely that NPR-A is physiologically regulated in the HeLa cells because NPR-A is endogenously expressed in HeLa cells and NPR-A is downregulated similarly in these cells as it is in endogenously expressing primary bovine aortic endothelial and overexpressing Chinese hamster ovary cells (Chapter 3; Figures 1B and 4B).

Previous investigators have used ^{125}I-ANP to track NPR-A internalization in various cell lines. However, the usefulness of this technique in the analysis of NPR-A is debatable because of the rapid release of ^{125}I-ANP from this receptor at physiologic temperatures (Koh *et al.*, 1992). When cells expressing NPR-A are allowed to bind ^{125}I-ANP at 4°C and then are rapidly warmed to 37°C, 75% of the radioactivity is released from the cells by 5-10 min (Koh *et al.*, 1992; Pandey, 1993; Fan *et al.*, 2005). This observation is consistent and not under debate. However, whether the released radioactivity is associated with intact or mostly intact ANP vs. degraded ANP is arguable. Maack and colleagues reported that ANP is released intact from cells (Koh *et al.*, 1992). Our laboratory found that a mostly intact form of ^{125}I-ANP was released from cells if an extracellular neutral endopeptidase inhibitor was included in the medium (Fan *et al.*, 2005). Neither group observed any effect of lysosomal inhibitors on ^{125}I-ANP degradation in cells expressing NPR-A, but did observe that the inhibitors significantly delayed ^{125}I-ANP degradation in cells expressing NPR-C. In contrast, a different group reported that the majority of the radioactivity released from cells expressing NPR-A is associated with a mostly degraded form of ^{125}I-ANP and that lysosomal inhibitors delayed this process (Pandey, 1993). Thus, published reports indicate that NPR-A is not internalized at all or is rapidly internalized. The current study is not hampered by the pitfalls associated with previous reports because it does not require ligand binding to track the receptor. Furthermore, it measured ligand-independent internalization as well as the effect of ANP on the basal internalization rate.

At the start of the accumulation assay, presumably labeled receptors can only remain at the cell surface or move inside the cell. Thus, the initial linear slope indicates the receptor internalization rate. However, at longer time points, sorting, recycling, and

degradation processes can contribute to the accumulation of NPR-A. Basal NPR-A accumulation reached steady state after 20 min. The presence of ANP increased FLAG-NPR-A accumulation at all stages of the uptake curve, which is consistent with ANP stimulating the transfer rate of receptors from outside to inside the cell. However, the difference in accumulation at longer time periods can also be explained by differential intracellular sorting, which affects the proportion of receptors that are either degraded or recycled back to the membrane. Differential sorting enables downregulation of many signaling receptors to occur in the presence, but not the absence, of an activating ligand, and is likely to play an important role in regulating NPR-A degradation as well. NPR-A accumulation reached a plateau during the last 40 min of the basal accumulation assay, which is consistent with the rate of recycling equaling the rate of internalization. Pandey and colleagues have reported recycling of the ^{125}I-ANP-NPR-A complex in multiple cell lines at rates of approximately 5%/min, which is considerably faster than the rate of internalization observed in our study (Pandey, 1992, 1993; Pandey *et al.*, 2002). K44A Dyn1 did not affect the initial NPR-A internalization rate; however, after steady state had been reached, intracellular NPR-A accumulation was elevated in cells expressing the K44A Dyn1 mutant. The fact that dynamin inhibition only increased NPR-A uptake at longer time points is consistent with dynamin participating in the recycling but not the internalization process (Figures 6 and 7). A study documenting dynamin-dependent recycling of transferrin receptors in HeLa cells has been reported (van Dam and Stoorvogel, 2002).

The dominant negative K44A Dyn1 mutant had no effect on either ANP-dependent NPR-A downregulation or basal or ANP-stimulated NPR-A internalization even though it blocked transferrin uptake (Figures 5-7). In contrast, earlier work with the EGF receptor

demonstrated that the K44A Dyn1 mutant potently inhibits ligand-induced endocytosis of the EGF receptor (Vieira *et al.*, 1996). Interestingly, initial NPR-A uptake was significantly increased in cells depleted of clathrin, but the robust accumulation was lost around 20 min (Figure 8, C and D). In the presence of ANP, NPR-A accumulation in control cells approached that observed in the clathrin knock down cells at longer time periods, which is consistent with the two processes converging on a common point in the NPR-A trafficking pathway. The robust initial uptake of NPR-A observed in the cells lacking clathrin may result from upregulation of a NPR-A transporting pathway. To our knowledge, this is the first example of clathrin depletion increasing the uptake of any receptor, consistent with the novel nature of NPR-A trafficking. This observation may be useful to investigators that study endocytic pathways and may eventually shed light on the upregulated pathway. Regardless, these studies clearly indicate that NPR-A is not internalized by a clathrin-coated pit mechanism in these cells.

To our knowledge, the specific mechanisms and pathways that mediate NPR-A internalization and degradation have not been examined before this study. The experimental approaches used to demonstrate requirements for clathrin and dynamin in the internalization of most other cell surface signaling receptors blocked internalization of the transferrin receptor in our studies, but failed to block cellular uptake of NPR-A. In conclusion, these data indicate that the majority of neither basal nor ANP-stimulated NPR-A internalization proceeds through a clathrin- or dynamin-dependent endocytic pathway. Additionally, the data suggest that clathrin suppression increases the initial transport of NPR-A into the cell. The inescapable conclusion from our studies is that NPR-A is regulated by a novel trafficking pathway that has little or no overlap with known pathways.

Figure 1

Intracellular accumulation assay. A cell with receptors at the cell surface is incubated at 4°C to slow receptor internalization. Primary antibody recognizing the extracellular domain of the receptor is added at 4°C to bind receptor at the cell surface. Radiolabeled secondary antibody is subsequently added to radioactively label the extracellular receptor-primary antibody complex. Incubation in a 37°C water bath initiates internalization of the receptor-antibody complexes. The cell is acid washed at 4°C to remove surface radioactivity and the remaining (intracellular) radioactivity is counted.

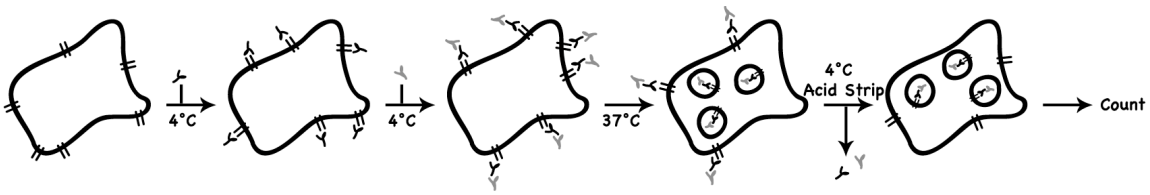
4°C
4°C
37°C
4°C
Acid Strip
Count

Figure 2

FLAG-NPR-A is slowly internalized by a process that is stimulated by ANP, and prolonged ANP exposure decreases FLAG-NPR-A at the cell surface. HeLa cells transiently transfected with FLAG-NPR-A were labeled at 4°C with anti-FLAG M2 antibody and ^{125}I-anti-mouse IgG as described under Materials and Methods. (A) The cells were incubated at 37°C in the absence or presence of 1 μM ANP for the periods of time shown and then acid-washed and counted. (B and C) Cells were incubated in 10 μg/ml cycloheximide in the absence or presence of 200 nM ANP for 8 h prior to the accumulation assay. ANP was also included in the internalization assay. (B) Total counts were normalized to the cells with no ANP exposure. Statistical significance was determined by a paired t-test where * indicates $p < 0.0001$ for no ANP vs. ANP. (A and C) Data points represent the mean ± SEM and were graphed as a percent of total counts where N = 12 for (A) and (C), respectively. Initial internalization rates (slopes) and statistical significance, determined by a paired t-test, were based on time points 2-10 min ($p < 0.05$) in (A) and 2-10 min (basal) or 2-20 min (ANP) ($p < 0.001$) in (C).

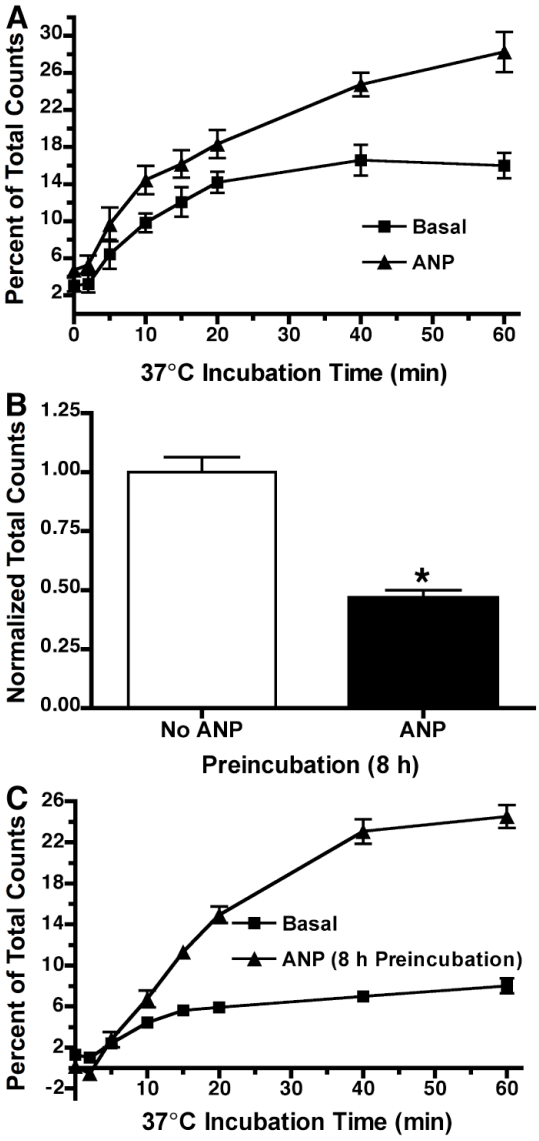
A
Percent of Total Counts
30
26
22
18
14
10
6
2
0
10
20
30
40
50
60
Basal
ANP
37°C Incubation Time (min)
B
Normalized Total Counts
1.25
1.00
0.75
0.50
0.25
0.00
*
No ANP
ANP
Preincubation (8 h)
C
Percent of Total Counts
26
22
18
14
10
6
2
-2
10
20
30
40
50
60
Basal
ANP (8 h Preincubation)
37°C Incubation Time (min)

Figure 3

Characterization of CD8-NPR-A. (A) CD8-NPR-A is expressed and activated at the cell surface. Tetracycline transactivator (tTA) HeLa cells transfected with GFP or NPR-A (wildtype), or infected with CD8-NPR-A adenoviruses (pAdCMV(+) or pAdtet7) were stimulated with 1 μM ANP and cGMP levels were measured. CD8-NPR-A-infected cells were also stimulated with anti-CD8 antibody or 1 μM ANP and anti-CD8 antibody. Data points are represented as mean ± SEM, where N = 4. (B) ANP exposure increases intracellular CD8-NPR-A accumulation. tTA HeLa cells were infected overnight with the pAdtet7-CD8-NPR-A adenovirus. CD8-NPR-A intracellular accumulation was measured as described under Materials and Methods in the absence and presence of 1 μM ANP. Data points represent the mean ± SEM and were graphed as a percent of total counts where N = 12. Initial internalization rates (slopes) and statistical significance, determined by a paired t-test, were based on time points 0-15 min ($p > 0.05$). (C) CD8-NPR-A is not significantly degraded after an 8 h ANP exposure. tTA HeLa cells were infected (top) or transiently transfected (bottom) with CD8-NPR-A and incubated with 10 μg/ml cycloheximide in the absence or presence of 200 nM ANP for 8 h. CD8-NPR-A was immunoprecipitated with antibody to NPR-A and detected by immunoblot using antibody to CD8α.

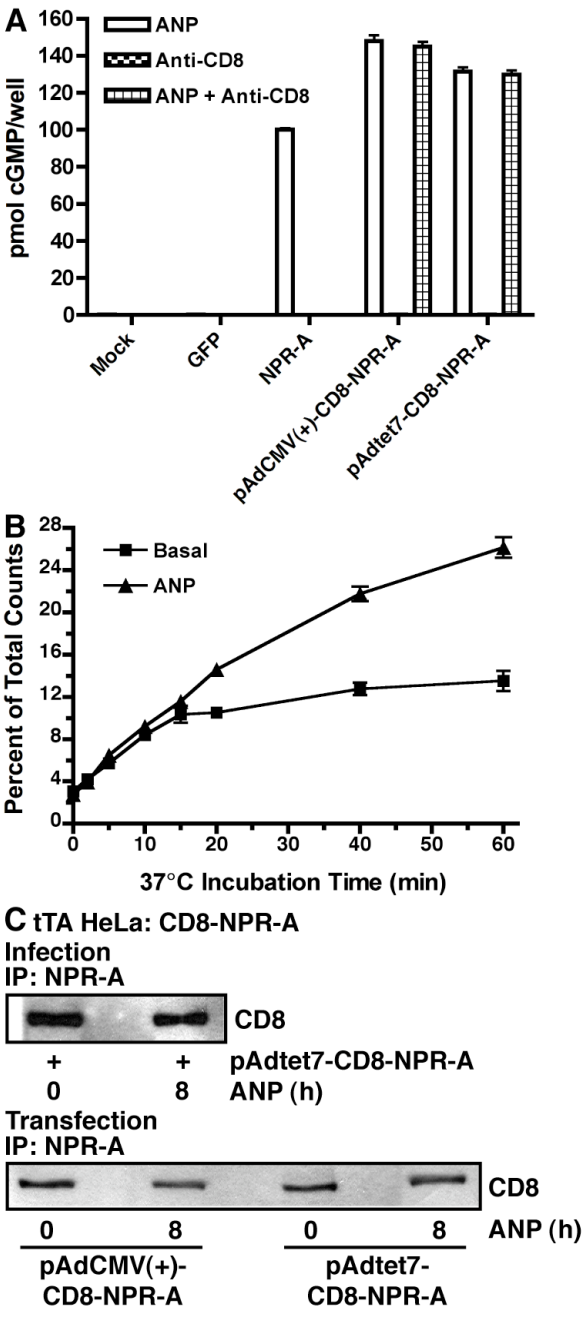
A
ANP
Anti-CD8
ANP + Anti-CD8
pmol cGMP/well
160
140
120
100
80
60
40
20
0
Mock
GFP
NPR-A
pAdCMV(+)-CD8-NPR-A
pAdtet7-CD8-NPR-A
B
Basal
ANP
Percent of Total Counts
28
24
20
16
12
8
4
0
0
10
20
30
40
50
60
37°C Incubation Time (min)
C tTA HeLa: CD8-NPR-A
Infection
IP: NPR-A
CD8
+
+
pAdtet7-CD8-NPR-A
0
8
ANP (h)
Transfection
IP: NPR-A
CD8
0
8
0
8
ANP (h)
pAdCMV(+)-
CD8-NPR-A
pAdtet7-
CD8-NPR-A

Figure 4

Clathrin heavy chain reductions do not inhibit ANP-dependent NPR-A degradation. HeLa cells were transfected with siRNA against glyceraldehyde 3-phosphate dehydrogenase (GAPDH) or clathrin heavy chain (CHC). (A) Clathrin protein levels are reduced in cells transfected with siRNA against CHC. (B) Transferrin uptake is inhibited in cells transfected with siRNA against CHC. (C) Cells were incubated in 10 μg/ml cycloheximide in the absence or presence of 200 nM ANP for 10 h. NPR-A was immunoprecipitated and detected by immunoblot. (D) Data from four independent experiments like that shown in (C) were quantified, normalized to GAPDH siRNA NPR-A protein levels, and presented as a mean ± SEM. Statistical significance was determined by a paired t-test. * indicates $p < 0.001$ for GAPDH siRNA vs. GAPDH siRNA + ANP, and # indicates $p < 0.05$ for CHC siRNA vs. CHC siRNA + ANP.

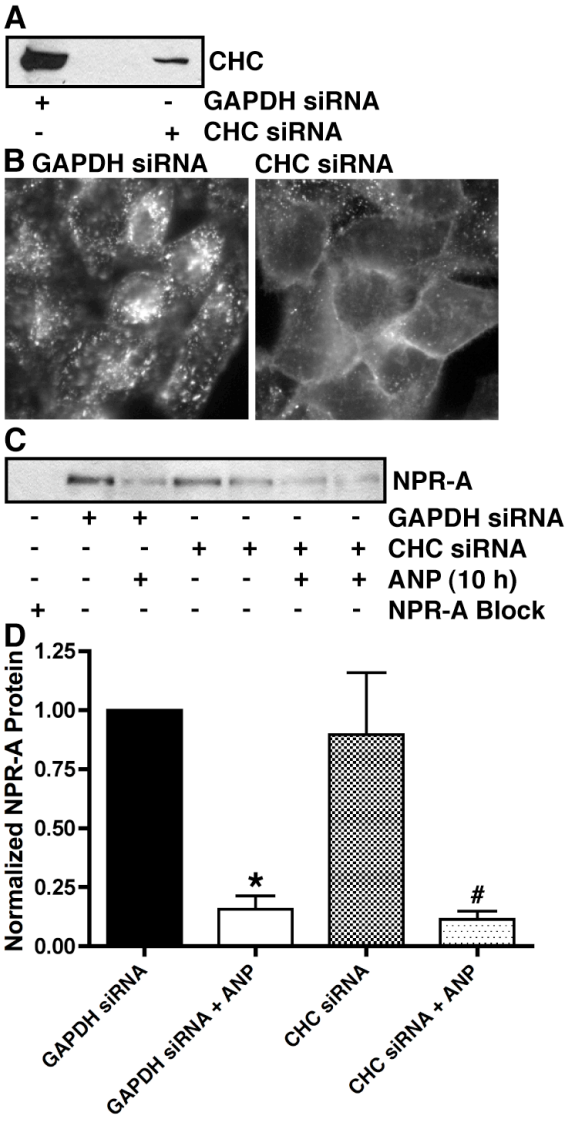
A
CHC
+ - GAPDH siRNA
- + CHC siRNA
B GAPDH siRNA
CHC siRNA
C
NPR-A
- + + - - - - GAPDH siRNA
- - - + + + + CHC siRNA
- - + - - + + ANP (10 h)
+ - - - - - - NPR-A Block
D
Normalized NPR-A Protein
1.25
1.00
0.75
0.50
0.25
0.00
*
#
GAPDH siRNA
GAPDH siRNA + ANP
CHC siRNA
CHC siRNA + ANP

Figure 5

Reduced dynamin activity does not inhibit ANP-dependent NPR-A degradation. tTA HeLa cells were infected overnight without or with an adenovirus encoding K44A dynamin-1 (Dyn1). (A) Transferrin uptake is inhibited in cells expressing K44A Dyn1. (B) Cells were incubated with 10 μg/ml cycloheximide in the absence or presence of 200 nM ANP for 10 h. NPR-A was immunoprecipitated and detected by immunoblot. (C) Data from five independent experiments like that shown in (B) were quantified, normalized to NPR-A levels measured in cells not expressing K44A Dyn1, and represented as mean ± SEM. Statistical significance was determined by an unpaired t-test. * indicates $p < 0.01$ for No Treatment vs. ANP, and # indicates $p < 0.0001$ for K44A Dyn1 vs. K44A Dyn1 + ANP.

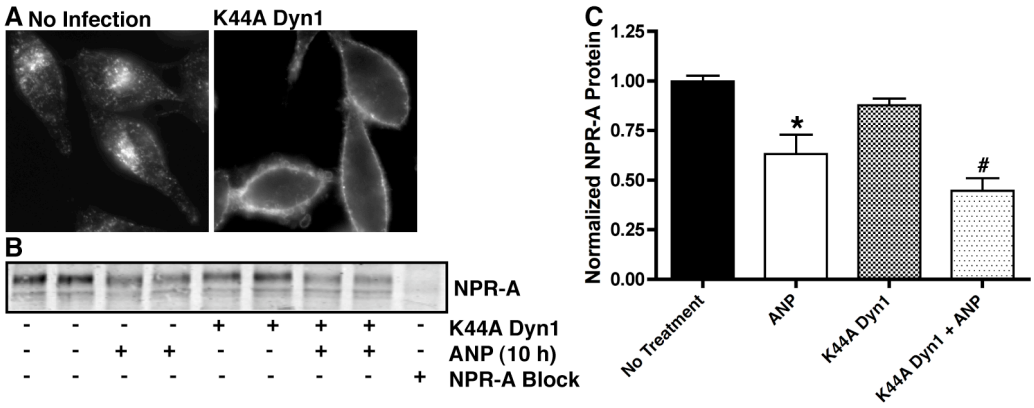
A No Infection
K44A Dyn1
B
NPR-A
- - - - + + + + - K44A Dyn1
- - + + - - + + - ANP (10 h)
- - - - - - - - + NPR-A Block
C
Normalized NPR-A Protein
1.25
1.00
0.75
0.50
0.25
0.00
*
#
No Treatment
ANP
K44A Dyn1
K44A Dyn1 + ANP

Figure 6

Reduced dynamin activity increases intracellular accumulation of FLAG-NPR-A at longer but not shorter time periods. FLAG-NPR-A transfected tTA HeLa cells were infected with either pAdtet or dominant negative K44A Dyn1 adenovirus and incubated in the absence or presence of 10-20 ng/ml tetracycline for 10-12 h prior to the accumulation assay. (A) Less than 5% of the cells from each treatment were fractionated by SDS-PAGE and proteins were detected by immunoblot with antibody to the HA epitope (top) or β-tubulin (bottom). K44A Dyn1 mutant expression was severely reduced in the presence of tetracycline. The immunoblot is representative of all experiments. (B) The accumulation assay was conducted as described in Figure 2 in the absence of ANP. (C) Cells were incubated at 37°C in the presence of 1 μM ANP. Data points represent the mean ± SEM and were graphed as a percent of total counts where N = 10 and N = 8 for (B) and (C), respectively. Initial internalization rates (slopes) and statistical significance, determined by a paired t-test, were based on time points 0-10 min ($p > 0.05$ for all comparisons) in (B) and 2-15 min ($p > 0.05$ for pAdtet vs. K44A Dyn1, $p > 0.05$ for pAdtet vs. K44A Dyn1 + Tetracycline, and $p < 0.05$ for K44A Dyn1 vs. K44A Dyn1 + Tetracycline) in (C).

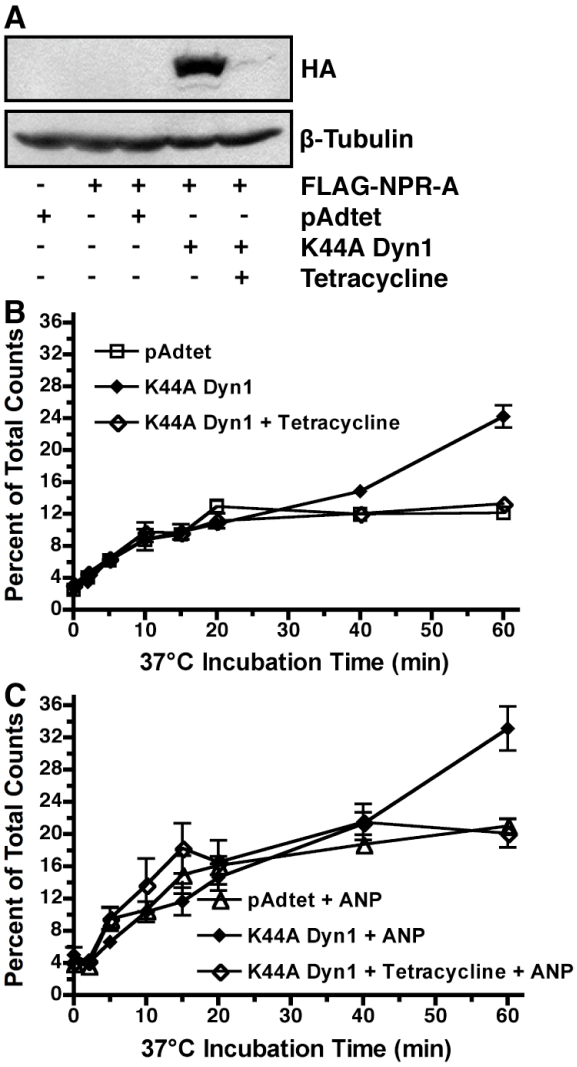
A
HA
β-Tubulin
- + + + +
+ - + - -
- - - + +
- - - - +
FLAG-NPR-A
pAdtet
K44A Dyn1
Tetracycline
B
Percent of Total Counts
pAdtet
K44A Dyn1
K44A Dyn1 + Tetracycline
37°C Incubation Time (min)
C
Percent of Total Counts
pAdtet + ANP
K44A Dyn1 + ANP
K44A Dyn1 + Tetracycline + ANP
37°C Incubation Time (min)

Figure 7

Intracellular accumulation of CD8-NPR-A is similar to that of FLAG-NPR-A in the presence of the dominant negative K44A Dyn1 mutant. tTA HeLa cells were infected 10-12 h with pAdtet7-CD8-NPR-A adenovirus, and one group was also infected with K44A Dyn1 adenovirus. Basal CD8-NPR-A intracellular accumulation was measured as described under Materials and Methods. Data points represent the mean ± SEM and were graphed as a percent of total counts where N = 12. Initial internalization rates (slopes) and statistical significance, determined by a paired t-test, were based on time points 0-15 min ($p > 0.05$). (Inset) A portion of cells were solubilized, fractionated by SDS-PAGE, and detected by immunoblot with antibody to the HA epitope to verify K44A Dyn1 expression. The immunoblot is representative of all experiments.

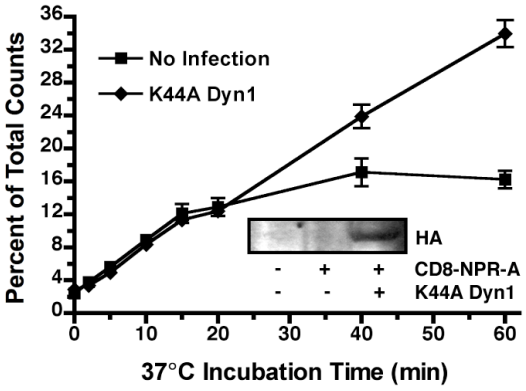
Percent of Total Counts
36
32
28
24
20
16
12
8
4
0
No Infection
K44A Dyn1
HA
- + + CD8-NPR-A
- - + K44A Dyn1
0
10
20
30
40
50
60
37°C Incubation Time (min)

Figure 8

Clathrin heavy chain reductions stimulate NPR-A internalization. tTA HeLa cells were transfected twice with siRNA against negative control #2 or clathrin heavy chain (CHC) and once with FLAG-NPR-A. (A) Solubilized cells were fractionated by SDS-PAGE and detected by immunoblot with antibody to either CHC (top) or β-tubulin (bottom). The immunoblot shown is representative of all experiments. (B) Clathrin heavy chain reductions markedly reduced ^{125}I-transferrin uptake. (C) The accumulation assay was conducted as described in Figure 2 in the absence of ANP. (D) Cells were incubated at 37°C in the presence of 1 μM ANP. Data points represent the mean ± SEM and were graphed as a percent of total counts where N = 7, N = 11, and N = 14 for (B), (C), and (D), respectively. Initial internalization rates (slopes) and statistical significance, determined by a paired t-test, were based on time points 0-10 min ($p < 0.005$) in (C) and 0-5 min ($p < 0.0005$) in (D).

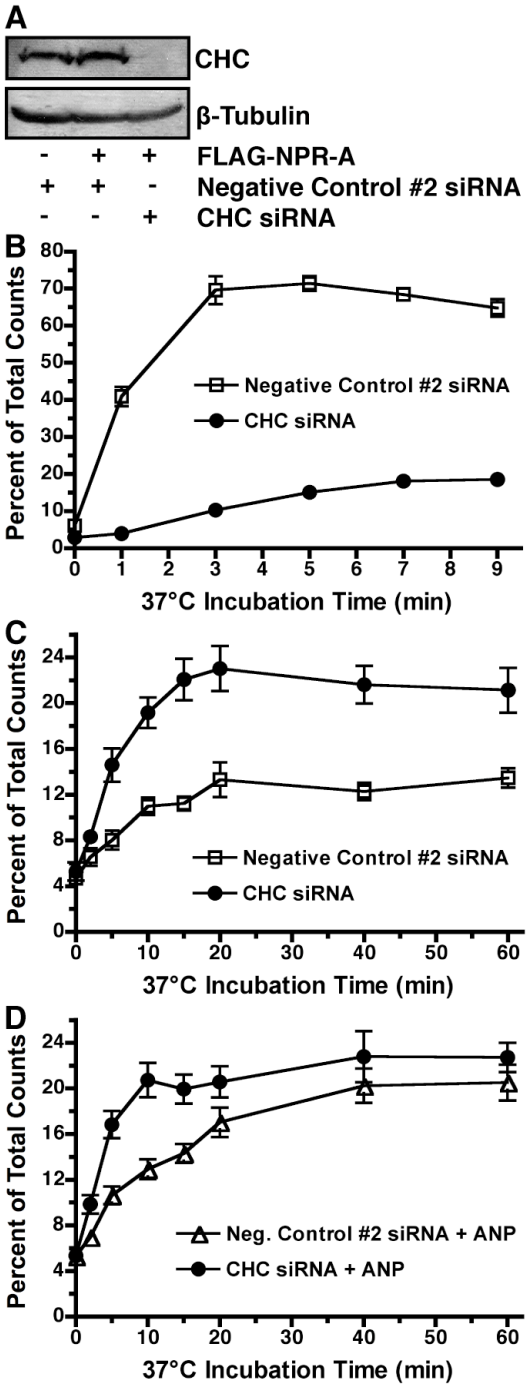
A
CHC
β-Tubulin
- + + FLAG-NPR-A
+ + - Negative Control #2 siRNA
- - + CHC siRNA
B
Percent of Total Counts
Negative Control #2 siRNA
CHC siRNA
37°C Incubation Time (min)
C
Percent of Total Counts
Negative Control #2 siRNA
CHC siRNA
37°C Incubation Time (min)
D
Percent of Total Counts
Neg. Control #2 siRNA + ANP
CHC siRNA + ANP
37°C Incubation Time (min)

CHAPTER 5

Conclusions and Future Directions

Summary

Cardiac natriuretic peptides are important endogenous regulators of cardiovascular homeostasis, and imbalances in the natriuretic peptide system lead to cardiovascular disease. Elevations in circulating atrial natriuretic peptide (ANP) and B-type natriuretic peptide (BNP) concentrations are correlated with disease progression; however, the molecular mechanisms responsible for disease progression in the presence of high natriuretic peptide concentrations are poorly understood. Here, a pressure-overload mouse model of congestive heart failure revealed that natriuretic peptide receptor-A (NPR-A), the receptor by which ANP and BNP mediate their physiological effects, is downregulated in the failed heart. Unexpectedly, the related natriuretic peptide receptor-B (NPR-B) was found to contribute to the majority of hormone-dependent guanylyl cyclase activity in the failed heart. Subsequent data demonstrated that prolonged ANP exposure resulted in degradation of NPR-A in various cell culture systems. Furthermore, ANP exposure reduced the number of receptors at the cell surface. To investigate potential mechanisms responsible for NPR-A downregulation, a novel antibody-based intracellular accumulation assay was developed and it revealed that NPR-A is basally internalized by a relatively slow clathrin- and dynamin-independent process that is stimulated by ANP. The rate of NPR-A internalization also increased in cells depleted of clathrin. Finally, although recycling of NPR-A has not been directly tested in these studies, dynamin inhibition increased intracellular NPR-A concentrations 40-60 min after initiation of internalization suggesting that NPR-A is recycled and that dynamin participates in this process.

Significance

The results from the congestive heart failure studies are significant in that they demonstrated for the first time *in vivo* differential regulation of natriuretic peptide receptors in the failed heart. It is well-established that activation of NPR-B by C-type natriuretic peptide (CNP) stimulates long bone growth; however, growing evidence has indicated that the CNP/NPR-A pathway may play a significant role in the heart as well (Kalra *et al.*, 2003; Del Ry *et al.*, 2005; Soeki *et al.*, 2005; Langenickel *et al.*, 2006). For the first time we found that NPR-B is responsible for a significant portion of natriuretic peptide-dependent guanylyl cyclase activity in the non-failed heart and the majority of activity in the failed heart. Conversely, NPR-A is downregulated in the failed heart, which is consistent with reports of a blunted natriuretic peptide response in heart-failed patients (Cody *et al.*, 1986; Tsutamoto *et al.*, 1993). These findings suggest that heart-failure drugs capable of stimulating NPR-B alone or in combination with NPR-A may be more effective than current treatment with nesiritide, which only activates NPR-A. Of additional significance, these studies demonstrated the ability to measure natriuretic peptide-dependent guanylyl cyclase activity and natriuretic peptide receptor concentrations in human heart tissue.

Our *in vivo* observation of NPR-A downregulation was consistently replicated in various cell culture systems, suggesting that ANP-dependent downregulation of NPR-A is a universal property. Development of novel NPR-A immunolocalization and intracellular accumulation assays allowed NPR-A levels to be measured qualitatively and quantitatively, respectively, at the plasma membrane. To our knowledge, this is the first time that NPR-A has been visualized exclusively at the cell surface. Significantly, in contrast to previous studies in cell culture, none of the studies relied on ^{125}I-ANP binding to NPR-A, but rather followed the receptor itself. Not only are ^{125}I-ANP binding studies

subject to various interpretation issues due to changing binding affinities, prior receptor occupation, and expression of both NPR-A and NPR-C (Schiffrin *et al.*, 1991; Jewett *et al.*, 1993), but they have created controversy as to whether or not NPR-A is internalized and degraded (Koh *et al.*, 1992; Pandey, 1992; Pandey *et al.*, 2002; Fan *et al.*, 2005). Because we followed the receptor and not a ^{125}I-ANP-NPR-A complex, we observed basal internalization of NPR-A for the first time, and found that intracellular accumulation of NPR-A was increased in the presence of ANP.

Most signaling receptors are internalized via a clathrin- and dynamin-mediated pathway, yet up to 50% of the total endocytic activity in the cell may be clathrin-independent (Gong *et al.*, 2007; Sorkin and von Zastrow, 2009). Endocytosis of the endothelial growth factor (EGF) receptor is one of the most well characterized models for studying the kinetics and mechanisms of endocytic pathways. The schematic in Figure 1 summarizes trafficking of a typical cell surface signaling receptor (top), such as the EGF or β-adrenergic receptors, and NPR-A (bottom) in the absence and presence of ligand. In the absence of an activating ligand, EGF receptors are slowly, but constitutively, internalized ($t_{1/2} \sim 30$ min) and the majority of receptors are rapidly recycled back to the cell surface (Figure 1, top left) (Wiley, 2003). Meanwhile, activated EGF receptors are rapidly internalized (5-10-fold over basal) and trafficked toward degradation, not recycling, endosomes, which decreases the number of receptors at the cell surface (Figure 1, top right) (Wiley, 2003). ANP increased the rate of NPR-A internalization and degradation (Figure 1, bottom right). However, in contrast to most signaling receptors, NPR-A is internalized by a slow pathway that neither requires clathrin-coated pits nor dynamin-dependent vesicle scission (Figure 1, bottom). The slow rate of NPR-A internalization was strikingly evident when compared to the internalization rate of the

transferrin receptor in the same tTA HeLa cells; the initial internalization rate of the transferrin receptor was increased more than 30-fold compared to that of NPR-A (Figure 2). At the moment, little is known about the sorting, recycling, and degradation mechanisms of NPR-A (Figure 1, bottom). Our findings are significant not only because they are the first to link NPR-A to common internalization pathways, but also because they suggest that the majority of NPR-A is internalized by a novel clathrin- and dynamin-independent pathway. Additionally, depletion of clathrin increased the initial rate of NPR-A uptake, which, to our knowledge, is the first example of clathrin depletion increasing the uptake of any receptor.

The body of work presented here represents a significant advancement in the understanding of the natriuretic peptide system in congestive heart failure and provides insight into the mechanisms involved in the regulation of this system. More importantly, this work provides a framework for future studies, particularly in regards to trafficking of the natriuretic peptide receptors. Patients with cardiovascular disease would benefit from therapies that either preserve or increased the number of receptors available for ligand binding in order to increase natriuresis and diuresis, and therefore, lower the hemodynamic load on the heart. Understanding NPR-A downregulation is essential for the development of cardiovascular drugs that disrupt this process.

Regulation of NPR-A and NPR-B in Cardiovascular Disease

Circulating levels of natriuretic peptides are exaggerated in cardiovascular disease, and the increase is positively correlated with disease severity (Ruskoaho, 2003). In our mouse studies, transverse aortic constriction was performed to induced congestive heart failure. As a result of NPR-A downregulation, ANP-stimulated guanylyl cyclase activities

were significantly reduced in the mouse ventricle, whereas CNP-stimulated guanylyl cyclase activities were slightly increased. A separate study in a rat monocrotaline model for right ventricular hypertrophy reported that cyclase activities of both NPR-A and NPR-B were reduced in endocardial cells from the right ventricle (Kim *et al.*, 1999). Nevertheless, similar to our study, NPR-B-dependent guanylyl cyclase activity was greater than NPR-A-dependent guanylyl cyclase activity in the diseased animals. It is unclear whether these differences are due to disease severity, model type, heart region, and/or cell type. Future studies in animal models of cardiovascular disease may shed light on these differences, as well as provide insight as to how NPR-A and NPR-B are regulated at different stages and types of cardiovascular disease.

Hypertension is a major risk factor for heart failure. To compensate for the increased peripheral resistance associated with hypertension, the left ventricle of the heart progressively enlarges and becomes fibrotic resulting in reduced contractility (Deedwania, 1997). Eventually heart failure occurs when the hypertrophied and fibrotic heart is no longer able to maintain a normal cardiac output. To investigate the regulation of NPR-A and NPR-B in the hypertensive heart, we performed a few pilot experiments using two different rat models of hypertension obtained from Dr. John Osborn (University of Minnesota; Minneapolis, MN).

In the first model, hypertension was induced by deoxycorticosterone acetate (DOCA) and high salt in unilateral nephrectimized rats. Heart tissue was collected from both normotensive (control) and hypertensive rats, and membranes were prepared as described in Chapter 2. Similar to our observations in the heart-failed mice, ANP-dependent guanylyl cyclase activity was slightly decreased in the DOCA-treated animals, while CNP-dependent guanylyl cyclase activity remained the same or slightly increased

(Figure 3A). Unlike the mouse hearts, which had to be pooled, protein concentrations could be determined from individual rat hearts. This may be due to the increased amount of starting material in the rat heart compared to the mouse heart. Consistent with the cyclase results, NPR-A protein levels were clearly reduced in the hypertensive heart (Figure 3B, top). The trend in the NPR-B protein levels was difficult to decipher due to sample variation (Figure 3B, bottom).

The second model induced hypertension in rats by a high salt diet and infusion of angiotensin II (Ang II). In contrast to the DOCA-salt model, which is characterized by low renin and angiotensin II levels, the Ang II-salt model causes hypertension in a high angiotensin II setting. ANP-dependent guanylyl cyclase activity was reduced in heart membranes from Ang II-infused animals (Figure 3C); however, interestingly, NPR-A protein levels were not consistently reduced in these same animals (Figure 3D, top). This is consistent with a dephosphorylation-dependent, not a protein-dependent, mechanism responsible for the reduced ANP-dependent guanylyl cyclase activity. To determine the contribution of receptor phosphorylation to this observation a phosphoprotein stain could be used. Although CNP-dependent guanylyl cyclase activity represented a significant portion of the cyclase activity in the heart, surprisingly, the cyclase activity was reduced in the hypertensive heart (Figure 3C). No differences in the NPR-B protein levels were detected in the control and Ang II-infused hearts (Figure 3D, bottom). Thus, the guanylyl cyclase activities observed in the Ang II-salt are more reflective of those reported by Kim and colleagues in a monocrotaline model of right ventricular hypertrophy (Kim *et al.*, 1999).

Understanding the regulation of NPR-A and NPR-B in other tissues will also be important to effectively treat patients with cardiovascular disease. Recently our group

reported that renal hyporesponsiveness in mice with congestive heart failure resulted from decreased NPR-A protein concentrations in the kidney (Bryan *et al.*, 2007). Hence, in addition to heart tissue, tissue from the aorta, kidney, and mesenteric arteries were collected in the pilot hypertension studies. The immunoprecipitation-immunoblot data from these tissues yielded two interesting observations, of which both were noted in all of the independent studies. First, immunoblot detection of NPR-B in the rat kidney could only be partially blocked by a recombinant carboxyl-terminal NPR-B blocking peptide (Figure 4A). The peptide block worked because it completely blocked detection of the positive control for NPR-B. Immunoblotting with two separate polyclonal antibodies, both recognizing the carboxyl-terminus of NPR-B, produced the same result, and no protein was detected in all of the samples when antiserum against NPR-A was used. Secondly, in addition to the typical NPR-A band around 130 kDa, a doublet band appeared around 85 kDa when NPR-A was immunoprecipitated from rat mesenteric arteries (Figure 4B). Both bands were absent in the presence of the peptide block. Interestingly, the intensity of the doublet typically increased in the hypertensive animals. The bands observed in these tissues may be due to splice variants as splice variants have been reported in natriuretic peptide receptors. Interestingly, a splice variant of NPR-B was reported in the human kidney (Hirsch *et al.*, 2003). This NPR-B splice variant lacks a functional intracellular guanylyl cyclase domain because 31 unrelated amino acids have replaced the last 84 amino acids at the carboxyl-terminal of NPR-B (Hirsch *et al.*, 1999).

Internalization of Natriuretic Peptide Receptor-A

To investigate the mechanisms responsible for the downregulation of NPR-A observed both in cell culture and *in vivo*, an antibody-based intracellular accumulation

assay was developed. This assay requires an antibody to the extracellular domain of NPR-A in order to follow the path of receptors at the cell surface. Since our polyclonal antibody to NPR-A recognizes the intracellular carboxyl-terminus of NPR-A, a tag was placed on the amino-terminus of NPR-A. Briefly, cells were incubated at 4°C to slow internalization and allow for cell surface receptors to be labeled with antibody to the amino-terminal tag and a ^{125}I-conjugated secondary antibody. Labeled cells were incubated at 37°C to initiate internalization, and then acid-washed at 4°C to remove antibody at the cell surface. Radioactivity was counted to determine receptor internalization.

Sensitivity has proven to be a challenge with this assay. Part of the problem stems from the nature of NPR-A—the receptor is not robustly internalized. In the absence of ligand about 10% of the cell surface receptors are internalized within 1 h, and addition of ANP approximately doubles receptor accumulation. Half of the EGF receptors on the cell surface are internalized after 30 min in the absence of ligand, and this rate increases 5-10-fold following ligand activation (Wiley, 2003). Even the related clearance receptor, NPR-C, internalizes much slower than other clearance and/or transport receptors, such as the low density lipoprotein and transferrin receptors. NPR-C was reported to internalized at a rate of 5%/min, while more than 50% of transferrin receptors are internalized within 3 min (Chapter 4; Figure 8) (Nussenzveig *et al.*, 1990). Given the limited rate of NPR-A internalization, without a sufficient number of counts it is difficult to reliably observe internalization, particularly when looking for changes in the internalization pattern.

FLAG-NPR-A was transiently transfected into cells for the majority of the intracellular accumulation data presented here; thus, a significant portion of the cells assayed were

not expressing FLAG-NPR-A. Although this should not affect the percent of receptors internalized in each cell expressing FLAG-NPR-A, it does affect the range of the radioactive counts in the overall assay and is therefore a valid concern given the nature of the receptor. To increase the population of cells expressing FLAG-NPR-A, we attempted to stably express the FLAG-NPR-A construct in HeLa cells; this approach was unsuccessful. Adenoviruses expressing an amino-terminal CD8-tagged receptor held promise until it was discovered that CD8-NPR-A does not undergo ANP-dependent downregulation within an 8 h time frame. This suggested that CD8-NPR-A trafficking is different than trafficking of FLAG-NPR-A and endogenous NPR-A. Future strategies include stably expressing FLAG-NPR-A in another cell line, and creating a virus expressing the FLAG-NPR-A construct. Although these strategies should increase overall expression levels, it should be noted that overexpression could create a model that is no longer physiologically relevant. It is well established that EGF-induced downregulation of the EGF receptor is impaired in cells that overexpress the EGF receptor (Gilligan *et al.*, 1992). Furthermore, we found that the rate of NPR-A degradation was significantly reduced in 293T cells overexpressing NPR-A compared to the rate observed in bAEC and HeLa cells. However, NPR-A was downregulated with relatively normal kinetics in 293 cells (Potter and Hunter, 1999).

The data presented in Chapter 4 clearly indicated that NPR-A internalization is clathrin-independent. To our knowledge, NPR-A is the first receptor to accelerate uptake in response to clathrin depletion. It is possible that in response to inhibition of clathrin mediated-endocytosis the pathway responsible for NPR-A internalization is functionally upregulated (Doherty and McMahon, 2009). Once this pathway is identified, it would be

interesting to see if its components are indeed upregulated in the presence of clathrin depletion.

The GTPase dynamin in involved in multiple endocytic pathways, including clathrin-mediated endocytosis. Thus, although internalization of a receptor is clathrin-independent, it is not necessarily dynamin-independent. A dominant negative K44A dynamin-1 (K44A Dyn1) mutant was used in Chapter 4 to inhibit dynamin activity. The K44A Dyn1 mutant has been shown to inhibit the internalization of many cell surface receptors. For example, in the presence of EGF, cells expressing wildtype dynamin rapidly and efficiently cleared the EGF receptor from the cell surface, but in the presence of the K44A Dyn1 mutant more than 80% of the cell surface receptors remained at the plasma membrane (Vieira *et al.*, 1996). Our combined experiments with the K44A Dyn1 mutant indicated that NPR-A is internalized via a dynamin-independent pathway in both the absence and presence of ligand; however, some of the individual experiments suggested that dynamin may have a minor role in NPR-A internalization, particularly in the presence of ANP. It is not unusual for signaling receptors to be internalized by more than one pathway. In addition to clathrin-mediated endocytosis, the EGF receptor has been shown to slowly internalize via clathrin-independent pathways, although the contribution of these pathways to endocytosis of the EGF receptor is likely minimal *in vivo* (Sorkin and Goh, 2008). Regardless, if dynamin does play a role in NPR-A internalization, it appears to be minor, particularly when considering the effect of the K44A Dyn1 mutant on internalization of the EGF receptor. siRNA targeting dynamin-2, the ubiquitously expressed form of dynamin, or the cell-permeable dynamin inhibitor dynasore may help to clarify the potential role of dynamin in NPR-A internalization.

Under physiological conditions (low ligand concentrations and moderate receptor expression levels), the EGF receptor is internalized almost exclusively by rapid clathrin-mediated endocytosis. However, increasing EGF concentrations decrease the rate of receptor uptake presumably because the rapid internalization pathway has limited capacity (Wiley, 1988; Lund *et al.*, 1990). Interestingly, when high concentrations of EGF were added to cells, EGF receptor internalization was not significantly affected by siRNA knock down of the clathrin heavy chain or overexpression of the K44A Dyn1 mutant (Sorkin and Goh, 2008). Saturating concentrations (1 μM) of ANP were used in all of the accumulation experiments presented here. It is possible that the clathrin knock down and K44A Dyn1 mutant failed to affect NPR-A internalization simply because the ligand concentrations used were not physiological. Future studies should examine the effect of low ANP concentrations on NPR-A uptake.

Accumulating evidence suggests that clathrin-independent endocytosis accounts for a significant portion of the total endocytic activity in the cell; however, understanding of the endocytic mechanisms, the implicated cargoes, and the other proteins involved is still evolving. Caveolae-dependent, glycosylphosphatidylinositol (GPI)-enriched endosomal compartment (GEEC), flotillin-dependent, RhoA-dependent, and Arf6-dependent pathways are some of the identified clathrin-independent endocytic pathways (Gong *et al.*, 2007). Dynamin is implicated in caveolae-dependent, RhoA-dependent, and flotillin-dependent pathways (Oh *et al.*, 1998; Payne *et al.*, 2007; Doherty and McMahon, 2009). Because so little is known about these pathways, siRNA against their known key components may be a reasonable approach to determine their involvement in NPR-A internalization. Additionally, dominant negative T19N RhoA and Q67L Arf6 may be useful to investigate the RhoA- and Arf6-dependent pathways, respectively (Gong *et al.*,

2007). It is also possible that the majority of NPR-A is internalized by a completely undescribed pathway.

Many signaling receptors have been reported to contain intracellular motifs that regulate receptor internalization and intracellular trafficking. Pandey and colleagues used deletion mutagenesis to determine the role of cytoplasmic domains of NPR-A in the internalization and sequestration of ^{125}I-ANP-NPR-A complexes; deletion of both the intracellular kinase homology and guanylyl cyclase domains had the greatest impact on internalization (Pandey *et al.*, 2000). Five years later he reported that an acidic tyrosine-based GDAY motif in the carboxyl-terminal domain of NPR-A decreased internalization of the ligand-receptor complex by nearly 50% when the glycine and/or tyrosine residues of the GDAY motif were mutated to alanine (Pandey *et al.*, 2005). Ligand-mediated downregulation and receptor recycling were reduced 35-40% and 40%, respectively, in these mutant receptors (Pandey *et al.*, 2005). It would be interesting to see if these mutations affect ANP-dependent NPR-A downregulation and NPR-A internalization detected by immunoblot analysis or by our antibody-based accumulation assay, respectively.

An immunolocalization protocol was developed in Chapter 3, which allowed us to confidently visualize NPR-A at the plasma membrane for the first time. In this protocol, live cells were labeled with primary antibody prior to fixation with formaldehyde; thus, the primary antibody only bound receptors on the cell surface. Unfortunately, studies utilizing this new protocol were difficult because the FLAG-NPR-A transient transfections created a population of cells with varying FLAG-NPR-A expression levels. As mentioned previously, attempts to create a HeLa cell line stably expressing the FLAG-NPR-A construct were unsuccessful. Although our laboratory commonly uses HEK 293 cells to

stably express natriuretic peptide receptors, it may be difficult to study trafficking in these cells due to their small size and large nucleus-to-cell ratio. The monoclonal anti-CD8 antibody used to measure CD8-NPR-A intracellular accumulation failed to identify CD8-NPR-A by immunolocalization. CD8-NPR-A could only be visualized in cells exposed to polyclonal rabbit anti-CD8α antibody after fixation with formaldehyde; thus, CD8-NPR-A was never visualized exclusively at the cell surface. Live cell imaging may allow NPR-A trafficking to be examined in the presence of a heterogeneous cell population, as trafficking of the receptor could be followed in a few cells over time.

Considering the nature of NPR-A internalization, assay sensitivity is another concern. Data from our NPR-A accumulation assay demonstrates that NPR-A is internalized; however, in the immunolocalization assay, NPR-A loss from the cell surface could only be detected after long (8 h), but not short ($\leq$ 1 h) ANP exposures. Based on the internalization assay, approximately 10% of receptors are basally internalized in 1 h, and intracellular NPR-A accumulation is approximately 2-fold greater in cells incubated in the presence of ANP (Chapter 4). The sensitivity of the assay is not high enough to qualitatively detect this small change. It is also important to note that the control is not static due to basal internalization, thus the differences in cell surface receptor appear even less significant. To add further complexity, as mentioned above, it is difficult to compare minor changes in cell surface expression between cells and/or treatments when FLAG-NPR-A expression levels are initially different.

Regardless of the aforementioned challenges to NPR-A immunolocalization, with additional optimization, immunolocalization has the potential to be an invaluable tool in uncovering the trafficking pathway(s) of NPR-A. A significant portion of trafficking studies use immunolocalization techniques, thus a wide variety of chemical trafficking inhibitors

and fluorescent cellular markers are commercially available. Colocalization of NPR-A with one of these intracellular markers would provide insight into potential NPR-A trafficking pathways. Immunolocalization studies would be a positive compliment to experiments using the NPR-A intracellular accumulation assay.

The techniques developed to examine NPR-A internalization could be applied to the other mammalian natriuretic peptide receptors as well. Published literature on NPR-B internalization and trafficking is scarce. One study found that NPR-B is neither internalized nor degraded upon ligand binding (Fan *et al.*, 2005). Another report indicated that the missense mutations in NPR-B that are associated with acromesomelic dysplasia-type Maroteaux (AMDM), a rare form of human dwarfism, primarily affect NPR-B function by arresting trafficking of the receptor at the endoplasmic reticulum (Hume *et al.*, 2009). It is probable that the intracellular trafficking properties of NPR-A and NPR-B are similar since the extracellular and intracellular domains of rat NPR-B share a 43% and 78% amino acid sequence identity, respectively, to rat NPR-A (Schulz *et al.*, 1989). The natriuretic peptide clearance receptor, NPR-C, which has an intracellular domain of only 37 amino acids, undergoes extensive internalization and recycling (Nussenzveig *et al.*, 1990). This process is constitutive as it occurs in the absence and presence of ligand, and because the internalization rates are similar under both conditions it was suggested that ligand binding does not induce massive clustering of the receptors into coated pits (Nussenzveig *et al.*, 1990). Hypertonic sucrose experiments indicated that NPR-C is endocytosed through a clathrin-mediated pathway (Cohen *et al.*, 1996), although to our knowledge no other studies have indicated clathrin-dependence or -independence. It would be interesting to see if NPR-C internalization is

inhibited using our intracellular accumulation assay and siRNA against the clathrin heavy chain.

Natriuretic Peptide Receptor-A Recycling

Recycling of the ^{125}I-ANP-NPR-A complex has been reported in various cell lines (Pandey, 1992, 1993; Pandey *et al.*, 2002). Consistent with these earlier reports, results from the NPR-A accumulation assay suggest that NPR-A is recycled. Basal internalization of NPR-A, but not ANP-induced internalization, reaches equilibrium after 20 min, suggesting that receptor movement into and out of the cell is the same (Chapter 4). Under basal conditions, many internalized signaling receptors are predominantly recycled back to the plasma membrane, which is consistent with our observation. Furthermore, in the presence of the dominant negative K44A Dyn1 mutant the rate of intracellular accumulation was relatively linear throughout the assay (Chapter 4; Figures 6 and 7). By 60 min, accumulation approximately doubled in cells expressing the K44A Dyn1 mutant compared to control cells and, because expression is controlled by a tet-off system, this effect was absent in the presence of tetracycline. Hence, our data suggests that internalized NPR-A is recycled back to the cell surface and that dynamin participates in this process. A role for dynamin in NPR-A recycling is not unfeasible because dynamin-dependent transferrin receptor recycling has been reported (van Dam and Stoorvogel, 2002).

Although data from the NPR-A accumulation assay suggests that NPR-A is recycled, we do not have concrete proof that recycling occurs. The NPR-A intracellular accumulation assay can be modified to measure receptor recycling. Following the internalization period at 37°C, cells are acid-washed at 4°C to remove antibody from

receptors at the cell surface. Only labeled receptors that have internalized should be remaining inside the cells at this point. Cells are then incubated in a 37°C water bath to reinitiate receptor trafficking. Labeled receptors that are recycled back to the cell surface during this incubation are removed by a second acid-wash at 4°C. Loss of counts from the cell pellets after the second incubation at 37°C would be indicative of receptor recycling. No recycling was observed in our initial attempts to measure receptor recycling. Nonetheless, this does not imply that NPR-A is not recycled.

The initial recycling studies were performed in the presence of ANP in order to internalize more receptor. Unfortunately, based on other signaling receptors, a small proportion of internalized receptors are recycled in the presence of ligand, which would make it more difficult to detect recycling. Thus, even though fewer receptors are internalized under basal conditions, it is more probable that recycling would be observed. A sufficient number of receptors must be internalized in order to confidently observe recycling. Due to the nature of NPR-A, only a small percentage of total labeled receptors are internalized, particular under basal conditions. Hence, it is essential to start the assay with a high number of counts. Since the initial studies, improvements in the NPR-A accumulation assay have lead to increased intracellular counts, which inadvertently improves the probability of success with the recycling assay. Increased expression of the amino-terminal-tagged receptor, either through a virus or stably transfected cells, may also improve the probability of success with this assay.

Degradation of Natriuretic Peptide Receptor-A

Prolonged exposure to ANP causes significant degradation of NPR-A; however, the mechanism by which NPR-A is degraded is unclear. Based on ^{125}I-ANP studies, Pandey

and colleagues suggested that NPR-A is degraded by the lysosome (Pandey *et al.*, 2002). Pilot experiments to determine whether NPR-A degradation proceeds through a lysosomal or proteasomal pathway were unsuccessful, but also lacked appropriate controls. Neither inhibitors of the lysosome (bafilomycin A1, ammonium chloride, and chloroquine) nor proteosome (MG132 and lactacystin) blocked ANP-dependent NPR-A degradation (Figure 5). Different inhibitor concentrations and combinations all yielded the same results. Perhaps these results allude to the novel nature of NPR-A trafficking. Nevertheless, these studies should be revisited in the future.

Figure 1

Schematic representation of basal and ligand-dependent receptor trafficking. (Top) Ligand-independent (left) and –dependent (right) trafficking of many cell surface signaling receptors, such as the EGF and β-adrenergic receptors. Receptors are internalized via a clathrin- and dynamin-dependent pathway. Internalized inactive receptors are primarily recycled back to the cell surface (left). Receptor activation results in accelerated internalization and downregulation (degradation) (right). (Bottom) Basal (left) and ANP-dependent (right) NPR-A trafficking. The majority of NPR-A internalization occurs through a clathrin- and dynamin-independent pathway. NPR-A likely recycles back to the plasma membrane, as the K44A Dyn1 mutant increases intracellular accumulation at longer time points (Chapter 4; Figures 6 and 7). In ANP-exposed cells, fewer receptors are on the cell surface and NPR-A degradation is enhanced by an unidentified mechanism (right).

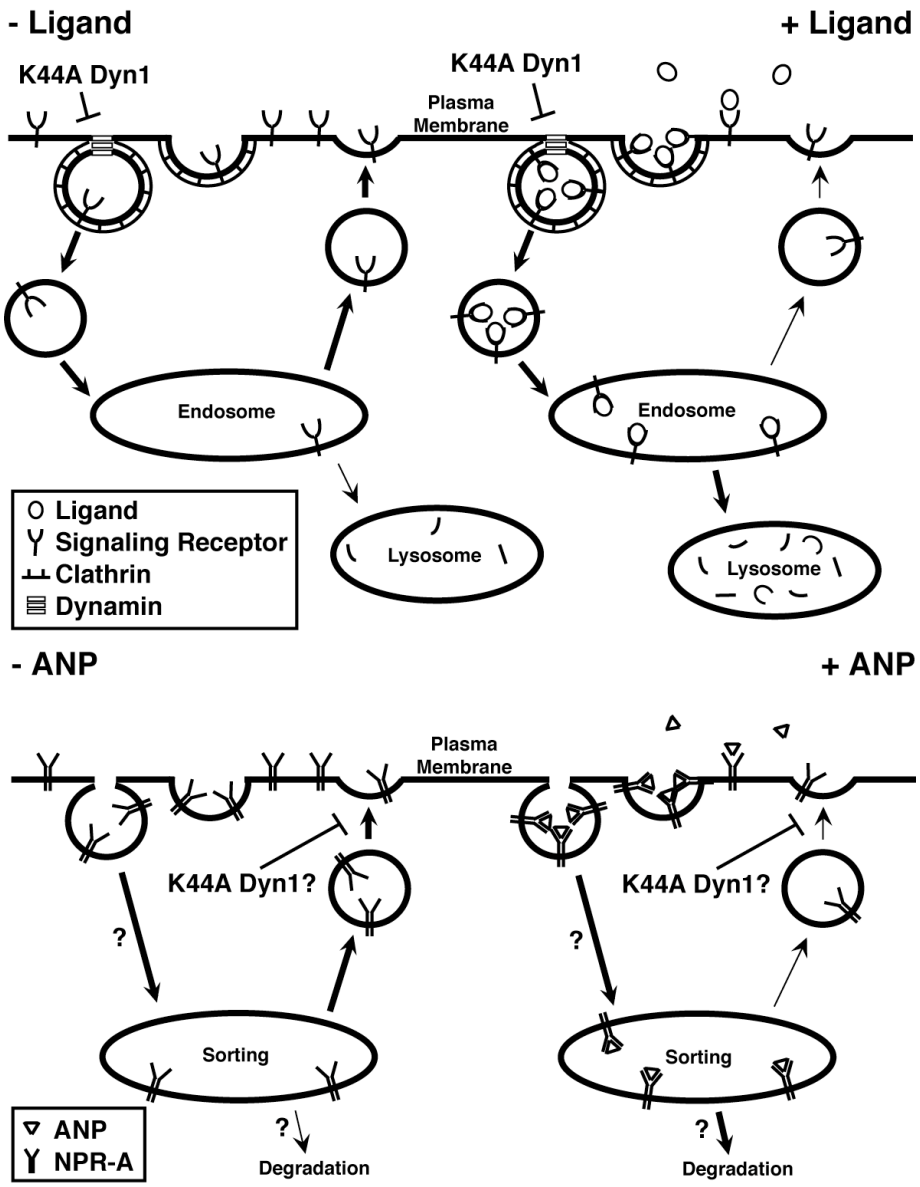
- Ligand
+ Ligand
K44A Dyn1
K44A Dyn1
Plasma Membrane
Endosome
Endosome
Ligand
Signaling Receptor
Clathrin
Dynamin
Lysosome
Lysosome
- ANP
+ ANP
Plasma Membrane
K44A Dyn1?
K44A Dyn1?
?
?
Sorting
Sorting
ANP
NPR-A
?
?
Degradation
Degradation

Figure 2

The ligand-dependent internalization rate of the transferrin receptor and NPR-A are strikingly different. Control ligand-dependent receptor accumulation curves for the transferrin receptor (TfnR) and NPR-A. Data is from Figure 8, B and D. Data points represent the mean ± SEM and were graphed as a percent of total counts where N = 7 and N = 14 for Transferrin/TfnR and ANP/NPR-A, respectively. Initial internalization (slopes) were based on time points 0-1 min for Transferrin/TfnR and 0-5 min for ANP/NPR-A.

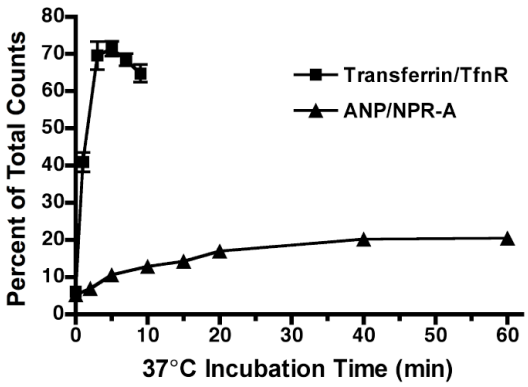
Percent of Total Counts
80
70
60
50
40
30
20
10
0
0
10
20
30
40
50
60
37°C Incubation Time (min)
Transferrin/TfnR
ANP/NPR-A

Figure 3

Natriuretic peptide-dependent guanylyl cyclase activities and receptor concentrations in the hypertensive rat heart. Hypertension was induced in rats with a high salt diet and either deoxycorticosterone acetate (DOCA) (A and B) or infusion of angiotensin II (Ang II) (C and D). Crude heart membranes were prepared from control or hypertensive animals. (A and C) A portion of the membranes were assayed for guanylyl cyclase activity under basal (no natriuretic peptide), 50 nM ANP, 1 μM ANP, 50 nM CNP, 1 μM CNP, or Triton X-100 conditions. (B and D) NPR-A (top) and NPR-B (bottom) were sequentially purified by immunoprecipitation from another portion of the heart membranes and detected by immunoblot. Each lane represents one rat heart. 293T NPR-A and NPR-B are positive controls. Data generated in (A), (B), and (D) by Darcy R. Flora and in (C) by Deborah M. Dickey.

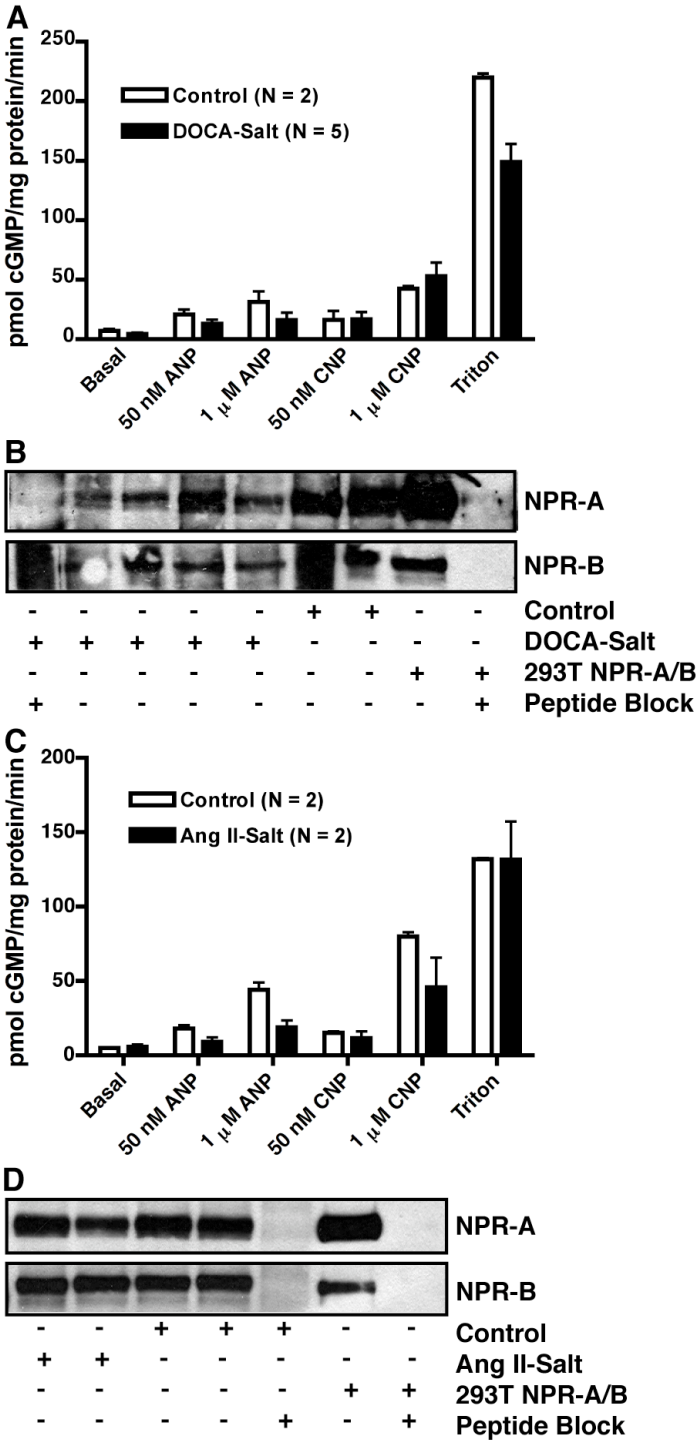
A
pmol cGMP/mg protein/min
250
200
150
100
50
0
Control (N = 2)
DOCA-Salt (N = 5)
Basal
50 nM ANP
1 μM ANP
50 nM CNP
1 μM CNP
Triton
B
NPR-A
NPR-B
- - - - - + + - - Control
+ + + + + - - - - DOCA-Salt
- - - - - - - + + 293T NPR-A/B
+ - - - - - - - + Peptide Block
C
pmol cGMP/mg protein/min
200
150
100
50
0
Control (N = 2)
Ang II-Salt (N = 2)
Basal
50 nM ANP
1 μM ANP
50 nM CNP
1 μM CNP
Triton
D
NPR-A
NPR-B
- - + + + - - Control
+ + - - - - - Ang II-Salt
- - - - - + + 293T NPR-A/B
- - - - + - + Peptide Block

Figure 4

Immunoblot observations in the kidney and mesenteric arteries of hypertensive rats. Hypertension was induced in rats by infusion of angiotensin II (Ang II) and a high salt diet. Crude membranes were prepared from the kidney (A) or mesenteric arteries (B) of control and hypertensive animals. NPR-B (A) and NPR-A (B) were purified by immunoprecipitation and detected by immunoblot. Each lane represents one rat heart. 293T NPR-A and NPR-B are positive controls. Arrows indicate interesting observations: (A) NPR-B detected in the rat kidney is not blocked by the peptide block, and (B) A doublet band around 85 kDa was detected by antibody to NPR-A in rat mesenteric arteries.

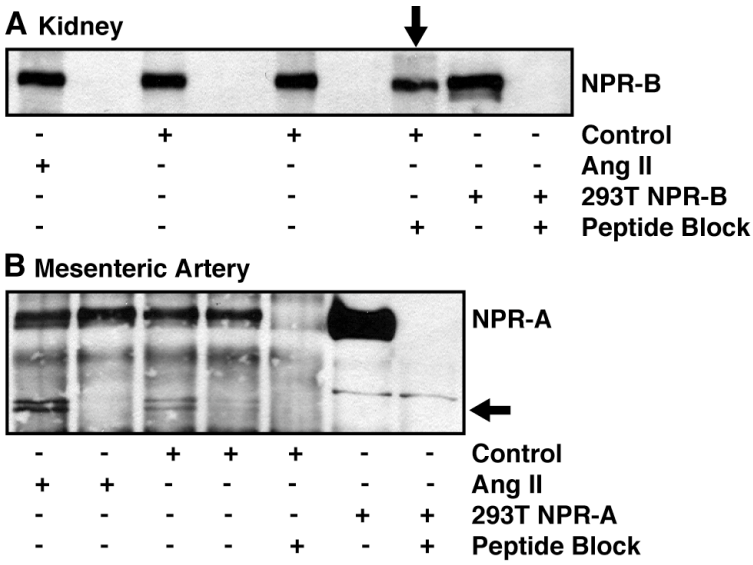
A Kidney
NPR-B
- + + + - - Control
+ - - - - - Ang II
- - - - + + 293T NPR-B
- - - + - + Peptide Block
B Mesenteric Artery
NPR-A
- - + + + - - Control
+ + - - - - - Ang II
- - - - - + + 293T NPR-A
- - - - + - + Peptide Block

Figure 5

Lysosomal and proteasomal inhibitors do not inhibit ANP-dependent NPR-A degradation. (A) HeLa cells were incubated for 8 h with 10 μg/ml cycloheximide and at least one lysosomal inhibitor (10 mM ammonium chloride, 100 nM bafilomycin A1, 200 μM chloroquine) in the absence or presence of 200 nM rat ANP. NPR-A was immunoprecipitated and detected by immunoblot with antibody to the NPR-A carboxyl-terminus. (B) HeLa cells were prepared as described in (A) except cells were incubated with proteasomal inhibitors (10 μM lactacystin or 10 μM MG132), instead of lysosomal inhibitors.

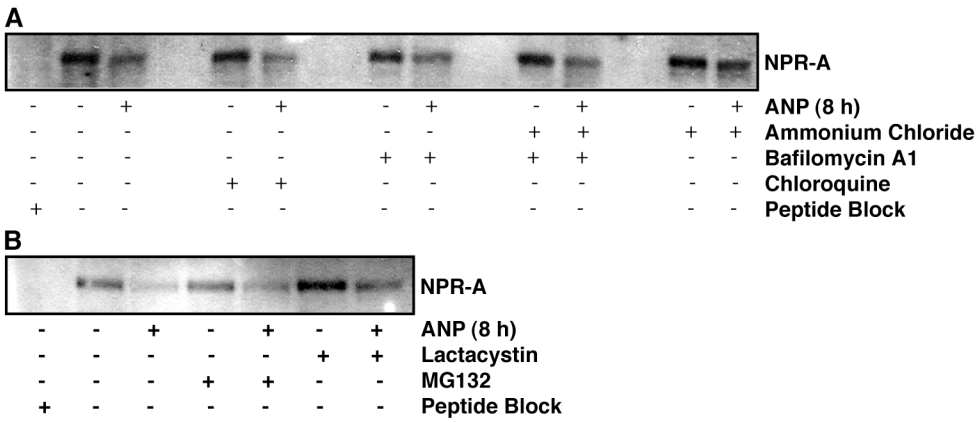
A
NPR-A
- - + - + - + - + - +
- - - - - - - + + + +
- - - - - + + + + - -
- - - + + - - - - - -
+ - - - - - - - - - -
ANP (8 h)
Ammonium Chloride
Bafilomycin A1
Chloroquine
Peptide Block
B
NPR-A
- - + - + - +
- - - - - + +
- - - + + - -
+ - - - - - -
ANP (8 h)
Lactacystin
MG132
Peptide Block

REFERENCES

Abbey, S.E., and Potter, L.R. (2002). Vasopressin-dependent inhibition of the C-type natriuretic peptide receptor, NPR-B/GC-B, requires elevated intracellular calcium concentrations. J Biol Chem *277*, 42423-42430.

Abdelalim, E.M., and Tooyama, I. (2009). BNP signaling is crucial for embryonic stem cell proliferation. PLoS One *4*, e5341.

Airhart, N., Yang, Y.F., Roberts, C.T., Jr., and Silberbach, M. (2003). Atrial natriuretic peptide induces natriuretic peptide receptor-cGMP-dependent protein kinase interaction. J Biol Chem *278*, 38693-38698.

Allgren, R.L., Marbury, T.C., Rahman, S.N., Weisberg, L.S., Fenves, A.Z., Lafayette, R.A., Sweet, R.M., Genter, F.C., Kurnik, B.R., Conger, J.D., and Sayegh, M.H. (1997). Anaritide in acute tubular necrosis. Auriculin Anaritide Acute Renal Failure Study Group. N Engl J Med *336*, 828-834.

Almeida, F.A., Suzuki, M., and Maack, T. (1986). Atrial natriuretic factor increases hematocrit and decreases plasma volume in nephrectomized rats. Life Sci *39*, 1193-1199.

Anand-Srivastava, M.B. (2005). Natriuretic peptide receptor-C signaling and regulation. Peptides *26*, 1044-1059.

Andreassi, M.G., Del Ry, S., Palmieri, C., Clerico, A., Biagini, A., and Giannessi, D. (2001). Up-regulation of 'clearance' receptors in patients with chronic heart failure: a possible explanation for the resistance to biological effects of cardiac natriuretic hormones. Eur J Heart Fail *3*, 407-414.

Arora, R.R., Venkatesh, P.K., and Molnar, J. (2006). Short and long-term mortality with nesiritide. Am Heart J *152*, 1084-1090.

Barbee, R.W., Perry, B.D., Re, R.N., Murgo, J.P., and Field, L.J. (1994). Hemodynamics in transgenic mice with overexpression of atrial natriuretic factor. Circ Res *74*, 747-751.

Bartels, C.F., Bukulmez, H., Padayatti, P., Rhee, D.K., van Ravenswaaij-Arts, C., Pauli, R.M., Mundlos, S., Chitayat, D., Shih, L.Y., Al-Gazali, L.I., Kant, S., Cole, T., Morton, J., Cormier-Daire, V., Faivre, L., Lees, M., Kirk, J., Mortier, G.R., Leroy, J., Zabel, B., Kim, C.A., Crow, Y., Braverman, N.E., van den Akker, F., and Warman, M.L. (2004). Mutations in the transmembrane natriuretic peptide receptor NPR-B impair skeletal growth and cause acromesomelic dysplasia, type Maroteaux. Am J Hum Genet *75*, 27-34.

Bennett, B.D., Bennett, G.L., Vitangcol, R.V., Jewett, J.R., Burnier, J., Henzel, W., and Lowe, D.G. (1991). Extracellular domain-IgG fusion proteins for three human natriuretic peptide receptors. Hormone pharmacology and application to solid phase screening of synthetic peptide antisera. J Biol Chem *266*, 23060-23067.

Bocciardi, R., Giorda, R., Buttgereit, J., Gimelli, S., Divizia, M.T., Beri, S., Garofalo, S., Tavella, S., Lerone, M., Zuffardi, O., Bader, M., Ravazzolo, R., and Gimelli, G. (2007). Overexpression of the C-type natriuretic peptide (CNP) is associated with overgrowth and bone anomalies in an individual with balanced t(2;7) translocation. Hum Mutat *28*, 724-731.

Brown, L.A., Nunez, D.J., and Wilkins, M.R. (1993). Differential regulation of natriuretic peptide receptor messenger RNAs during the development of cardiac hypertrophy in the rat. J Clin Invest *92*, 2702-2712.

Bruneau, B.G., Piazza, L.A., and de Bold, A.J. (1997). BNP gene expression is specifically modulated by stretch and ET-1 in a new model of isolated rat atria. Am J Physiol *273*, H2678-2686.

Bryan, P.M., Xu, X., Dickey, D.M., Chen, Y., and Potter, L.R. (2007). Renal hyporesponsiveness to atrial natriuretic peptide in congestive heart failure results from reduced atrial natriuretic peptide receptor concentrations. Am J Physiol Renal Physiol *292*, F1636-1644.

Burnett, J.C., Jr., Kao, P.C., Hu, D.C., Heser, D.W., Heublein, D., Granger, J.P., Opgenorth, T.J., and Reeder, G.S. (1986). Atrial natriuretic peptide elevation in congestive heart failure in the human. Science *231*, 1145-1147.

Cahill, P.A., Redmond, E.M., and Keenan, A.K. (1990). Vascular atrial natriuretic factor receptor subtypes are not independently regulated by atrial peptides. J Biol Chem *265*, 21896-21906.

Chan, J.C., Knudson, O., Wu, F., Morser, J., Dole, W.P., and Wu, Q. (2005). Hypertension in mice lacking the proatrial natriuretic peptide convertase corin. Proc Natl Acad Sci U S A *102*, 785-790.

Charles, C.J., Prickett, T.C., Espiner, E.A., Rademaker, M.T., Richards, A.M., and Yandle, T.G. (2006). Regional sampling and the effects of experimental heart failure in sheep: differential responses in A, B and C-type natriuretic peptides. Peptides *27*, 62-68.

Charloux, A., Piquard, F., Doutreleau, S., Brandenberger, G., and Geny, B. (2003). Mechanisms of renal hyporesponsiveness to ANP in heart failure. Eur J Clin Invest *33*, 769-778.

Chikuda, H., Kugimiya, F., Hoshi, K., Ikeda, T., Ogasawara, T., Shimoaka, T., Kawano, H., Kamekura, S., Tsuchida, A., Yokoi, N., Nakamura, K., Komeda, K., Chung, U.I., and Kawaguchi, H. (2004). Cyclic GMP-dependent protein kinase II is a molecular switch from proliferation to hypertrophic differentiation of chondrocytes. Genes Dev *18*, 2418-2429.

Chinkers, M., and Wilson, E.M. (1992). Ligand-independent oligomerization of natriuretic peptide receptors. Identification of heteromeric receptors and a dominant negative mutant. J Biol Chem *267*, 18589-18597.

Chrisman, T.D., Schulz, S., Potter, L.R., and Garbers, D.L. (1993). Seminal plasma factors that cause large elevations in cellular cyclic GMP are C-type natriuretic peptides. J Biol Chem *268*, 3698-3703.

Christoffersen, T.E., Aplin, M., Strom, C.C., Sheikh, S.P., Skott, O., Busk, P.K., Haunso, S., and Nielsen, L.B. (2006). Increased natriuretic peptide receptor A and C gene expression in rats with pressure-overload cardiac hypertrophy. Am J Physiol Heart Circ Physiol *290*, H1635-1641.

Chun, T.H., Itoh, H., Ogawa, Y., Tamura, N., Takaya, K., Igaki, T., Yamashita, J., Doi, K., Inoue, M., Masatsugu, K., Korenaga, R., Ando, J., and Nakao, K. (1997). Shear stress augments expression of C-type natriuretic peptide and adrenomedullin. Hypertension *29*, 1296-1302.

Chusho, H., Tamura, N., Ogawa, Y., Yasoda, A., Suda, M., Miyazawa, T., Nakamura, K., Nakao, K., Kurihara, T., Komatsu, Y., Itoh, H., Tanaka, K., Saito, Y., and Katsuki, M. (2001). Dwarfism and early death in mice lacking C-type natriuretic peptide. Proc Natl Acad Sci U S A *98*, 4016-4021.

Clavell, A.L., Stingo, A.J., Aarhus, L.L., and Burnett, J.C., Jr. (1993a). Biological actions of brain natriuretic peptide in thoracic inferior vena caval constriction. Am J Physiol *265*, R1416-1422.

Clavell, A.L., Stingo, A.J., Wei, C.M., Heublein, D.M., and Burnett, J.C., Jr. (1993b). C-type natriuretic peptide: a selective cardiovascular peptide. Am J Physiol *264*, R290-295.

Cody, R.J., Atlas, S.A., Laragh, J.H., Kubo, S.H., Covit, A.B., Ryman, K.S., Shaknovich, A., Pondolfino, K., Clark, M., Camargo, M.J., and et al. (1986). Atrial natriuretic factor in normal subjects and heart failure patients. Plasma levels and renal, hormonal, and hemodynamic responses to peptide infusion. J Clin Invest *78*, 1362-1374.

Cohen, D., Koh, G.Y., Nikonova, L.N., Porter, J.G., and Maack, T. (1996). Molecular determinants of the clearance function of type C receptors of natriuretic peptides. J Biol Chem *271*, 9863-9869.

Conner, S.D., and Schmid, S.L. (2003). Regulated portals of entry into the cell. Nature *422*, 37-44.

Currie, M.G., Geller, D.M., Cole, B.R., Siegel, N.R., Fok, K.F., Adams, S.P., Eubanks, S.R., Galluppi, G.R., and Needleman, P. (1984). Purification and sequence analysis of bioactive atrial peptides (atriopeptins). Science *223*, 67-69.

Damke, H., Baba, T., Warnock, D.E., and Schmid, S.L. (1994). Induction of mutant dynamin specifically blocks endocytic coated vesicle formation. J Cell Biol *127*, 915-934.

Damke, H., Gossen, M., Freundlieb, S., Bujard, H., and Schmid, S.L. (1995). Tightly regulated and inducible expression of dominant interfering dynamin mutant in stably transformed HeLa cells. Methods Enzymol *257*, 209-220.

de Bold, A.J. (1982). Tissue fractionation studies on the relationship between an atrial natriuretic factor and specific atrial granules. Can J Physiol Pharmacol *60*, 324-330.

de Bold, A.J., Borenstein, H.B., Veress, A.T., and Sonnenberg, H. (1981). A rapid and potent natriuretic response to intravenous injection of atrial myocardial extract in rats. Life Sci *28*, 89-94.

de Bold, A.J., Bruneau, B.G., and Kuroski de Bold, M.L. (1996). Mechanical and neuroendocrine regulation of the endocrine heart. Cardiovasc Res *31*, 7-18.

Deedwania, P.C. (1997). The progression from hypertension to heart failure. Am J Hypertens *10*, 280S-288S.

Del Ry, S., Passino, C., Maltinti, M., Emdin, M., and Giannessi, D. (2005). C-type natriuretic peptide plasma levels increase in patients with chronic heart failure as a function of clinical severity. Eur J Heart Fail *7*, 1145-1148.

Dickey, D.M., Flora, D.R., Bryan, P.M., Xu, X., Chen, Y., and Potter, L.R. (2007). Differential regulation of membrane guanylyl cyclases in congestive heart failure: natriuretic peptide receptor (NPR)-B, Not NPR-A, is the predominant natriuretic peptide receptor in the failing heart. Endocrinology *148*, 3518-3522.

Doherty, G.J., and McMahon, H.T. (2009). Mechanisms of endocytosis. Annu Rev Biochem *78*, 857-902.

Drewett, J.G., Fendly, B.M., Garbers, D.L., and Lowe, D.G. (1995). Natriuretic peptide receptor-B (guanylyl cyclase-B) mediates C-type natriuretic peptide relaxation of precontracted rat aorta. J Biol Chem *270*, 4668-4674.

Edwards, B.S., Zimmerman, R.S., Schwab, T.R., Heublein, D.M., and Burnett, J.C., Jr. (1988). Atrial stretch, not pressure, is the principal determinant controlling the acute release of atrial natriuretic factor. Circ Res *62*, 191-195.

Fan, D., Bryan, P.M., Antos, L.K., Potthast, R.J., and Potter, L.R. (2005). Down-regulation does not mediate natriuretic peptide-dependent desensitization of natriuretic peptide receptor (NPR)-A or NPR-B: guanylyl cyclase-linked natriuretic peptide receptors do not internalize. Mol Pharmacol *67*, 174-183.

Flynn, T.G., de Bold, M.L., and de Bold, A.J. (1983). The amino acid sequence of an atrial peptide with potent diuretic and natriuretic properties. Biochem Biophys Res Commun *117*, 859-865.

Forssmann, W.G., Birr, C., Carlquist, M., Christmann, M., Finke, R., Henschen, A., Hock, D., Kirchheim, H., Kreye, V., Lottspeich, F., and et al. (1984). The auricular myocardiocytes of the heart constitute an endocrine organ. Characterization of a porcine cardiac peptide hormone, cardiodilatin-126. Cell Tissue Res *238*, 425-430.

Franco, F., Dubois, S.K., Peshock, R.M., and Shohet, R.V. (1998). Magnetic resonance imaging accurately estimates LV mass in a transgenic mouse model of cardiac hypertrophy. Am J Physiol *274*, H679-683.

Fuller, F., Porter, J.G., Arfsten, A.E., Miller, J., Schilling, J.W., Scarborough, R.M., Lewicki, J.A., and Schenk, D.B. (1988). Atrial natriuretic peptide clearance receptor. Complete sequence and functional expression of cDNA clones. J Biol Chem *263*, 9395-9401.

Furuya, M., Yoshida, M., Hayashi, Y., Ohnuma, N., Minamino, N., Kangawa, K., and Matsuo, H. (1991). C-type natriuretic peptide is a growth inhibitor of rat vascular smooth muscle cells. Biochem Biophys Res Commun *177*, 927-931.

Garcia, R., Bonhomme, M.C., and Schiffrin, E.L. (1992). Divergent regulation of atrial natriuretic factor receptors in high-output heart failure. Am J Physiol *263*, H1790-1797.

Gardner, D.G. (2003). Natriuretic peptides: markers or modulators of cardiac hypertrophy? Trends Endocrinol Metab *14*, 411-416.

Gardner, D.G., Deschepper, C.F., Ganong, W.F., Hane, S., Fiddes, J., Baxter, J.D., and Lewicki, J. (1986). Extra-atrial expression of the gene for atrial natriuretic factor. Proc Natl Acad Sci U S A *83*, 6697-6701.

Gilligan, A., Bushmeyer, S., and Knowles, B.B. (1992). Variation in EGF-induced EGF receptor downregulation in human hepatoma-derived cell lines expressing different amounts of EGF receptor. Exp Cell Res *200*, 235-241.

Gong, Q., Huntsman, C., and Ma, D. (2007). Clathrin-independent internalization and recycling. J Cell Mol Med.

Goy, M.F., Oliver, P.M., Purdy, K.E., Knowles, J.W., Fox, J.E., Mohler, P.J., Qian, X., Smithies, O., and Maeda, N. (2001). Evidence for a novel natriuretic peptide receptor that prefers brain natriuretic peptide over atrial natriuretic peptide. Biochem J *358*, 379-387.

Grepin, C., Dagnino, L., Robitaille, L., Haberstroh, L., Antakly, T., and Nemer, M. (1994). A hormone-encoding gene identifies a pathway for cardiac but not skeletal muscle gene transcription. Mol Cell Biol *14*, 3115-3129.

Hagiwara, H., Sakaguchi, H., Itakura, M., Yoshimoto, T., Furuya, M., Tanaka, S., and Hirose, S. (1994). Autocrine regulation of rat chondrocyte proliferation by natriuretic peptide C and its receptor, natriuretic peptide receptor-B. J Biol Chem *269*, 10729-10733.

Hawkridge, A.M., Heublein, D.M., Bergen, H.R., 3rd, Cataliotti, A., Burnett, J.C., Jr., and Muddiman, D.C. (2005). Quantitative mass spectral evidence for the absence of circulating brain natriuretic peptide (BNP-32) in severe human heart failure. Proc Natl Acad Sci U S A *102*, 17442-17447.

Heim, J.M., Singh, S., and Gerzer, R. (1996). Effect of glycosylation on cloned ANF-sensitive guanylyl cyclase. Life Sci *59*, PL61-68.

Herman, J.P., Dolgas, C.M., Rucker, D., and Langub, M.C., Jr. (1996). Localization of natriuretic peptide-activated guanylate cyclase mRNAs in the rat brain. J Comp Neurol *369*, 165-187.

Hirsch, J.R., Meyer, M., Magert, H.J., Forssmann, W.G., Mollerup, S., Herter, P., Weber, G., Cermak, R., Ankorina-Stark, I., Schlatter, E., and Kruhoffer, M. (1999). cGMP-

dependent and -independent inhibition of a K+ conductance by natriuretic peptides: molecular and functional studies in human proximal tubule cells. J Am Soc Nephrol *10*, 472-480.

Hirsch, J.R., Skutta, N., and Schlatter, E. (2003). Signaling and distribution of NPR-Bi, the human splice form of the natriuretic peptide receptor type B. Am J Physiol Renal Physiol *285*, F370-374.

Holtwick, R., van Eickels, M., Skryabin, B.V., Baba, H.A., Bubikat, A., Begrow, F., Schneider, M.D., Garbers, D.L., and Kuhn, M. (2003). Pressure-independent cardiac hypertrophy in mice with cardiomyocyte-restricted inactivation of the atrial natriuretic peptide receptor guanylyl cyclase-A. J Clin Invest *111*, 1399-1407.

Hosoda, K., Nakao, K., Mukoyama, M., Saito, Y., Jougasaki, M., Shirakami, G., Suga, S., Ogawa, Y., Yasue, H., and Imura, H. (1991). Expression of brain natriuretic peptide gene in human heart. Production in the ventricle. Hypertension *17*, 1152-1155.

Hume, A.N., Buttgereit, J., Al-Awadhi, A.M., Al-Suwaidi, S.S., John, A., Bader, M., Seabra, M.C., Al-Gazali, L., and Ali, B.R. (2009). Defective cellular trafficking of missense NPR-B mutants is the major mechanism underlying acromesomelic dysplasia-type Maroteaux. Hum Mol Genet *18*, 267-277.

Hunt, P.J., Richards, A.M., Espiner, E.A., Nicholls, M.G., and Yandle, T.G. (1994). Bioactivity and metabolism of C-type natriuretic peptide in normal man. J Clin Endocrinol Metab *78*, 1428-1435.

Hunt, P.J., Richards, A.M., Nicholls, M.G., Yandle, T.G., Doughty, R.N., and Espiner, E.A. (1997). Immunoreactive amino-terminal pro-brain natriuretic peptide (NT-PROBNP): a new marker of cardiac impairment. Clin Endocrinol (Oxf) *47*, 287-296.

Iervasi, G., Clerico, A., Berti, S., Pilo, A., Biagini, A., Bianchi, R., and Donato, L. (1995). Altered tissue degradation and distribution of atrial natriuretic peptide in patients with idiopathic dilated cardiomyopathy and its relationship with clinical severity of the disease and sodium handling. Circulation *91*, 2018-2027.

Igaki, T., Itoh, H., Suga, S., Hama, N., Ogawa, Y., Komatsu, Y., Mukoyama, M., Sugawara, A., Yoshimasa, T., Tanaka, I., and Nakao, K. (1996). C-type natriuretic peptide in chronic renal failure and its action in humans. Kidney Int Suppl *55*, S144-147.

Inoue, K., Naruse, K., Yamagami, S., Mitani, H., Suzuki, N., and Takei, Y. (2003). Four functionally distinct C-type natriuretic peptides found in fish reveal evolutionary history of the natriuretic peptide system. Proc Natl Acad Sci U S A *100*, 10079-10084.

Itakura, M., Iwashina, M., Mizuno, T., Ito, T., Hagiwara, H., and Hirose, S. (1994). Mutational analysis of disulfide bridges in the type C atrial natriuretic peptide receptor. J Biol Chem *269*, 8314-8318.

Iwata, T., Uchida-Mizuno, K., Katafuchi, T., Ito, T., Hagiwara, H., and Hirose, S. (1991). Bifunctional atrial natriuretic peptide receptor (type A) exists as a disulfide-linked tetramer in plasma membranes of bovine adrenal cortex. J Biochem *110*, 35-39.

Jamieson, J.D., and Palade, G.E. (1964). Specific Granules in Atrial Muscle Cells. J Cell Biol *23*, 151-172.

Jaubert, J., Jaubert, F., Martin, N., Washburn, L.L., Lee, B.K., Eicher, E.M., and Guenet, J.L. (1999). Three new allelic mouse mutations that cause skeletal overgrowth involve the natriuretic peptide receptor C gene (Npr3). Proc Natl Acad Sci U S A *96*, 10278-10283.

Jeandel, L., Okamura, H., Belles-Isles, M., Chabot, J.G., Dihl, F., Morel, G., Kelly, P.A., and Heisler, S. (1989). Immunocytochemical localization, binding, and effects of atrial natriuretic peptide in rat adipocytes. Mol Cell Endocrinol *62*, 69-78.

Jewett, J.R., Koller, K.J., Goeddel, D.V., and Lowe, D.G. (1993). Hormonal induction of low affinity receptor guanylyl cyclase. Embo J *12*, 769-777.

Jiao, Y., Yan, J., Jiao, F., Yang, H., Donahue, L.R., Li, X., Roe, B.A., Stuart, J., and Gu, W. (2007). A single nucleotide mutation in Nppc is associated with a long bone abnormality in lbab mice. BMC Genet *8*, 16.

John, S.W., Krege, J.H., Oliver, P.M., Hagaman, J.R., Hodgin, J.B., Pang, S.C., Flynn, T.G., and Smithies, O. (1995). Genetic decreases in atrial natriuretic peptide and salt-sensitive hypertension. Science *267*, 679-681.

John, S.W., Veress, A.T., Honrath, U., Chong, C.K., Peng, L., Smithies, O., and Sonnenberg, H. (1996). Blood pressure and fluid-electrolyte balance in mice with reduced or absent ANP. Am J Physiol *271*, R109-114.

Joubert, S., Labrecque, J., and De Lean, A. (2001). Reduced activity of the NPR-A kinase triggers dephosphorylation and homologous desensitization of the receptor. Biochemistry *40*, 11096-11105.

Kalra, P.R., Clague, J.R., Bolger, A.P., Anker, S.D., Poole-Wilson, P.A., Struthers, A.D., and Coats, A.J. (2003). Myocardial production of C-type natriuretic peptide in chronic heart failure. Circulation *107*, 571-573.

Kangawa, K., Tawaragi, Y., Oikawa, S., Mizuno, A., Sakuragawa, Y., Nakazato, H., Fukuda, A., Minamino, N., and Matsuo, H. (1984). Identification of rat gamma atrial natriuretic polypeptide and characterization of the cDNA encoding its precursor. Nature *312*, 152-155.

Kenny, A.J., Bourne, A., and Ingram, J. (1993). Hydrolysis of human and pig brain natriuretic peptides, urodilatin, C-type natriuretic peptide and some C-receptor ligands by endopeptidase-24.11. Biochem J *291 (Pt 1)*, 83-88.

Kim, S.Z., Cho, K.W., and Kim, S.H. (1999). Modulation of endocardial natriuretic peptide receptors in right ventricular hypertrophy. Am J Physiol *277*, H2280-2289.

Kishimoto, I., Dubois, S.K., and Garbers, D.L. (1996). The heart communicates with the kidney exclusively through the guanylyl cyclase-A receptor: acute handling of sodium and water in response to volume expansion. Proc Natl Acad Sci U S A *93*, 6215-6219.

Kishimoto, I., Rossi, K., and Garbers, D.L. (2001). A genetic model provides evidence that the receptor for atrial natriuretic peptide (guanylyl cyclase-A) inhibits cardiac ventricular myocyte hypertrophy. Proc Natl Acad Sci U S A *98*, 2703-2706.

Knecht, M., Pagel, I., Langenickel, T., Philipp, S., Scheuermann-Freestone, M., Willnow, T., Bruemmer, D., Graf, K., Dietz, R., and Willenbrock, R. (2002). Increased expression of renal neutral endopeptidase in severe heart failure. Life Sci *71*, 2701-2712.

Knowles, J.W., Esposito, G., Mao, L., Hagaman, J.R., Fox, J.E., Smithies, O., Rockman, H.A., and Maeda, N. (2001). Pressure-independent enhancement of cardiac hypertrophy in natriuretic peptide receptor A-deficient mice. J Clin Invest *107*, 975-984.

Koh, G.Y., Nussenzveig, D.R., Okolicany, J., Price, D.A., and Maack, T. (1992). Dynamics of atrial natriuretic factor-guanylate cyclase receptors and receptor-ligand complexes in cultured glomerular mesangial and renomedullary interstitial cells. J Biol Chem *267*, 11987-11994.

Kohno, M., Yokokawa, K., Yasunari, K., Kano, H., Minami, M., Ueda, M., and Yoshikawa, J. (1997). Effect of natriuretic peptide family on the oxidized LDL-induced migration of human coronary artery smooth muscle cells. Circ Res *81*, 585-590.

Koller, K.J., Lipari, M.T., and Goeddel, D.V. (1993). Proper glycosylation and phosphorylation of the type A natriuretic peptide receptor are required for hormone-stimulated guanylyl cyclase activity. J Biol Chem *268*, 5997-6003.

Koller, K.J., Lowe, D.G., Bennett, G.L., Minamino, N., Kangawa, K., Matsuo, H., and Goeddel, D.V. (1991). Selective activation of the B natriuretic peptide receptor by C-type natriuretic peptide (CNP). Science *252*, 120-123.

Kuhn, M. (2003). Structure, regulation, and function of mammalian membrane guanylyl cyclase receptors, with a focus on guanylyl cyclase-A. Circ Res *93*, 700-709.

Kuhn, M., Holtwick, R., Baba, H.A., Perriard, J.C., Schmitz, W., and Ehler, E. (2002). Progressive cardiac hypertrophy and dysfunction in atrial natriuretic peptide receptor (GC-A) deficient mice. Heart *87*, 368-374.

Lang, R.E., Tholken, H., Ganten, D., Luft, F.C., Ruskoaho, H., and Unger, T. (1985). Atrial natriuretic factor--a circulating hormone stimulated by volume loading. Nature *314*, 264-266.

Langenickel, T., Buttgereit, J., Pagel, I., Dietz, R., Willenbrock, R., and Bader, M. (2004). Forced homodimerization by site-directed mutagenesis alters guanylyl cyclase activity of natriuretic peptide receptor B. Hypertension *43*, 460-465.

Langenickel, T.H., Buttgereit, J., Pagel-Langenickel, I., Lindner, M., Monti, J., Beuerlein, K., Al-Saadi, N., Plehm, R., Popova, E., Tank, J., Dietz, R., Willenbrock, R., and Bader, M. (2006). Cardiac hypertrophy in transgenic rats expressing a dominant-negative mutant of the natriuretic peptide receptor B. Proc Natl Acad Sci U S A *103*, 4735-4740.

Langub, M.C., Jr., Dolgas, C.M., Watson, R.E., Jr., and Herman, J.P. (1995). The C-type natriuretic peptide receptor is the predominant natriuretic peptide receptor mRNA expressed in rat hypothalamus. J Neuroendocrinol *7*, 305-309.

Lee, C.Y., Lieu, H., and Burnett, J.C., Jr. (2009). Designer natriuretic peptides. J Investig Med *57*, 18-21.

Leitman, D.C., Andresen, J.W., Kuno, T., Kamisaki, Y., Chang, J.K., and Murad, F. (1986). Identification of multiple binding sites for atrial natriuretic factor by affinity cross-linking in cultured endothelial cells. J Biol Chem *261*, 11650-11655.

Leskinen, H., Vuolteenaho, O., and Ruskoaho, H. (1997). Combined inhibition of endothelin and angiotensin II receptors blocks volume load-induced cardiac hormone release. Circ Res *80*, 114-123.

Lewis, J., Salem, M.M., Chertow, G.M., Weisberg, L.S., McGrew, F., Marbury, T.C., and Allgren, R.L. (2000). Atrial natriuretic factor in oliguric acute renal failure. Anaritide Acute Renal Failure Study Group. Am J Kidney Dis *36*, 767-774.

Liang, F., and Gardner, D.G. (1998). Autocrine/paracrine determinants of strain-activated brain natriuretic peptide gene expression in cultured cardiac myocytes. J Biol Chem *273*, 14612-14619.

Lopez, M.J., Garbers, D.L., and Kuhn, M. (1997). The guanylyl cyclase-deficient mouse defines differential pathways of natriuretic peptide signaling. J Biol Chem *272*, 23064-23068.

Lopez, M.J., Wong, S.K., Kishimoto, I., Dubois, S., Mach, V., Friesen, J., Garbers, D.L., and Beuve, A. (1995). Salt-resistant hypertension in mice lacking the guanylyl cyclase-A receptor for atrial natriuretic peptide. Nature *378*, 65-68.

Lowe, D.G., Chang, M.S., Hellmiss, R., Chen, E., Singh, S., Garbers, D.L., and Goeddel, D.V. (1989). Human atrial natriuretic peptide receptor defines a new paradigm for second messenger signal transduction. Embo J *8*, 1377-1384.

Lowe, D.G., and Fendly, B.M. (1992). Human natriuretic peptide receptor-A guanylyl cyclase. Hormone cross-linking and antibody reactivity distinguish receptor glycoforms. J Biol Chem *267*, 21691-21697.

Lowe, D.G., Klisak, I., Sparkes, R.S., Mohandas, T., and Goeddel, D.V. (1990). Chromosomal distribution of three members of the human natriuretic peptide receptor/guanylyl cyclase gene family. Genomics *8*, 304-312.

Lund, K.A., Opresko, L.K., Starbuck, C., Walsh, B.J., and Wiley, H.S. (1990). Quantitative analysis of the endocytic system involved in hormone-induced receptor internalization. J Biol Chem *265*, 15713-15723.

Maack, T. (1992). Receptors of atrial natriuretic factor. Annu Rev Physiol *54*, 11-27.

Maack, T., Suzuki, M., Almeida, F.A., Nussenzveig, D., Scarborough, R.M., McEnroe, G.A., and Lewicki, J.A. (1987). Physiological role of silent receptors of atrial natriuretic factor. Science *238*, 675-678.

Maeda, K., Tsutamoto, T., Wada, A., Hisanaga, T., and Kinoshita, M. (1998). Plasma brain natriuretic peptide as a biochemical marker of high left ventricular end-diastolic pressure in patients with symptomatic left ventricular dysfunction. Am Heart J *135*, 825-832.

Margulies, K.B., and Burnett, J.C., Jr. (1994). Inhibition of cyclic GMP phosphodiesterases augments renal responses to atrial natriuretic factor in congestive heart failure. J Card Fail *1*, 71-80.

Matsukawa, N., Grzesik, W.J., Takahashi, N., Pandey, K.N., Pang, S., Yamauchi, M., and Smithies, O. (1999). The natriuretic peptide clearance receptor locally modulates the physiological effects of the natriuretic peptide system. Proc Natl Acad Sci U S A *96*, 7403-7408.

McDonough, P.M., Brown, J.H., and Glembotski, C.C. (1993). Phenylephrine and endothelin differentially stimulate cardiac PI hydrolysis and ANF expression. Am J Physiol *264*, H625-630.

McGregor, A., Richards, M., Espiner, E., Yandle, T., and Ikram, H. (1990). Brain natriuretic peptide administered to man: actions and metabolism. J Clin Endocrinol Metab *70*, 1103-1107.

Mills, R.M., LeJemtel, T.H., Horton, D.P., Liang, C., Lang, R., Silver, M.A., Lui, C., and Chatterjee, K. (1999). Sustained hemodynamic effects of an infusion of nesiritide (human b-type natriuretic peptide) in heart failure: a randomized, double-blind, placebo-controlled clinical trial. Natrecor Study Group. J Am Coll Cardiol *34*, 155-162.

Miyagi, M., and Misono, K.S. (2000). Disulfide bond structure of the atrial natriuretic peptide receptor extracellular domain: conserved disulfide bonds among guanylate cyclase-coupled receptors. Biochim Biophys Acta *1478*, 30-38.

Miyagi, M., Zhang, X., and Misono, K.S. (2000). Glycosylation sites in the atrial natriuretic peptide receptor: oligosaccharide structures are not required for hormone binding. Eur J Biochem *267*, 5758-5768.

Mizuno, T., Iwashina, M., Itakura, M., Hagiwara, H., and Hirose, S. (1993). A variant form of the type C atrial natriuretic peptide receptor generated by alternative RNA splicing. J Biol Chem *268*, 5162-5167.

Moffatt, P., Thomas, G., Sellin, K., Bessette, M.C., Lafreniere, F., Akhouayri, O., St-Arnaud, R., and Lanctot, C. (2007). Osteocrin is a specific ligand of the natriuretic Peptide clearance receptor that modulates bone growth. J Biol Chem *282*, 36454-36462.

Moncla, A., Missirian, C., Cacciagli, P., Balzamo, E., Legeai-Mallet, L., Jouve, J.L., Chabrol, B., Le Merrer, M., Plessis, G., Villard, L., and Philip, N. (2007). A cluster of

translocation breakpoints in 2q37 is associated with overexpression of NPPC in patients with a similar overgrowth phenotype. Hum Mutat *28*, 1183-1188.

Mukoyama, M., Nakao, K., Hosoda, K., Suga, S., Saito, Y., Ogawa, Y., Shirakami, G., Jougasaki, M., Obata, K., Yasue, H., and et al. (1991). Brain natriuretic peptide as a novel cardiac hormone in humans. Evidence for an exquisite dual natriuretic peptide system, atrial natriuretic peptide and brain natriuretic peptide. J Clin Invest *87*, 1402-1412.

Murakami, Y., Shimada, T., Inoue, S., Shimizu, H., Ohta, Y., Katoh, H., Nakamura, K., and Ishibashi, Y. (2002). New insights into the mechanism of the elevation of plasma brain natriuretic polypeptide levels in patients with left ventricular hypertrophy. Can J Cardiol *18*, 1294-1300.

Nagase, M., Katafuchi, T., Hirose, S., and Fujita, T. (1997). Tissue distribution and localization of natriuretic peptide receptor subtypes in stroke-prone spontaneously hypertensive rats. J Hypertens *15*, 1235-1243.

Nakao, K., Itoh, H., Kambayashi, Y., Hosoda, K., Saito, Y., Yamada, T., Mukoyama, M., Arai, H., Shirakami, G., Suga, S., and et al. (1990). Rat brain natriuretic peptide. Isolation from rat heart and tissue distribution. Hypertension *15*, 774-778.

Nakao, K., Sugawara, A., Morii, N., Sakamoto, M., Yamada, T., Itoh, H., Shiono, S., Saito, Y., Nishimura, K., Ban, T., and et al. (1986). The pharmacokinetics of alpha-human atrial natriuretic polypeptide in healthy subjects. Eur J Clin Pharmacol *31*, 101-103.

Nakayama, T., Soma, M., Takahashi, Y., Rehemudula, D., Kanmatsuse, K., and Furuya, K. (2000). Functional deletion mutation of the 5'-flanking region of type A human

natriuretic peptide receptor gene and its association with essential hypertension and left ventricular hypertrophy in the Japanese. Circ Res *86*, 841-845.

Nathke, I.S., Heuser, J., Lupas, A., Stock, J., Turck, C.W., and Brodsky, F.M. (1992). Folding and trimerization of clathrin subunits at the triskelion hub. Cell *68*, 899-910.

Nussenzveig, D.R., Lewicki, J.A., and Maack, T. (1990). Cellular mechanisms of the clearance function of type C receptors of atrial natriuretic factor. J Biol Chem *265*, 20952-20958.

Ogawa, H., Qiu, Y., Ogata, C.M., and Misono, K.S. (2004). Crystal structure of hormone-bound atrial natriuretic peptide receptor extracellular domain: rotation mechanism for transmembrane signal transduction. J Biol Chem *279*, 28625-28631.

Ogawa, Y., Itoh, H., Tamura, N., Suga, S., Yoshimasa, T., Uehira, M., Matsuda, S., Shiono, S., Nishimoto, H., and Nakao, K. (1994). Molecular cloning of the complementary DNA and gene that encode mouse brain natriuretic peptide and generation of transgenic mice that overexpress the brain natriuretic peptide gene. J Clin Invest *93*, 1911-1921.

Ogawa, Y., Nakao, K., Nakagawa, O., Komatsu, Y., Hosoda, K., Suga, S., Arai, H., Nagata, K., Yoshida, N., and Imura, H. (1992). Human C-type natriuretic peptide. Characterization of the gene and peptide. Hypertension *19*, 809-813.

Oh, P., McIntosh, D.P., and Schnitzer, J.E. (1998). Dynamin at the neck of caveolae mediates their budding to form transport vesicles by GTP-driven fission from the plasma membrane of endothelium. J Cell Biol *141*, 101-114.

Okamura, H., Kelly, P.A., Chabot, J.G., Morel, G., Belles-Isles, M., and Heisler, S. (1988). Atrial natriuretic peptide receptors are present in brown adipose tissue. Biochem Biophys Res Commun *156*, 1000-1006.

Oliver, P.M., Fox, J.E., Kim, R., Rockman, H.A., Kim, H.S., Reddick, R.L., Pandey, K.N., Milgram, S.L., Smithies, O., and Maeda, N. (1997). Hypertension, cardiac hypertrophy, and sudden death in mice lacking natriuretic peptide receptor A. Proc Natl Acad Sci U S A *94*, 14730-14735.

Oliver, P.M., John, S.W., Purdy, K.E., Kim, R., Maeda, N., Goy, M.F., and Smithies, O. (1998). Natriuretic peptide receptor 1 expression influences blood pressures of mice in a dose-dependent manner. Proc Natl Acad Sci U S A *95*, 2547-2551.

Olney, R.C., Bukulmez, H., Bartels, C.F., Prickett, T.C., Espiner, E.A., Potter, L.R., and Warman, M.L. (2006). Heterozygous mutations in natriuretic peptide receptor-B (NPR2) are associated with short stature. J Clin Endocrinol Metab *91*, 1229-1232.

Pandey, K.N. (1992). Kinetic analysis of internalization, recycling and redistribution of atrial natriuretic factor-receptor complex in cultured vascular smooth-muscle cells. Ligand-dependent receptor down-regulation. Biochem J *288 (Pt 1)*, 55-61.

Pandey, K.N. (1993). Stoichiometric analysis of internalization, recycling, and redistribution of photoaffinity-labeled guanylate cyclase/atrial natriuretic factor receptors in cultured murine Leydig tumor cells. J Biol Chem *268*, 4382-4390.

Pandey, K.N. (2005). Internalization and trafficking of guanylyl cyclase/natriuretic peptide receptor-A. Peptides *26*, 985-1000.

Pandey, K.N., Inagami, T., and Misono, K.S. (1986). Atrial natriuretic factor receptor on cultured Leydig tumor cells: ligand binding and photoaffinity labeling. Biochemistry *25*, 8467-8472.

Pandey, K.N., Kumar, R., Li, M., and Nguyen, H. (2000). Functional domains and expression of truncated atrial natriuretic peptide receptor-A: the carboxyl-terminal

regions direct the receptor internalization and sequestration in COS-7 cells. Mol Pharmacol *57*, 259-267.

Pandey, K.N., Nguyen, H.T., Garg, R., Khurana, M.L., and Fink, J. (2005). Internalization and trafficking of guanylyl (guanylate) cyclase/natriuretic peptide receptor A is regulated by an acidic tyrosine-based cytoplasmic motif GDAY. Biochem J *388*, 103-113.

Pandey, K.N., Nguyen, H.T., Sharma, G.D., Shi, S.J., and Kriegel, A.M. (2002). Ligand-regulated internalization, trafficking, and down-regulation of guanylyl cyclase/atrial natriuretic peptide receptor-A in human embryonic kidney 293 cells. J Biol Chem *277*, 4618-4627.

Pandey, K.N., and Singh, S. (1990). Molecular cloning and expression of murine guanylate cyclase/atrial natriuretic factor receptor cDNA. J Biol Chem *265*, 12342-12348.

Payne, C.K., Jones, S.A., Chen, C., and Zhuang, X. (2007). Internalization and trafficking of cell surface proteoglycans and proteoglycan-binding ligands. Traffic *8*, 389-401.

Pedro, L., Fenrick, R., Marquis, M., McNicoll, N., and De Lean, A. (1998). Characterization of the phosphorylation state of natriuretic peptide receptor-C. Mol Cell Biochem *178*, 95-101.

Pfeifer, A., Aszodi, A., Seidler, U., Ruth, P., Hofmann, F., and Fassler, R. (1996). Intestinal secretory defects and dwarfism in mice lacking cGMP-dependent protein kinase II. Science *274*, 2082-2086.

Porter, J.G., Arfsten, A., Fuller, F., Miller, J.A., Gregory, L.C., and Lewicki, J.A. (1990). Isolation and functional expression of the human atrial natriuretic peptide clearance receptor cDNA. Biochem Biophys Res Commun *171*, 796-803.

Potter, L.R. (2005). Domain analysis of human transmembrane guanylyl cyclase receptors: implications for regulation. Front Biosci *10*, 1205-1220.

Potter, L.R., Abbey-Hosch, S., and Dickey, D.M. (2006). Natriuretic peptides, their receptors, and cyclic guanosine monophosphate-dependent signaling functions. Endocr Rev *27*, 47-72.

Potter, L.R., and Garbers, D.L. (1992). Dephosphorylation of the guanylyl cyclase-A receptor causes desensitization. J Biol Chem *267*, 14531-14534.

Potter, L.R., and Hunter, T. (1998a). Identification and characterization of the major phosphorylation sites of the B-type natriuretic peptide receptor. J Biol Chem *273*, 15533-15539.

Potter, L.R., and Hunter, T. (1998b). Phosphorylation of the kinase homology domain is essential for activation of the A-type natriuretic peptide receptor. Mol Cell Biol *18*, 2164-2172.

Potter, L.R., and Hunter, T. (1999). A constitutively "phosphorylated" guanylyl cyclase-linked atrial natriuretic peptide receptor mutant is resistant to desensitization. Mol Biol Cell *10*, 1811-1820.

Potter, L.R., and Hunter, T. (2001). Guanylyl cyclase-linked natriuretic peptide receptors: structure and regulation. J Biol Chem *276*, 6057-6060.

Potter, L.R., Yoder, A.R., Flora, D.R., Antos, L.K., and Dickey, D.M. (2009). Natriuretic peptides: their structures, receptors, physiologic functions and therapeutic applications. Handb Exp Pharmacol, 341-366.

Rahmutula, D., Nakayama, T., Soma, M., Kosuge, K., Aoi, N., Izumi, Y., Kanmatsuse, K., and Ozawa, Y. (2002). Structure and polymorphisms of the human natriuretic peptide receptor C gene. Endocrine *17*, 85-90.

Rathinavelu, A., and Isom, G.E. (1991). Differential internalization and processing of atrial-natriuretic-factor B and C receptor in PC12 cells. Biochem J *276 (Pt 2)*, 493-497.

Rehemudula, D., Nakayama, T., Soma, M., Takahashi, Y., Uwabo, J., Sato, M., Izumi, Y., Kanmatsuse, K., and Ozawa, Y. (1999). Structure of the type B human natriuretic peptide receptor gene and association of a novel microsatellite polymorphism with essential hypertension. Circ Res *84*, 605-610.

Richards, A.M., Cleland, J.G., Tonolo, G., McIntyre, G.D., Leckie, B.J., Dargie, H.J., Ball, S.G., and Robertson, J.I. (1986). Plasma alpha natriuretic peptide in cardiac impairment. Br Med J (Clin Res Ed) *293*, 409-412.

Richards, A.M., Crozier, I.G., Holmes, S.J., Espiner, E.A., Yandle, T.G., and Frampton, C. (1993a). Brain natriuretic peptide: natriuretic and endocrine effects in essential hypertension. J Hypertens *11*, 163-170.

Richards, A.M., Crozier, I.G., Yandle, T.G., Espiner, E.A., Ikram, H., and Nicholls, M.G. (1993b). Brain natriuretic factor: regional plasma concentrations and correlations with haemodynamic state in cardiac disease. Br Heart J *69*, 414-417.

Richards, A.M., Lainchbury, J.G., Troughton, R.W., Espiner, E.A., and Nicholls, M.G. (2004). Clinical applications of B-type natriuretic peptides. Trends Endocrinol Metab *15*, 170-174.

Richards, A.M., Tonolo, G., Montorsi, P., Finlayson, J., Fraser, R., Inglis, G., Towrie, A., and Morton, J.J. (1988). Low dose infusions of 26- and 28-amino acid human atrial natriuretic peptides in normal man. J Clin Endocrinol Metab *66*, 465-472.

Rose, R.A., and Giles, W.R. (2008). Natriuretic peptide C receptor signalling in the heart and vasculature. J Physiol *586*, 353-366.

Ruskoaho, H. (2003). Cardiac hormones as diagnostic tools in heart failure. Endocr Rev *24*, 341-356.

Sabrane, K., Kruse, M.N., Fabritz, L., Zetsche, B., Mitko, D., Skryabin, B.V., Zwiener, M., Baba, H.A., Yanagisawa, M., and Kuhn, M. (2005). Vascular endothelium is critically involved in the hypotensive and hypovolemic actions of atrial natriuretic peptide. J Clin Invest *115*, 1666-1674.

Sackner-Bernstein, J.D., Kowalski, M., Fox, M., and Aaronson, K. (2005a). Short-term risk of death after treatment with nesiritide for decompensated heart failure: a pooled analysis of randomized controlled trials. JAMA *293*, 1900-1905.

Sackner-Bernstein, J.D., Skopicki, H.A., and Aaronson, K.D. (2005b). Risk of worsening renal function with nesiritide in patients with acutely decompensated heart failure. Circulation *111*, 1487-1491.

Saito, Y., Nakao, K., Nishimura, K., Sugawara, A., Okumura, K., Obata, K., Sonoda, R., Ban, T., Yasue, H., and Imura, H. (1987). Clinical application of atrial natriuretic polypeptide in patients with congestive heart failure: beneficial effects on left ventricular function. Circulation *76*, 115-124.

Sakamoto, M., Nakao, K., Kihara, M., Morii, N., Sugawara, A., Suda, M., Shimokura, M., Kiso, Y., Yamori, Y., and Imura, H. (1985). Existence of atrial natriuretic polypeptide in kidney. Biochem Biophys Res Commun *128*, 1281-1287.

Schachner, T., Zou, Y., Oberhuber, A., Mairinger, T., Tzankov, A., Laufer, G., Ott, H., and Bonatti, J. (2004). Perivascular application of C-type natriuretic peptide attenuates neointimal hyperplasia in experimental vein grafts. Eur J Cardiothorac Surg *25*, 585-590.

Schiffrin, E.L., Turgeon, A., Tremblay, J., and Deslongchamps, M. (1991). Effects of ANP, angiotensin, vasopressin, and endothelin on ANP receptors in cultured rat vascular smooth muscle cells. Am J Physiol *260*, H58-65.

Schulz, S., Singh, S., Bellet, R.A., Singh, G., Tubb, D.J., Chin, H., and Garbers, D.L. (1989). The primary structure of a plasma membrane guanylate cyclase demonstrates diversity within this new receptor family. Cell *58*, 1155-1162.

Schweitz, H., Vigne, P., Moinier, D., Frelin, C., and Lazdunski, M. (1992). A new member of the natriuretic peptide family is present in the venom of the green mamba (Dendroaspis angusticeps). J Biol Chem *267*, 13928-13932.

Sengenes, C., Berlan, M., De Glisezinski, I., Lafontan, M., and Galitzky, J. (2000). Natriuretic peptides: a new lipolytic pathway in human adipocytes. Faseb J *14*, 1345-1351.

Sengenes, C., Bouloumie, A., Hauner, H., Berlan, M., Busse, R., Lafontan, M., and Galitzky, J. (2003). Involvement of a cGMP-dependent pathway in the natriuretic peptide-mediated hormone-sensitive lipase phosphorylation in human adipocytes. J Biol Chem *278*, 48617-48626.

Sengenes, C., Zakaroff-Girard, A., Moulin, A., Berlan, M., Bouloumie, A., Lafontan, M., and Galitzky, J. (2002). Natriuretic peptide-dependent lipolysis in fat cells is a primate specificity. Am J Physiol Regul Integr Comp Physiol *283*, R257-265.

Sever, S., Damke, H., and Schmid, S.L. (2000). Dynamin:GTP controls the formation of constricted coated pits, the rate limiting step in clathrin-mediated endocytosis. J Cell Biol *150*, 1137-1148.

Shinomiya, M., Tashiro, J., Saito, Y., Yoshida, S., Furuya, M., Oka, N., Tanaka, S., Kangawa, K., and Matsuo, H. (1994). C-type natriuretic peptide inhibits intimal thickening

of rabbit carotid artery after balloon catheter injury. Biochem Biophys Res Commun *205*, 1051-1056.

Singh, G., Kuc, R.E., Maguire, J.J., Fidock, M., and Davenport, A.P. (2006). Novel snake venom ligand dendroaspis natriuretic peptide is selective for natriuretic peptide receptor-A in human heart: downregulation of natriuretic peptide receptor-A in heart failure. Circ Res *99*, 183-190.

Smith, M.W., Espiner, E.A., Yandle, T.G., Charles, C.J., and Richards, A.M. (2000). Delayed metabolism of human brain natriuretic peptide reflects resistance to neutral endopeptidase. J Endocrinol *167*, 239-246.

Soeki, T., Kishimoto, I., Okumura, H., Tokudome, T., Horio, T., Mori, K., and Kangawa, K. (2005). C-type natriuretic peptide, a novel antifibrotic and antihypertrophic agent, prevents cardiac remodeling after myocardial infarction. J Am Coll Cardiol *45*, 608-616.

Sorkin, A., and Goh, L.K. (2008). Endocytosis and intracellular trafficking of ErbBs. Exp Cell Res *314*, 3093-3106.

Sorkin, A., and von Zastrow, M. (2009). Endocytosis and signalling: intertwining molecular networks. Nat Rev Mol Cell Biol *10*, 609-622.

Steinhelper, M.E., Cochrane, K.L., and Field, L.J. (1990). Hypotension in transgenic mice expressing atrial natriuretic factor fusion genes. Hypertension *16*, 301-307.

Stenger, R.J., and Spiro, D. (1961). The ultrastructure of mammalian cardiac muscle. J Biophys and Biochem Cytol *9*, 325-351.

Stephenson, S.L., and Kenny, A.J. (1987). The hydrolysis of alpha-human atrial natriuretic peptide by pig kidney microvillar membranes is initiated by endopeptidase-24.11. Biochem J *243*, 183-187.

Stults, J.T., O'Connell, K.L., Garcia, C., Wong, S., Engel, A.M., Garbers, D.L., and Lowe, D.G. (1994). The disulfide linkages and glycosylation sites of the human natriuretic peptide receptor-C homodimer. Biochemistry *33*, 11372-11381.

Sudoh, T., Kangawa, K., Minamino, N., and Matsuo, H. (1988). A new natriuretic peptide in porcine brain. Nature *332*, 78-81.

Sudoh, T., Minamino, N., Kangawa, K., and Matsuo, H. (1990). C-type natriuretic peptide (CNP): a new member of natriuretic peptide family identified in porcine brain. Biochem Biophys Res Commun *168*, 863-870.

Suga, S., Itoh, H., Komatsu, Y., Ogawa, Y., Hama, N., Yoshimasa, T., and Nakao, K. (1993). Cytokine-induced C-type natriuretic peptide (CNP) secretion from vascular endothelial cells--evidence for CNP as a novel autocrine/paracrine regulator from endothelial cells. Endocrinology *133*, 3038-3041.

Suga, S., Nakao, K., Hosoda, K., Mukoyama, M., Ogawa, Y., Shirakami, G., Arai, H., Saito, Y., Kambayashi, Y., Inouye, K., and et al. (1992a). Receptor selectivity of natriuretic peptide family, atrial natriuretic peptide, brain natriuretic peptide, and C-type natriuretic peptide. Endocrinology *130*, 229-239.

Suga, S., Nakao, K., Itoh, H., Komatsu, Y., Ogawa, Y., Hama, N., and Imura, H. (1992b). Endothelial production of C-type natriuretic peptide and its marked augmentation by transforming growth factor-beta. Possible existence of "vascular natriuretic peptide system". J Clin Invest *90*, 1145-1149.

Suga, S., Nakao, K., Mukoyama, M., Arai, H., Hosoda, K., Ogawa, Y., and Imura, H. (1992c). Characterization of natriuretic peptide receptors in cultured cells. Hypertension *19*, 762-765.

Supaporn, T., Sandberg, S.M., Borgeson, D.D., Heublein, D.M., Luchner, A., Wei, C.M., Dousa, T.P., and Burnett, J.C., Jr. (1996). Blunted cGMP response to agonists and enhanced glomerular cyclic 3',5'-nucleotide phosphodiesterase activities in experimental congestive heart failure. Kidney Int *50*, 1718-1725.

Takahashi, Y., Nakayama, T., Soma, M., Izumi, Y., and Kanmatsuse, K. (1998). Organization of the human natriuretic peptide receptor A gene. Biochem Biophys Res Commun *246*, 736-739.

Takeuchi, H., Ohmori, K., Kondo, I., Oshita, A., Shinomiya, K., Yu, Y., Takagi, Y., Mizushige, K., Kangawa, K., and Kohno, M. (2003). Potentiation of C-type natriuretic peptide with ultrasound and microbubbles to prevent neointimal formation after vascular injury in rats. Cardiovasc Res *58*, 231-238.

Tamura, N., Doolittle, L.K., Hammer, R.E., Shelton, J.M., Richardson, J.A., and Garbers, D.L. (2004). Critical roles of the guanylyl cyclase B receptor in endochondral ossification and development of female reproductive organs. Proc Natl Acad Sci U S A *101*, 17300-17305.

Tamura, N., and Garbers, D.L. (2003). Regulation of the guanylyl cyclase-B receptor by alternative splicing. J Biol Chem *278*, 48880-48889.

Tamura, N., Ogawa, Y., Chusho, H., Nakamura, K., Nakao, K., Suda, M., Kasahara, M., Hashimoto, R., Katsuura, G., Mukoyama, M., Itoh, H., Saito, Y., Tanaka, I., Otani, H., and Katsuki, M. (2000). Cardiac fibrosis in mice lacking brain natriuretic peptide. Proc Natl Acad Sci U S A *97*, 4239-4244.

Thibault, G., Amiri, F., and Garcia, R. (1999). Regulation of natriuretic peptide secretion by the heart. Annu Rev Physiol *61*, 193-217.

Thibault, G., Garcia, R., Gutkowska, J., Bilodeau, J., Lazure, C., Seidah, N.G., Chretien, M., Genest, J., and Cantin, M. (1987). The propeptide Asn1-Tyr126 is the storage form of rat atrial natriuretic factor. Biochem J *241*, 265-272.

Thuerauf, D.J., Hanford, D.S., and Glembotski, C.C. (1994). Regulation of rat brain natriuretic peptide transcription. A potential role for GATA-related transcription factors in myocardial cell gene expression. J Biol Chem *269*, 17772-17775.

Tokudome, T., Horio, T., Soeki, T., Mori, K., Kishimoto, I., Suga, S., Yoshihara, F., Kawano, Y., Kohno, M., and Kangawa, K. (2004). Inhibitory effect of C-type natriuretic peptide (CNP) on cultured cardiac myocyte hypertrophy: interference between CNP and endothelin-1 signaling pathways. Endocrinology *145*, 2131-2140.

Tsuji, T., and Kunieda, T. (2005). A loss-of-function mutation in natriuretic peptide receptor 2 (Npr2) gene is responsible for disproportionate dwarfism in cn/cn mouse. J Biol Chem *280*, 14288-14292.

Tsutamoto, T., Kanamori, T., Morigami, N., Sugimoto, Y., Yamaoka, O., and Kinoshita, M. (1993). Possibility of downregulation of atrial natriuretic peptide receptor coupled to guanylate cyclase in peripheral vascular beds of patients with chronic severe heart failure. Circulation *87*, 70-75.

Vacquier, V.D., and Moy, G.W. (1986). Stoichiometry of phosphate loss from sea urchin sperm guanylate cyclase during fertilization. Biochem Biophys Res Commun *137*, 1148-1152.

Valentin, J.P., Qiu, C., Muldowney, W.P., Ying, W.Z., Gardner, D.G., and Humphreys, M.H. (1992). Cellular basis for blunted volume expansion natriuresis in experimental nephrotic syndrome. J Clin Invest *90*, 1302-1312.

van Dam, E.M., and Stoorvogel, W. (2002). Dynamin-dependent transferrin receptor recycling by endosome-derived clathrin-coated vesicles. Mol Biol Cell *13*, 169-182.

Vieira, A.V., Lamaze, C., and Schmid, S.L. (1996). Control of EGF receptor signaling by clathrin-mediated endocytosis. Science *274*, 2086-2089.

Vieira, M.A., Gao, M., Nikonova, L.N., and Maack, T. (2001). Molecular and cellular physiology of the dissociation of atrial natriuretic peptide from guanylyl cyclase a receptors. J Biol Chem *276*, 36438-36445.

Wang, Y., de Waard, M.C., Sterner-Kock, A., Stepan, H., Schultheiss, H.P., Duncker, D.J., and Walther, T. (2007). Cardiomyocyte-restricted over-expression of C-type natriuretic peptide prevents cardiac hypertrophy induced by myocardial infarction in mice. Eur J Heart Fail *9*, 548-557.

Wilcox, J.N., Augustine, A., Goeddel, D.V., and Lowe, D.G. (1991). Differential regional expression of three natriuretic peptide receptor genes within primate tissues. Mol Cell Biol *11*, 3454-3462.

Wiley, H.S. (1988). Anomalous binding of epidermal growth factor to A431 cells is due to the effect of high receptor densities and a saturable endocytic system. J Cell Biol *107*, 801-810.

Wiley, H.S. (2003). Trafficking of the ErbB receptors and its influence on signaling. Exp Cell Res *284*, 78-88.

Wilson, I.A., Niman, H.L., Houghten, R.A., Cherenson, A.R., Connolly, M.L., and Lerner, R.A. (1984). The structure of an antigenic determinant in a protein. Cell *37*, 767-778.

Witteles, R.M., Kao, D., Christopherson, D., Matsuda, K., Vagelos, R.H., Schreiber, D., and Fowler, M.B. (2007). Impact of nesiritide on renal function in patients with acute

decompensated heart failure and pre-existing renal dysfunction a randomized, double-blind, placebo-controlled clinical trial. J Am Coll Cardiol *50*, 1835-1840.

Wu, C., Wu, F., Pan, J., Morser, J., and Wu, Q. (2003). Furin-mediated processing of Pro-C-type natriuretic peptide. J Biol Chem *278*, 25847-25852.

Yamamoto, K., Burnett, J.C., Jr., Jougasaki, M., Nishimura, R.A., Bailey, K.R., Saito, Y., Nakao, K., and Redfield, M.M. (1996). Superiority of brain natriuretic peptide as a hormonal marker of ventricular systolic and diastolic dysfunction and ventricular hypertrophy. Hypertension *28*, 988-994.

Yamashita, Y., Takeshige, K., Inoue, A., Hirose, S., Takamori, A., and Hagiwara, H. (2000). Concentration of mRNA for the natriuretic peptide receptor-C in hypertrophic chondrocytes of the fetal mouse tibia. J Biochem *127*, 177-179.

Yan, W., Wu, F., Morser, J., and Wu, Q. (2000). Corin, a transmembrane cardiac serine protease, acts as a pro-atrial natriuretic peptide-converting enzyme. Proc Natl Acad Sci U S A *97*, 8525-8529.

Yancy, C.W., Krum, H., Massie, B.M., Silver, M.A., Stevenson, L.W., Cheng, M., Kim, S.S., and Evans, R. (2007). The Second Follow-up Serial Infusions of Nesiritide (FUSION II) trial for advanced heart failure: study rationale and design. Am Heart J *153*, 478-484.

Yandle, T.G., Richards, A.M., Nicholls, M.G., Cuneo, R., Espiner, E.A., and Livesey, J.H. (1986). Metabolic clearance rate and plasma half life of alpha-human atrial natriuretic peptide in man. Life Sci *38*, 1827-1833.

Yasoda, A., Komatsu, Y., Chusho, H., Miyazawa, T., Ozasa, A., Miura, M., Kurihara, T., Rogi, T., Tanaka, S., Suda, M., Tamura, N., Ogawa, Y., and Nakao, K. (2004).

Overexpression of CNP in chondrocytes rescues achondroplasia through a MAPK-dependent pathway. Nat Med *10*, 80-86.

Yasoda, A., Ogawa, Y., Suda, M., Tamura, N., Mori, K., Sakuma, Y., Chusho, H., Shiota, K., Tanaka, K., and Nakao, K. (1998). Natriuretic peptide regulation of endochondral ossification. Evidence for possible roles of the C-type natriuretic peptide/guanylyl cyclase-B pathway. J Biol Chem *273*, 11695-11700.

Yasue, H., Obata, K., Okumura, K., Kurose, M., Ogawa, H., Matsuyama, K., Jougasaki, M., Saito, Y., Nakao, K., and Imura, H. (1989). Increased secretion of atrial natriuretic polypeptide from the left ventricle in patients with dilated cardiomyopathy. J Clin Invest *83*, 46-51.

Yeung, V.T., Ho, S.K., Nicholls, M.G., and Cockram, C.S. (1996). Binding of CNP-22 and CNP-53 to cultured mouse astrocytes and effects on cyclic GMP. Peptides *17*, 101-106.

Yoder, A.R., Kruse, A.C., Earhart, C.A., Ohlendorf, D.H., and Potter, L.R. (2008). Reduced ability of C-type natriuretic peptide (CNP) to activate natriuretic peptide receptor B (NPR-B) causes dwarfism in lbab -/- mice. Peptides *29*, 1575-1581.

Yoshimura, M., Yasue, H., Morita, E., Sakaino, N., Jougasaki, M., Kurose, M., Mukoyama, M., Saito, Y., Nakao, K., and Imura, H. (1991). Hemodynamic, renal, and hormonal responses to brain natriuretic peptide infusion in patients with congestive heart failure. Circulation *84*, 1581-1588.

Zahabi, A., Picard, S., Fortin, N., Reudelhuber, T.L., and Deschepper, C.F. (2003). Expression of constitutively active guanylate cyclase in cardiomyocytes inhibits the hypertrophic effects of isoproterenol and aortic constriction on mouse hearts. J Biol Chem *278*, 47694-47699.